BIOGEOCHEMISTRY IN THE COASTAL ZONE: CHANGING LAND USE, SALINITY INTRUSION, POREWATER STOICHIOMETRY AND THE MINERALIZATION OF ORGANIC MATTER IN ESTUARINE SEDIMENTS

by

N. Weston

(Under the Direction of Samantha Joye)

ABSTRACT

Thirty years of population growth, land use change, and nutrient loading from the subwatersheds of the Altamaha River, GA were analyzed. Population growth, mainly in the upper watershed near the cities of Atlanta and Athens, resulted in increased nitrate delivery to the rivers and transport to the coastal zone. Delivery of freshwater appears to be declining, due to climate change and water withdrawal within the watershed. The effects of upriver salinity intrusion on the biogeochemistry of sediments from the tidal freshwater portion of the Altamaha River were investigated. Methanogenesis, which dominated in the freshwater sediments, declined quickly following salinity intrusion. Sulfate reduction was the dominant pathway of microbial organic matter mineralization within two weeks of salinity intrusion, although increased iron-oxide availability during initial salinity intrusion appears to have stimulated high rates of microbial iron reduction for a short period. Salinity-driven desorption of ammonium and increased rates of silica and phosphorus mineral dissolution following salinity intrusion increased overall export of ammonium, phosphate and silicate from salinity-impacted sediments.

The mineralization of complex organic matter in sediments is mediated by a diverse consortium of microbes that hydrolyze, ferment, and terminally oxidize organic compounds. Patterns of estuarine sediment biogeochemistry, focusing on the role of dissolved organic carbon

(DOC) and nitrogen, were determined with a multi-site, multi-season survey of estuarine porewater profiles in Georgia and South Carolina. This survey demonstrated system-scale correlations between the inorganic products of terminal metabolism (dissolved inorganic carbon, ammonium and phosphate) and sulfate depletion. DOC, as the substrate for terminal metabolism, was not correlated with other variables indicating that production and consumption of DOC were tightly coupled, and bulk DOC is largely a recalcitrant pool. Controls on the coupling between the hydrolytic/fermentative and terminal metabolic bacterial communities in estuarine sediments were further investigated using anaerobic flow-through bioreactors. We documented the temperature-driven decoupling of the production and consumption of key DOC intermediates due to variable temperature responses of these functional microbial groups. Production of labile DOC exceeded terminal oxidation at colder temperatures, resulting in accumulation of labile DOC. At higher temperatures, potential terminal oxidation rates exceeded those of labile DOC production and labile DOC availability limited rates of terminal oxidation.

INDEX WORDS: Biogeochemistry, Estuary, Land use, Salinity, Porewater, Stoichiometry, Mineralization, Organic matter, Dissolved organic matter, Terminal metabolism, Fermentation, Hydrolysis, Sulfate reduction, Methanogenesis, Iron reduction, Denitrification, Watershed, Loading, Nutrient, Population, Salinity intrusion, Temperature, Dissolved organic carbon

BIOGEOCHEMISTRY IN THE COASTAL ZONE: CHANGING LAND USE, SALINITY INTRUSION, POREWATER STOICHIOMETRY AND THE MINERALIZATION OF ORGANIC MATTER IN ESTUARINE SEDIMENTS

by

NATHANIEL B. WESTON

B.A. Hampshire College, 1997

A Dissertation Submitted to the Graduate Faculty of the University of Georgia in Partial Fulfillment of the Requirements for the Degree

DOCTOR OF PHILOSOPHY

ATHENS, GEORGIA

2005

BIOGEOCHEMISTRY IN THE COASTAL ZONE: CHANGING LAND USE, SALINITY INTRUSION, POREWATER STOICHIOMETRY AND THE MINERALIZATION OF ORGANIC MATTER IN ESTUARINE SEDIMENTS

by

NATHANIEL B WESTON

Major Professor:	Samantha B. Joye
Committee:	James Hollibaugh Mary Ann Moran Christof Meile Charles Hopkinson

Electronic Version Approved:

Maureen Grasso
Dean of the Graduate School
The University of Georgia
August 2005

DEDICATION

This work is dedicated to the two people who, above all, made it possible for me to reach this point in life, my parents:

John and Susan Weston

Thank you.

ACKNOWLEDGMENTS

I would like to thank the various sources of funding that have made this work possible; the National Science Foundation Georgia Coastal Ecosystem Long Term Ecological Research project (OCE 99-82133), the National Oceanic and Atmospheric Administration's Georgia Sea Grant Program (NA06RG0029-R/WQ11 and R/WQ12A), and South Carolina Sea Grant Program (award number: NA960PO113), and the University of Georgia's University-Wide Fellowship Program.

There are many people I would like to thank who have helped in the field, in the laboratory, and with manuscripts, including Dan Albert, Steve Carini, Ji-Hong Dai, Hai-Bing Ding, Ray Dixon, Jennifer Edmonds, Rosalynn Lee, Steve MacAvoy, Pat Megonigal, Jessie Menken, Beth! Orcutt, Paula Olecki, Bill Porubsky, Tiffany Roberts, Vladimir Samarkin, Heide Schultz, Wade Sheldon, Ming-Yi Sun, and Liliana Velasquez. I would like to say a special thanks to Matthew Erickson, who has been extremely helpful and without whom this dissertation would not exist. I also would like to thank Charlene D'Avanzo for starting me on this path.

My dissertation committee, Mandy Joye, Tim Hollibaugh, Chuck Hopkinson, Christof Meile, and Mary Ann Moran, have been supportive and I am grateful for their encouragement and input. Christof Meile's critical reviews of manuscripts are invaluable, as well as the beers with him that follow. It has been an absolute pleasure to work with my advisor, Mandy Joye. Her support, both intellectually and financially, has been abundant and consistent for the duration of my research. I will very much miss the almost unfettered ability to play in the mud that Mandy has made possible.

Finally, I wish to thank Jessie Menken, who is my guiding star. I am eternally thankful for her love and support.

TABLE OF CONTENTS

CHAPTER 1

INTRODUCTION AND LITERATURE REVIEW

Human activities have greatly altered the quality, quantity and timing of delivery of materials to coastal waters. About one half of the world's population lives within 100 km of the coast (Vitousek et al. 1997), and changing land use in the watersheds of rivers impacts processes in the coastal zone (Howarth et al. 1996; Nixon 1995; Vitousek et al. 1997; Paerl et al. 1998). Nitrogen loading to estuaries is of particular concern, as coastal waters are often nitrogen limited and increased nitrogen delivery can fuel excess production and lead to eutrophication (Nixon et al. 1996).

Human activities have greatly increased global nitrogen fixation via the Haber-Bosch process (Vitousek et al. 1997). On average about 20% of nitrogen delivered to landscapes from fertilization of agricultural land (Turner and Rabalais 1991), atmospheric deposition (Fisher and Oppenheimer 1991), direct human waste (Cole et al. 1993) and other sources is exported by rivers (Howarth 1998; Van Breemen et al. 2002). Nitrogen export has increased in many of the world's rivers due to these human activities (Howarth et al. 1996).

In **CHAPTER 2**, I explore long-term changes in land use and population in the Altamaha River watershed, and concentrations of nutrients and organic matter in the rivers and loading to the coastal zone. The Altamaha River in Georgia drains one of the largest watersheds on the East Coast (about 36,000 km^2), and the coastal zone of the Altamaha is an important and productive fishery. Although the watershed of the Altamaha remains relatively undisturbed, in recent years development pressure has increased in the basin. In 2002, the Altamaha River was

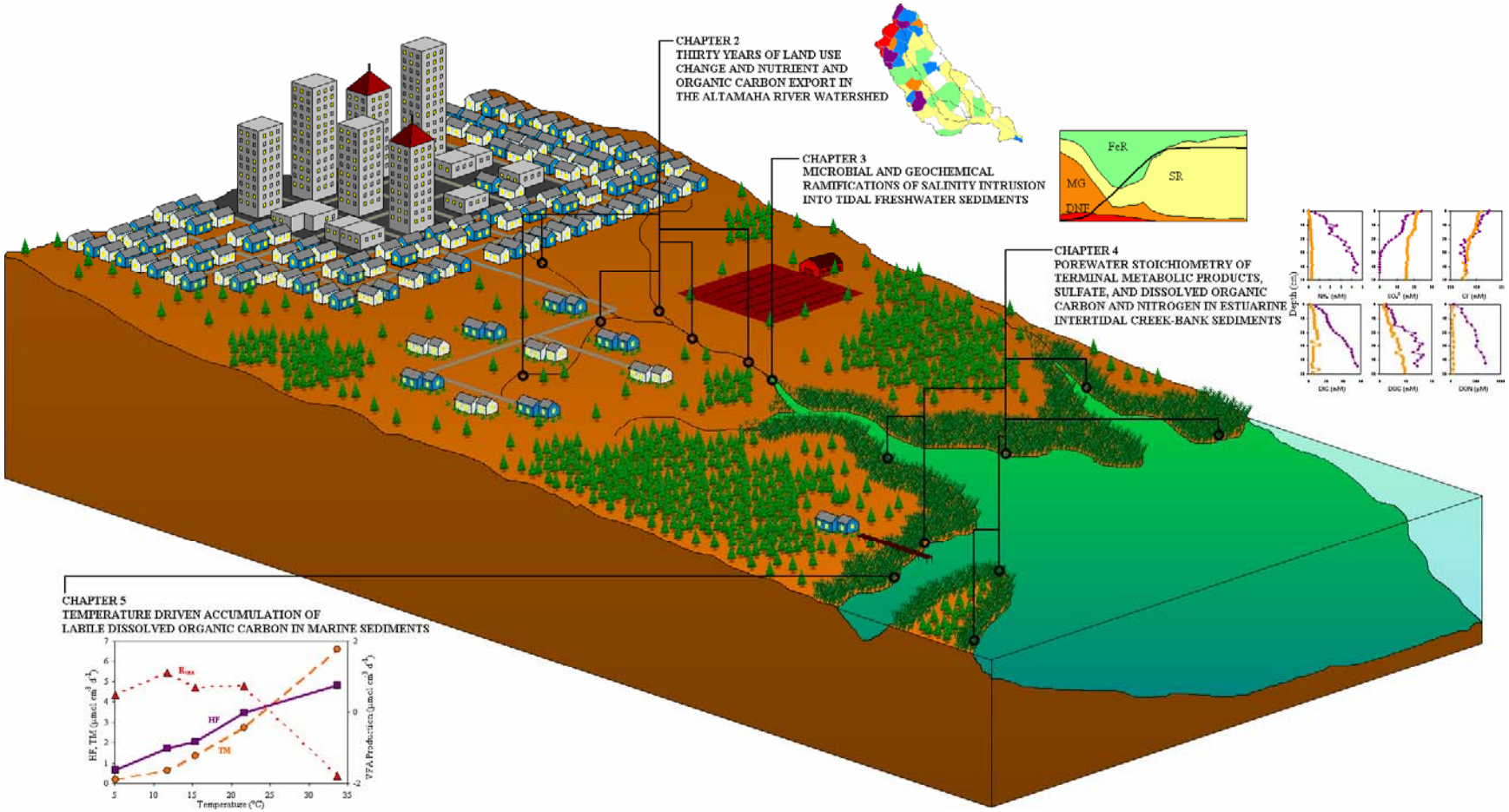

Figure 1.1. Diagram of a coastal watershed with mixed urban, suburban, agricultural and forested land use and coastal salt marshes. Locations of studies focusing on land use change and loading from sub-watersheds to the coastal zone (**Chapter 2**), the effects of salinity intrusion on tidal freshwater sediments (**Chapter 3**), system-scale stoichiometry of metabolic substrates and products in estuarine sediments (**Chapter 4**), and temperature effects on the coupling of hydrolysis/fermentation and terminal metabolism (**Chapter 5**) are indicated.

placed on the American Rivers Organization's list of most endangered rivers (American Rivers 2002). The National Oceanic and Atmospheric Administration (1996) described the Altamaha River estuary as currently minimally impacted but likely to exhibit increasing signs of eutrophication due to anthropogenic activities in the watershed.

Despite the size and importance of the Altamaha River watershed and estuary, relatively little is known about the effects of changing land use in the watershed on the rivers and nutrient export to the coastal zone. In this paper we analyze more than thirty years of nutrient and organic carbon data from fifteen United States Geological Survey water quality monitoring stations in the Altamaha River and its major tributaries. Trends in population and land use within the watershed are also examined. Long-term patterns and controls of river nutrient and organic carbon concentrations were investigated, and loading from the major sub-watersheds to the Altamaha River was estimated.

Climate change (Smith et al. 2005), rising sea-levels (Wigley 2005) and increases in water consumption due to human activities (Gleick 2003) has and will continue to alter riverine inputs of freshwater to coastal zones globally. As river discharge drops, saline ocean water intrudes upriver into previously freshwater zones (Hamilton 1990; Knowles 2002). Changes in salinity will alter both the abiotic geochemistry and microbial community of sediments. In **CHAPTER 3**, I discuss the effects of salinity intrusion on the biogeochemistry of tidal freshwater sediments of the Altamaha River, and the potential consequences of salinity intrusion on estuarine productivity. Along with abiotic geochemical alterations of freshwater sediment during salinity intrusion, microbial denitrification, sulfate reduction, methanogenesis and iron reduction are estimated to determine shifts in microbial metabolic pathways following salinity intrusion.

Understanding the controls on organic matter mineralization has long been a focus of terrestrial and aquatic biogeochemical studies because the long-term burial of organic carbon corresponds to the net accumulation of oxygen in the atmosphere, thus mediating the redox state of the Earth's biosphere and atmosphere (Berner 2003). Benthic-pelagic processes are tightly coupled in shallow coastal systems (Rowe et al. 1976), and sediment remineralization of organic matter provides a significant fraction of the inorganic nutrients required to support benthic and water-column primary production (Boynton & Kemp 1985, Hopkinson et al. 1999). Coastal sediments account for only a small fraction (7.5%) of the total area of marine sediments but support a disproportionately high amount of organic matter turnover (Wollast 1991; Middelburg et al. 1997).

High metabolic rates in coastal sediments deplete available oxygen, and the majority of organic matter mineralization proceeds via anaerobic metabolic pathways, mainly sulfate reduction (King 1988; Canfield 1993; Roden & Tuttle 1993; Roden et al. 1995). The mineralization of particulate organic matter (POM) in anaerobic sediments is achieved largely by the coupling of hydrolytic, fermentative and terminal metabolic processes (Fenchel & Findlay 1995). The microbes performing the terminal mineralization of organic matter to metabolic end products are limited largely to low molecular weight, labile dissolved organic carbon that can be transported across cellular membranes (< 600 Da, Weiss et al. 1991). Terminal metabolism thus requires the production of labile dissolved organic matter (Fenchel & Findlay 1995). Extracellular enzymatic hydrolysis initially converts particulate organic matter to high molecular weight dissolved organic matter, which is further hydrolyzed and fermented to labile dissolved organic matter and fermentation end products (Fenchel & Findlay 1995; Arnosti et al 1994; Burdige et al. 2000). Labile dissolved organic matter, which includes compounds such as

volatile fatty acids (VFAs) and amino acids, is available for terminal metabolism (Fenchel & Findaly 1995; Sørensen et al. 1981; Wellsbury & Parkes 1995).

Despite the importance of DOM as an intermediate in the degradation of organic matter, relatively little is known about DOM dynamics in estuarine sediments. In **CHAPTER 4**, I document seasonal and spatial patterns of DOC and DON along with, and in relation to, several other biogeochemical variables in shallow intertidal estuarine sediments at eight sites in coastal South Carolina and Georgia. Sediment porewater profiles were measured in porewater equilibration samplers to obtain seasonal steady-state inventories of DOC, DON, ammonium (NH_4^+), nitrate+nitrite (NO_x), phosphate (PO_4^{3-}), dissolved inorganic carbon (DIC), reduced iron (Fe^{2+}), chloride (Cl^-), sulfate (SO_4^{2-}), hydrogen sulfide (HS^-) and methane (CH_4) at sites across gradients in salinity in several estuarine systems. A large data set of over 700 individual profiles was obtained. A more limited amount of sediment solid phase particulate organic carbon (POC) and nitrogen (PON) pool size determinations and SO_4^{2-} reduction (SR) rate measurements were also made. This study provides a comprehensive system-scale description of sediment biogeochemistry with emphasis on DOC and DON in intertidal creek-bank environments. Rather than focus on metabolic pathways and nutrient and organic matter dynamics at any one site, I chose to evaluate patterns at the system-scale level. A site that appears to receive septic inputs from the adjacent residential community is discussed in more detail.

The coupling between hydrolytic/fermentative production and terminal metabolic consumption is further explored in **CHAPTER 5**. Temperature and substrate availability are primary drivers of microbial activity (Pomeroy & Wiebe 2001) and may regulate rates of organic matter mineralization (Westermann 1996). Rates of sulfate reduction in coastal sediments, for instance, generally follow a seasonal pattern similar to that of temperature (King 1988; Westrich

& Berner 1988). Although sulfate reduction and other anaerobic terminal metabolic processes depend on the labile organic carbon substrates produced by fermentation, the temperature dependence of organic carbon production via hydrolysis and fermentation and consumption via terminal metabolism may be quite different. In this study, I explore the temperature responses of hydrolysis/fermentation and terminal metabolism within a microbial community with slurry incubations. I then investigate the temperature responses of microbial communities adapted to *in situ* temperatures with flow-through bioreactor experiments conducted using sediments collected four times over the course of a year.

LITERATURE CITED

American Rivers. 2002. America's most endangered rivers of 2002. Washington, DC.

Arnosti, C., D.J. Repeta and N.V. Blough. 1994. Rapid bacterial-degradation of polysaccharides in anoxic marine systems. Geochimica et Cosmochimica Acta 58: 2369-2652.

Berner, R.A. The long-term carbon cycle, fossil fuels and atmospheric composition. Nature 426: 323-326.

Boynton W.R. and W.M. Kemp. 1985. Nutrient regeneration and oxygen consumption by sediments along an estuarine salinity gradient. Mar. Ecol. Prog. Ser. 23: 45-55.

Burdige, D.J., A. Skoog and K. Gardner. 2000. Dissolved and particulate carbohydrates in contrasting marine sediments. Geochimica et Cosmochimica Acta 64: 1029-1041.

Canfield, D.E. 1993. In *Interactions of C, N, P and S Biogeochemical Cycles*, R. Wollast, L. Chou, F. Mackenzie, Eds. Springer, Berlin, pp. 333-363.

Fenchel, T.M. and B.J. Findlay. 1995. *Ecology and evolution of anoxic worlds*. Oxford University Press, Oxford.

Fisher, D.C. and M. Oppenheimer. 1991. Atmospheric nitrogen deposition and the Chesapeake Bay estuary. Ambio 20: 102-108.

Gleick, P.H. 2003. Water use. Annual Review of Environment and Resources 28: 275-314.

Hamilton, P. 1990. Modeling salinity and circulation for the Columbia River Estuary. Progress in Oceanography 25: 113-156.

Hopkinson, C.S., A.E. Giblin, J. Tucker and R.H. Garritt. 1999. Benthic metabolism and nutrient cycling along an estuarine salinity gradient. Estuaries 22: 825-843.

Howarth, R.W., G. Billen, D. Swaney, A. Townsend, N. Jaworski, K. Lajtha, J. A. Downing, R. Elmgren, N. Caraco, T. Jordan, F. Berendse, J. Freney, V. Kudeyarov, P. Murdoch, and Zhu Zhao-Liang, 1996. Regional nitrogen budgets and riverine N & P fluxes for the drainages to the North Atlantic Ocean: Natural and human influences. *Biogeochemistry* 35: 75-139.

Howarth, R.W. 1998. An assessment of human influence on fluxes of nitrogen from the terrestrial landscape to the estuaries and continental shelves of the North Altantic Ocean. *Nutrient Cycling in Agroecosystems* 52: 213-233.

King, G.M. 1988. Patterns of sulfate reduction and the sulfur cycle in a South Carolina salt marsh. Limnol. Oceanogr. 33: 376-390.

Knowles, N. 2002. Natural and management influences on freshwater inflows and salinity in the San Francisco Estuary at monthly to interannual scales. Water Resources Research 38: 1289.

Middelburg, J.J., K. Soetart and P.M.J. Herman. 1997. Empirical relationships for use in global diagenetic models. Deep-Sea Res. 44: 327-344.

National Oceanic and Atmospheric Administration. 1996. NOAA's estuarine eutrophication survey. Volume 1: South Atlantic Region. Office of Ocean Resources Conservation Assessment, Silver Spring, Maryland.

Nixon, S.W. 1995. Coastal marine eutrophication: a definition, social causes, and future concerns. *Ophelia* 41:199-219.

Nixon, S.W., J.W. Ammermann, L.P. Atkinson, V.M. Berounsky, G.B Billen, W.C. Boicourt, W.R. Boynton, T.M. Church, D.M Ditoro, R. Elmgren, J.H. Garber, A.E. Giblin, R.A. Jahnke, N.J.P. Owens, M.E.Q. Pilson and S.P. Seitzinger. 1996. The fate of nitrogen and phosphorus at the land-sea margin of the North Atlantic Ocean. Biogeochemistry 35: 141-180.

Paerl, H.W., J.L. Pinckney, J.M. Fear and B.L. Peierls. 1998. Ecosystem responses to internal and watershed organic matter loading: Consequences for hypoxia in the eutrophying Neuse River Estuary, North Carolina, USA. *Marine Ecology Progress Series* 166: 17-25.

Pomeroy, L.R. and W.J. Wiebe. 2001. Temperature and substrates as interactive limiting factors for marine heterotrophic bacteria. Aquatic Microbial Ecology 23: 187-204.

Roden, E.E. and J.H. Tuttle. 1993. Inorganic sulfur turnover in oligohaline estuarine sediments. Biogeochemistry 22: 81-105.

Roden, E.E., J.H. Tuttle, W.R. Boynton and W.M. Kemp. 1995. Carbon cycling in mesohaline Chesapeake Bay sediments 1. POC deposition rates and mineralization pathways. Journal of Marine Research 53: 799-819.

Rowe GT, Clifford CH & Smith KL (1976) Benthic nutrient regeneration and its coupling to primary productivity in coastal waters. Nature 255: 215-217.

Sørensen, J. D. Christensen and B.B. Jørgensen. 1981. Volatile fatty acids and hydrogen as substrates for sulfate-reducing bacteria in anaerobic marine sediment. Applied and Environmental Microbiology 42: 5-11.

Turner, R.E. and N.N. Rabalais. 1991. Changes in Mississippi River water-quality this century. Bioscience 41: 140-147.

Van Breemen, N., E.W. Boyer, C.L. Goodale, N.A. Jaworski, K. Paustian, S.P. Seitzinger, K. Lajtha, B. Mayer, D. Van Dam, R.W. Howarth, K.J. Nadelhoffer, M. Eve and G. Billen. 2002. Where did all the nitrogen go? Fate of nitrogen inputs to large watersheds in the northeastern U.S.A. *Biogeochemsitry* 57/58: 267-293.

Vitousek, P.M., H.A. Mooney, J. Lubchenco and J.M. Melillo. 1997. Human domination of Earth's ecosystems. Science. 277: 494-499.

Weiss, M.S., U. Abele, J. Weckesser, W. Welte, E. Schiltz and G.E. Shultz. 1991. Molecular architecture and electrostatic properties of a bacterial porin. Science. 1627-1630.

Westermann, P. 1996. Temperature regulation of anaerobic degradation of organic matter. World Journal of Microbiology and Biotechnology 12: 497-503.

Wellsbury, P. and R.J. Parkes. 1995. Acetate bioavailability and turnover in estuarine sediment. FEMS Microbiology Ecology 17: 85-94.

Westrich, J.T. and R.A. Berner. 1988. The effect of temperature on rates of sulfate reduction in marine sediments. Geomicrobiology Journal 6: 99-117.

Wigley, T.M.L. 2005. The climate change commitment. Science 307: 1766-1769.

Wollast, R. 1991. in *Ocean Margin Processes in Global Change*, R.F.C. Mantoura, J.M. Martin, R. Wollast, Eds. Wiley, Chichester, pp. 365-381.

CHAPTER 2

THIRTY YEARS OF LAND USE CHANGE AND NUTRIENT AND ORGANIC CARBON EXPORT IN THE ALTAMAHA RIVER WATERSHED[1]

[1]Weston, N. B., J.T. Hollibaugh and S.B. Joye. Prepared for submission to *Water Research*

ABSTRACT

Thirty years of water quality monitoring data from the United States Geological Survey conducted at fifteen stations in the Altamaha River watershed was examined and related to population density and agricultural land use. Concentrations and sub-watershed specific export of ammonium (NH_4^+), nitrite+nitrate (NO_x), phosphorus (P) and organic carbon (OC) were determined for the Ocmulgee, Oconee, Ohoopee and Altamaha Rivers, and patterns over time, with variation in river discharge and temperature were examined. Population densities increased in the Altamaha River watershed from 1970 to 2000, most notably in the upper portions of the watershed near the cities of Atlanta and Athens, while agricultural land use declined throughout the watershed. NO_x and P concentrations were highest in the 2nd and 3rd order Ocmulgee and Oconee Rivers in the upper Altamaha River watershed. NO_x concentrations increased with time at many of the stations during the study period, and inorganic nitrogen export from rivers was related to population density. Agricultural land use apparently played a lesser role in nutrient delivery to rivers than urban and suburban landscapes, but may have been more important in OC loading to rivers. OC export to rivers was highest in the coastal plain, characterized by extensive freshwater wetlands. Altered hydrology in the Altamaha River due to climate change and lakes created by the damming of rivers may also have influenced the delivery and processing of nutrients and organic carbon by rivers. P and OC concentrations dropped significantly over three decades at many of the stations. The overall average load from the 36,259 km^2 Altamaha River watershed to the coastal zone during the study period was 1.1, 5.6, 0.8 and 255 kmol km^{-2} yr^{-1} for NH_4^+, NO_x, P and OC, respectively. This analysis of thirty years of water quality monitoring data indicates NO_x delivery to rivers is increasing

due to population growth in the Altamaha River watershed. Only wise management of growth, especially in the still largely undeveloped coastal zone of this watershed, will keep the Altamaha River estuary from being at risk of eutrophication.

INTRODUCTION

Changing land-use has altered the biogeochemical signatures and flow patterns of many rivers. Development within watersheds can impact both the river and coastal receiving waters (Howarth et al. 1996). Loading of nutrients and organic matter from rivers can cause and/or exacerbate eutrophication and result in harmful algal blooms and fish kills, reductions in water quality, disruptions of the heterotrophic/autotrophic balance and/or system-scale changes in production and trophic structure in estuaries (Nixon 1995; Vitousek et al. 1997; Paerl et al. 1998). Nitrogen loading to estuaries is of particular concern, as coastal waters are often nitrogen limited and increased nitrogen delivery can fuel excess production and lead to eutrophication (Nixon et al. 1996).

Human activities have greatly increased global nitrogen fixation via the Haber-Bosch process (Vitousek et al. 1997). On average about 20% of nitrogen delivered to landscapes from fertilization of agricultural land (Turner and Rabalais 1991), atmospheric deposition (Fisher and Oppenheimer 1991), direct human waste (Cole et al. 1993) and other sources is exported by rivers (Howarth 1998; Van Breemen et al. 2002). Nitrogen export has increased in many of the world's rivers due to these human activities (Howarth et al. 1996).

The Altamaha River in Georgia (Fig. 1) drains one of the largest basins on the East Coast (about 36,000 km^2). Although the watershed of the Altamaha remains relatively undisturbed, in recent years development pressure has increased in the basin. In 2002, the Altamaha River was

placed on the American Rivers Organization's list of most endangered rivers due to rapid population growth, increasing water withdrawal and reservoir construction (American Rivers 2002). The National Oceanic and Atmospheric Administration (1996) described the Altamaha River estuary as currently minimally impacted but likely to exhibit increasing signs of eutrophication due to anthropogenic activities in the watershed.

Despite the size and importance of the Altamaha River watershed and estuary, relatively little is known about the effects of changing land use in the watershed on the rivers and loading to the coastal zone. In this paper we analyze three decades of nutrient and organic carbon data from fifteen United States Geological Survey water quality monitoring stations in the Altamaha River and its major tributaries. Trends in population and land use within the watershed are also examined. Long-term patterns and controls of river nutrient and organic carbon concentrations were investigated, and loading from the major sub-watersheds to the Altamaha River was estimated.

METHODS

Study Site

The Altamaha River watershed lies entirely within the state of Georgia and drains 36,259 km^2, about one quarter of the state's land area (Fig. 2.1). Two main 3rd order tributaries, the Ocmulgee and Ohoopee Rivers, originate as 2nd order rivers in the Piedmont foothills of the Appalachian Mountains more than 600 km from the coast and about 200 m above sea-level, and join near Lumber City, GA to form the Altamaha River. The lower portions of the Ocmulgee and Oconee, the smaller 2nd order 'blackwater' Ohoopee and Little Ocmulgee Rivers, and the 4th order Altamaha River transit the coastal plain. Discharge from the Altamaha River averages

about 400 m^3 s^{-1}. Long term mean discharge exhibits a seasonal maximum in spring and a minimum in late summer and fall.

There are three major dams in the Altamaha River watershed that are operated for hydroelectric power generation (Fig. 2.1). Two dams, the Sinclair and Lloyd Shoals dams, creating Lakes Sinclair and Jackson on the Oconee and Ocmulgee Rivers, respectively, were completed before the time period of this study. The Wallace Dam on the Oconee River was completed in 1980, forming Lake Oconee. Total area of the lakes is about 150 km^2, with Lake Jackson on the Ocmulgee River accounting for only about 12% of the total.

Water Quality, Discharge and Precipitation

Nutrient, organic carbon, temperature and flow data were obtained from water quality stations in the Altamaha River watershed from the USGS website (www.usgs.gov). Six variables of interest were chosen; water temperature (USGS variable code 00010), river discharge (00061), ammonium (00610), nitrate+nitrite (00630), phosphorus (00665) and organic carbon (00680). Analyses were conducted on unfiltered water, and phosphorus and carbon measurements include both dissolved and particulate forms (see USGS website for methods details; www.usgs.gov). Data were included in the present analysis if the average gauged stream discharge exceeded 20 m^3 sec^{-1} (approximately 5% of the Altamaha River discharge), if 200 or more measurements of each variable of interest were made, and if monitoring was conducted through at least 1999. Separate records of long-term river discharge data (daily averages) from the USGS were also obtained from four stations in each of the sub-watersheds (Ocmulgee, Oconee, Ohoopee and Altamaha; Table 2.1). Watershed drainage area and elevation above sea level for each station (when available) was obtained from the USGS web site (www.usgs.gov).

Distance of each station up-watershed from the coast was estimated using GIS. Additionally, long-term daily precipitation data was obtained from the National Climate Data Center (NCDC) website (www.ncdc.noaa.gov) for five meteorological monitoring stations in different regions of the Altamaha River watershed.

Average water temperature, discharge (Q), ammonium (NH_4^+), nitrate+nitrite (NO_x), phosphorus (P) and organic carbon (OC) were compared across sites using analysis of variance (ANOVA) and Tukey's "honestly significantly different" test based on the studentized range distribution. Trends in NH_4^+, NO_x, P and OC concentration with time, discharge (natural log transformed) and temperature at each site were determined with multivariate regressions.

Average loading rates of nutrients and OC (kmol d^{-1}) were calculated from discrete concentration and stream discharge measurements at six USGS stations in the Altamaha River watershed [Table 1, stations denoted by (L)]. Sub-watershed average yields per area of watershed (kmol km^{-2} yr^{-1}) were then calculated from the loading rates and drainage area (Table 2.1). For stations 02215500, 02223600 and 02226010 that were down-river from other stations for which loading was calculated, the load and the land area of the up-rivers station(s) were subtracted to determine the areal loading from the specific sub-watershed.

Long-term trends in mean daily discharge (natural log transformed) from each of the major sub-watersheds and for the total Altamaha River watershed for the available period of record (Table 2.1) and from 1970 to 2002 were evaluated. A linear best-fit was applied to natural log-transformed mean daily discharge. Trends in precipitation were assessed using linear regressions against natural log-transformed precipitation data. In addition, whole-watershed precipitation was estimated assuming each precipitation station represented an equal fifth of the

watershed area, and total water delivery (m^3 s^{-1}) was calculated using the watershed area (Table 2.1).

Land Use

Data on population density and land area by county were obtained from the 1970 and 2000 United States Census (www.census.gov, U.S. Census Bureau 2003). Farm acreage and the distribution of agricultural land use by county for the Altamaha River watershed in 1969 and 2002 were obtained from the U.S. Department of Agriculture (1974, 2004). Sub-watershed specific population densities and agricultural land use [for stations designated (L); Table 2.1] were also estimated based on the ratio of each county situated within the sub-watershed. Note that these calculations could not account for population density or agricultural land use heterogeneity within any single county and even distributions were assumed, which may result in some error for counties that did not lie entirely within a single sub-watershed.

RESULTS

Fourteen USGS water quality monitoring stations fit the criteria for inclusion in this study (Table 2.1, Fig. 2.1), and one station (02225500) on the Ohoopee River was added despite a lower number of records to include this river in the watershed analysis. All stations were on the Ocmulgee, Oconee, Ohoopee or Altamaha Rivers with the exception of station 02208005 which was on the Yellow River, a tributary of the Ocmulgee. Seven of the water quality stations had continuous records from the 1970s or earlier through 2001 or later. Eight of the stations had gaps in sample collection, usually from 1994 to 1999 (Table 2.1).

Discharge and Precipitation

Long-term discharge data at the four water discharge stations indicated a significant decrease ($p < 0.001$) in discharge in all rivers for the available period of record (Table 2.1), as well as from 1970 to 2002 (Fig. 2.2). Discharge decreased by 1.12, 1.43, 0.26 and 4.15 $m^3 s^{-1}$ per year in the Oconee, Ocmulgee, Ohoopee and Altamaha Rivers, respectively, from 1970 to 2002 (Fig. 2.2).

Daily precipitation decreased significantly at two of the five NCDC meteorological monitoring stations in the Altamaha River watershed. Decreases of 2.8 and 1.9 mm yr^{-1} were observed at stations 090435 (P) and 092318 (P), respectively ($p < 0.05$) in the upper Oconee and upper Ocmulgee sub-watersheds. Estimated whole-watershed precipitation declined significantly ($p < 0.001$) from 1970 to 2002, resulting in a 4.13 $m^3 s^{-1}$ per year decrease in water delivery to the watershed (Fig. 2.1).

Station and Watershed Averages

Average river discharge at the USGS stations increased significantly down-watershed in the Oconee, Ocmulgee and Altamaha Rivers (Table 2.2, Fig. 2.3). Mean river temperature increased down-river, with the coolest sites at the head of the Ocmulgee and Oconee watersheds and the warmest water in the Altamaha River (Fig. 2.3, Table 2.2). Temperature appears to have been correlated with river discharge [$T = 1.2 \ln(Q) + 13.5$, $r^2 = 0.74$, $p < 0.01$] more than with distance from the coast.

Mean NH_4^+ concentrations were variable from station to station in the Ocmulgee and Oconee Rivers (Table 2.2). However, there was a significant drop in average NH_4^+ values down-

river (Table 2.2, Fig. 2.3). When all stations were grouped by river, mean NH_4^+ was lowest in the Altamaha and highest in the Ohoopee and Upper Oconee Rivers (Table 2.3).

The furthest up-stream Oconee River station exhibited the overall highest average NO_x concentration, and the Ohoopee River had the lowest average NO_x (Table 2.2). Grouped by river, the upper Oconee and both portions of the Ocmulgee River had the highest average NO_x (Table 2.3). This pattern resulted in a significant increase in NO_x concentrations with increasing distance from the coast (Fig. 2.3).

P concentrations were somewhat variable within the tributaries of the Altamaha River (Table 2.2). When grouped by river, P was highest in the lower Ocmulgee and upper Oconee and lowest in the Ohoopee and Altamaha Rivers (Table 2.3). However, there was no significant trend with distance in the rivers (Fig. 2.3). OC concentrations increased significantly down-river (Fig. 2.3), and were highest in the Ohoopee River, followed by the Altamaha River and lowest in the upper portions of the Oconee and Ocmulgee Rivers (Tables 2.2 & 2.3).

Correlations Between Nutrient and Organic Carbon Concentrations and Time, Temperature and River Discharge

Changes in nutrient and OC concentrations over time and with temperature and river discharge at each of the fifteen sites were explored. Generally little of the variation in NH_4^+ concentration could be explained by these variables (Table 2.4). NH_4^+ concentration decreased significantly with time at seven of the stations, and NH_4^+ decreased with discharge at nine of the stations. NH_4^+ decreases of up to about 0.8 $\mu M\ yr^{-1}$ were observed, though generally decreases were less (Table 2.4). An increase of about 0.2 $\mu M\ yr^{-1}$ was measured in the up-stream station on the Oconee River.

NO_x concentrations increased from the 1970s through the 1990s at many of the USGS stations in the Ocmulgee, Oconee and Altamaha Rivers (Table 2.5). Increases of over 1.0 μM yr^{-1} NO_x were documented in the upper portions of the Ocmulgee and Oconee Rivers. There appeared to be some attenuation of this increase further down-river, with smaller net increases of approximately 0.5, 0.2 and 0.2 μM yr^{-1} at the downriver stations of the Ocmulgee (02215500), Oconee (02223600) and Altamaha (02226010) Rivers, respectively (Table 2.5).

River temperature and discharge were also significantly correlated with NO_x at many of the stations. NO_x concentrations decreased with increasing temperature and discharge at eight of the stations (Table 2.5). Together with long-term changes over time, these variables explained at least 12% and up to 60% of the variation in NO_x concentrations in the Altamaha River watershed.

P concentrations decreased significantly with time at all stations in the Ocmulgee River, from 0.06 to 0.2 μM yr^{-1} (Table 2.6). River discharge also appeared to influence P concentrations at several of the sites, although not in a consistent manner. Multivariate regressions against date, water temperature and river discharge explained more than 20% of the variance in P at only three stations (in the Ocmulgee watershed) and, while significant at the majority of sites, did not explain a great deal of the variation in P concentration at most sites.

Decreasing OC concentrations over time were also observed at most of the sites in the Ocmulgee watershed, as well as two in the Oconee and one in the Altamaha River (Table 2.7). OC increased at warmer temperatures at several of the stations. Discharge, however, appeared to be the major control on OC concentrations at many of the monitoring sites. Concentrations of OC increased significantly with increasing river discharge at all but three of the sites, with increases of 15 to nearly 200 μM OC $(m^3\ sec^{-1})^{-1}$ (Table 2.7).

Nutrient and Organic Carbon Loading

The average volume of water discharged to the ocean from the Altamaha River [using long-term daily discharge data from USGS station 02226000 (Q)] was 382 m^3 sec^{-1} from 1974 through 2003. Of this total volume, 83.5 % was accounted for by discharge from the Ocmulgee, Oconee and Ohoopee Rivers [at USGS stations 02215500 (Q), 02223500 (Q) and 02225500 (Q), respectively, Fig. 2.1] to the Altamaha River. The Ocmulgee and Oconee Rivers supplied the majority of water to the Altamaha River (40.4% and 35.7% of total Altamaha flow, respectively), with the Ohoopee River contributing an additional 7.4%. The contribution from the Oconee River may be slightly underestimated, as the USGS monitoring station furthest down-watershed [02215500 (Q)] is about 100 km from the confluence with the Ocmulgee (Fig. 2.1). By difference, the lower Oconee River, the Little Ocmulgee and other minor tributaries in the lower portion of the Altamaha River contribute about 63 m^3 s^{-1} of water on average to the total Altamaha River flow. Average discharge from USGS water quality monitoring stations in the major sub-watersheds agrees with the long-term discharge results, although slightly less (77%) of the total Altamaha River discharge is accounted for by discharge from the sub-watersheds (Table 2.8). The fractional area and fractional discharge of each sub-watershed (in relation the total Altamaha River watershed area and discharge) differ at most by 3%.

The average load of NH_4^+, NO_x, P and OC from the Altamaha River (USGS station 02226010) to the coastal zone was 107, 536, 82, and 24,608 kmol d^{-1}, respectively, from 1974 through 2003 (Table 2.8). Over 95% of the average inorganic nitrogen (NH_4^+ and NO_x) load in the Altamaha River was supplied by the major sub-watersheds (Table 2.8). The Ocmulgee River alone supplied 57% of the NO_x to the Altamaha River, in relative excess of the 38% water delivery from this river. In contrast, the Ohoopee River supplied only 2% of the NO_x and 20%

of the NH_4^+ load while accounting for 8% of the water delivery. Both the NH_4^+ and NO_x load from the Oconee River to the Altamaha River were in slight excess of the water delivery from this river (Table 2.8). 86% and 57% of the average P and OC load in the Altamaha River, respectively, was accounted for by loading from the Ocmulgee, Oconee and Ohoopee Rivers (Table 2.8). The relative contributions of P from the Ocmulgee and Oconee Rivers to the Altamaha River were generally slightly higher and the relative contributions of OC were substantially lower than the relative water delivery from these rivers (Table 2.8).

Average loading rates per unit of watershed area reflected the sub-watershed trends in nutrient and OC loading. NO_x loading from the upper Ocmulgee River exceeded 12 kmol km^{-2} yr^{-1} (Fig. 2.4). The highest areal NH_4^+ loading was in the Ohoopee River watershed, and the lower portion of the Altamaha River watershed had the lowest areal NH_4^+ loading rate. The Ohoopee and Altamaha Rivers had the lowest areal P and NO_x loading rates, and the highest areal OC loading rates (Fig. 2.4). Total export from the Altamaha River per area of watershed was 1.1, 5.6, 0.8 and 255 kmol km^{-2} yr^{-1} of NH_4^+, NO_x, P and OC, respectively (Fig. 2.4).

Land Use

Population density was greatest near the metropolitan area of Atlanta and the cities of Macon and Athens, GA in both 1970 and 2000 (Fig. 2.5). All counties in the Altamaha River watershed experienced population growth between 1970 and 1990, with growth ranging from 4% to over 700%. The largest increases were concentrated in the upper portion of the Ocmulgee and Oconee watersheds, largely between Atlanta and Athens (Fig. 2.5). There was a doubling in population in only one county in the lower portion of the Altamaha watershed in three decades, despite the low starting population densities in 1970 (Fig. 2.5).

Sub-watershed specific population density estimates were lowest in the Ohoopee, Altamaha and lower Oconee watersheds, ranging from 10 to 15 individuals per km^{-2} in 1970, and increased by only 3 to 5 individuals km^{-2} in 2000 in all three of these sub-watersheds (Fig. 2.4). Density estimates and increases in density were larger in the upper Oconee and both Ocmulgee sub-watersheds. Density in 1970 was estimated at 27, 35 and 98 individuals km^{-2} in the upper Oconee, lower Ocmulgee and upper Ocmulgee sub-watersheds, respectively, and increased to 58, 46 and 238 individuals km^{-2} in 2000, respectively. Total average Altamaha watershed population density doubled from 35 individuals km^{-2} in 1970 to 70 individuals km^{-2} in 2000 (Fig. 2.4).

Agricultural land use by county ranged from less than 1% to over 75% in the Altamaha River watershed (Fig. 2.6). Every county with one exception lost farm acreage from 1969 to 2000 resulting in an overall decrease from 42.3% agriculture land use in 1969 to 28.2% in 2000, a decline of about one third (Fig. 2.4). Changes in agricultural land use by county from 1969 to 2002 ranged from a gain of 54 % to losses of almost 90 % of farm acreage (Fig. 2.6). However, estimated sub-watershed specific losses of agricultural land use had a much smaller range and no discernable pattern within the larger watershed (30 to 40 % loss in three decades; Fig. 2.4). The Ohoopee and Altamaha sub-watersheds had the highest estimated agricultural land use, and the upper Ocmulgee and lower Oconee had the lowest agricultural land use in both 1969 and 2002 (Fig. 2.4).

Land Use and Loading

The relationship between average sub-watershed specific estimated population densities and average riverine inorganic nitrogen ($NH_4^+ + NO_x$) export per area of watershed is significant

($p = 0.014$) and has a slope of 0.062 kmol N $person^{-1}$ yr^{-1} (Fig. 2.7). There was also a significant negative correlation between sub-watershed specific estimated agricultural land use and P loading [P Load = -0.0453 (% Agricultural Land Use) + 2.53, $R^2 = 0.81$, $p = 0.015$]. Although sub-watershed specific riverine P export was not significantly related to average sub-watershed population densities ($p = 0.14$), this trend was caused by a single sub-watershed (Lower Oconee, see Fig. 2.4). When this station was removed the relationship became significant [P = 0.0041 (Population) + 0.54, $R^2 = 0.97$, $p < 0.01$].

DISCUSSION

Development, increasing population, and changes in land use have altered the delivery of nutrients and organic matter to rivers and estuaries globally (Pickney et al. 2001). The watershed of the Altamaha River remains relatively undeveloped compared with most other rivers on the East Coast of the United States. This is especially true of the coastal portion of the Altamaha River watershed. On average globally, about 60% of the world's population lives within 100 km of the ocean (Vitousek et al. 1997). In the Altamaha River watershed the highest population densities are in the upper portion of the watershed near metropolitan Atlanta and the cities of Athens and Macon, GA (Figs. 2.4 & 2.5). Although every county in the watershed experienced population growth from 1970 to 2000, growth was also generally greatest in these same inland counties, markedly so in the upper Ocmulgee sub-watershed. Despite relatively low population densities in 1970 in the lower portion of the Altamaha River watershed, population growth was generally less than 50% in these areas (Figs. 2.4 & 2.5).

Over three decades of water quality monitoring by the United States Geological Survey have demonstrated spatial and temporal trends in the nutrient and organic carbon concentrations

of the Altamaha River watershed. Accompanying thirty years of population growth in the upper Altamaha River watershed was a significant long-term increase in nitrate concentration at many of the water quality monitoring stations in the Ocmulgee, Oconee and Altamaha Rivers (Table 2.5). Average NO_x concentrations over the study period are highest in the Ocmulgee River, followed by the Oconee River, and lowest in the Ohoopee River (Tables 2.2 & 2.3), creating a significant down-stream gradient of decreasing NO_x concentrations (Fig. 2.3). The increases with time are greatest (> 1 $\mu M\ yr^{-1}$) in the upper portions of the Ocmulgee and Oconee, and appear to be somewhat attenuated in the lower watershed (Table 2.5).

In the Altamaha River watershed, loading rates of NO_x per area of watershed were highest in the Ocmulgee and Oconee Rivers, especially in the upper Ocmulgee (Fig. 2.4). The relationship between sub-watershed specific population density and areal inorganic nitrogen ($NO_x + NH_4^+$) loading from these sub-watersheds was significant (Fig. 2.7). Agricultural land use was not correlated with riverine NH_4^+ loading, and was negatively correlated with NO_x loading (data not shown). This is likely due in large part to the inverse relationship between population density and agricultural land use in the Altamaha River watershed. Furthermore, increasing population density and decreasing agricultural land use (Figs. 2.4 & 2.5) are accompanied by increasing NO_x concentrations during the study period at many of the USGS stations in Altamaha River watershed (Table 2.5). This suggests that differences in inorganic nitrogen export in the rivers of the Altamaha River watershed was due largely to activities associated with higher human population densities, rather than with agricultural land use.

Sewage inputs associated with human populations (Cole et al. 1993), atmospheric deposition (Fisher and Oppenheimer 1991) and fertilizer use (Turner and Rabalais 1991) in watersheds associated with human activities may all increase nitrogen inputs to rivers. Howarth

et al. (1996) estimated major anthropogenic nitrogen inputs to watersheds in the Southeast United States to be 73, 84, 26 and 32 kmol N km^{-2} yr^{-1} from atmospheric deposition, fertilization, crop fixation and import of food products, respectively, for a total of 215 kmol N km^{-2} yr^{-1} (Howarth et al. 1996). Inorganic nitrogen export from the entire Altamaha River watershed to the coastal ocean averaged 6.7 kmol N km^{-2} yr^{-1} (Fig. 2.4), or only about 3% of the estimated regional scale anthropogenic inputs from Howarth et al. (1996). It is important to note that in the current study, we have not accounted for dissolved organic nitrogen (DON) or particulate nitrogen (PN) which can account for a substantial portion of total nitrogen, and thus it is not currently possible to make a total watershed nitrogen budget for the Altamaha River.

Peierls et al. (1991) found a significant relationship between the NO_x export and population density in the world's rivers and Cole et al. (1993) attribute much of the increased NO_x export directly to human sewage inputs. Humans consume about 0.36 kmol N yr^{-1} per capita (Garrow et al. 2000). Nitrogen exports from sewage treatment plants were estimated to be 0.22 kmol N $person^{-1}$ yr^{-1} in watersheds of the Northeastern United States (van Breemen 2002), indicating some retention and loss of N during sewage processing. The relationship between inorganic nitrogen export and population density from the sub-watersheds of the Altamaha River watershed was 0.062 kmol N $person^{-1}$ yr^{-1} (Fig. 2.7). Human waste can therefore account for all of the inorganic nitrogen export by rivers in this system, and, on average, about 20% of the human waste produced in the Altamaha River watershed appears to have been exported by rivers as inorganic nitrogen. It is interesting to note that Howarth (1998) and Van Breemen et al. (2002) found that on average 20% of human waste-derived nitrogen inputs to watersheds of the North Atlantic Ocean were exported by rivers, although those studies estimated total nitrogen rather than inorganic nitrogen as in the current study.

P concentrations in the Altamaha River Watershed may also be associated with activities related to high population densities in the watershed. Concentrations were higher at stations in the Ocmulgee and Oconee Rivers than in the Ohoopee and Altamaha Rivers (Tables 2.2 & 2.3). P export per area of watershed was negatively correlated with agricultural land use, and positively related to population density (when the lower Oconee sub-watershed was removed from the regression). In addition, average P concentrations were significantly correlated with average NO_x concentrations [data from Table 2.2, $P = 0.0652 (NO_x) + 1.186$, $R^2 = 0.72$, $p < 0.01$]. This suggests a similar mechanism of NO_x and P delivery to the rivers in this system, and P export was largely controlled by human population densities. In the Mississippi River basin, Lurry and Dunn (1997) found a relationship between P export and population density of 1.72 kmol km^{-2} yr^{-1} per 100 persons, and no significant relationship with the area of watershed in cropland. This is considerably higher than the 0.41 kmol km^{-2} yr^{-1} per 100 persons measured in the Altamaha River watershed during this study. Decreasing P concentrations during the three decades of monitoring at about half of the stations, and notably all of the Ocmulgee River stations (Table 2.6) suggest that phosphorus abatement initiatives (Litke 1999) may have decreased P input from urbanized and suburbanized landscapes to rivers in this watershed.

Average nutrient concentrations in the Altamaha River (station 02226010) were comparable to other Southeast coast United States rivers surveyed by Dame et al. (2000), and total average inorganic nitrogen export from the Altamaha River was higher than all but the Cape Fear and Pee Dee Rivers, and equivalent to the Savannah River (Dame et al. 2000). Howarth et al. (1996) estimated P export of 1 kmol km^{-2} yr^{-1} from the Southeast coast of the United States, which agrees with the 0.85 kmol km^{-2} yr^{-1} measured in the Altamaha River watershed (Fig. 2.4). In the Mississippi River watershed, Turner and Rabalais (2004) estimated export of 1.4 and 21.4

kmol km^{-2} yr^{-1} for P and NO_x, respectively. Export from the Altamaha River watershed (0.85 and 5.6 kmol km^{-2} yr^{-1}) were 60% and 26% of the Mississippi River export on a per area watershed basis, respectively (Fig. 2.4).

It is perhaps surprising that agricultural land use does not appear to play a more apparent role in delivery of nutrients to the rivers in the Altamaha River watershed, where up to 50 % of the land area of sub-watersheds was in farms. This may be due in part to relatively little variation in agricultural land use at the sub-watershed scale (Fig. 2.4), and some uncertainty about the amount of this agricultural land fertilized (presumably not the entirety of land categorized as farm acreage is fertilized). Concomitant decreases in NH_4^+, P and OC concentrations with time (Tables 2.4, 2.6 & 2.7) and agricultural land use (Fig. 2.4) during the study period may indicate some delivery of these constituents from agricultural landscapes. However, the relationships between agricultural land use and inorganic nitrogen ($NO_x + NH_4^+$) and P are significantly negative, suggesting that agriculture plays a relatively minor role in nutrient delivery to rivers in this system compared to areas of higher population density.

Agricultural land use may play a more significant role in OC delivery to the rivers in the Altamaha River watershed, although the relationship between sub-watershed specific agricultural land use and OC export is not significant ($p = 0.08$). Agricultural watersheds are often a major source of OC to rivers (Howarth et al. 1991). As mentioned, the lack of correlation between agricultural land use and OC export in this study may be a result of relatively little change in agricultural land use between sub-watersheds. Urbanized and suburbanized land and wetlands may also contribute substantial amounts of OC to rivers (Howarth et al. 1991, Hope et al. 1994), further masking the effects of agricultural loading. The distribution of forest cover in the Altamaha River watershed was not evaluated in this study, and forested landscapes can export

OC to rivers as well (Wahl et al. 1997). The dynamics of OC delivery to rivers, though largely controlled by hydrology as evidenced by the often strong relationship between river discharge and OC concentration (Table 2.7), can be more spatially and temporally variable than accounted for in this analysis (Hope et al. 1994; Warnken and Santschi 2004). Nevertheless, we expect that agriculture plays an important role in delivery of OC to rivers in the Altamaha River watershed due to the loss of soil organic content and higher rates of sediment erosion associated with agricultural land use (Lal 2002).

The hydrology of the Altamaha River watershed likely plays an important role in the delivery of nutrients and OC to the rivers, albeit one difficult to assess in this study. NO_x and NH_4^+ concentrations tended to be higher during periods of low discharge at most of the USGS monitoring stations (Tables 2.4 & 2.5), suggesting that inorganic nitrogen in the Altamaha River watershed was largely delivered through groundwater discharge as baseflow (Schilling and Zhang 2004). Increasing NO_x concentrations in the Upper Floridan aquifer have been documented in Georgia (Leeth et al. 2003), although the sites described in this paper were not within the Altamaha River watershed.

Hydrology in the Altamaha River watershed has been altered from its pristine condition through land use change, perhaps most notably by damming and the creation of three major lakes (two on the Oconee and one on the Ocmulgee, Fig. 2.1). Lakes may complicate nutrient and OC transport dynamics in the Altamaha River watershed as water movement slows and particles sink. It is important to note that both P and OC measurements include dissolved (reactive phosphate and dissolved organic carbon, respectively) and particulate components. Lakes can be a sink for particulate phosphorus through sedimentation, and a source of reactive phosphate via mobilization processes (James and Barko 2004).

It is difficult to assess the importance of landscape or in-stream processing of inorganic nutrients without direct rate measurements. The down-watershed gradients of decreasing inorganic N and P concentrations in the rivers (Fig. 2.3) may be due in part to uptake and transformations during transport to the rivers and by riparian biota, combined with dilution from less developed watersheds. NO_x concentrations are negatively correlated with temperature at most of the sites in the Altamaha River watershed (Table 2.5). This suggests that landscape and/or in-stream uptake and denitrification may play a role in attenuating NO_x concentrations on a seasonal basis (Groffman et al. 1996, Mulholland 2004).

Seitzinger et al. (2002) describe nitrogen removal in rivers as a function of the ratio of depth and time of travel, such that as the ratio of the water depth to the water transit time decreases, nitrogen is removed through denitrification more efficiently. The three lakes formed by dams on the Oconee and Ocmulgee Rivers cover about 150 km^2 combined (88% of which is in the Oconee River watershed), and it is likely that the depth to transit time decreases substantially in these lakes. It is interesting to note the substantial drop in NO_x from the two most up-river stations in the Ocmulgee and Oconee Rivers (02208005 and 02218000, respectively) to stations just down-stream from the lakes in each watershed (02210500 and 0223000, respectively; Table 2.2). Lakes formed by the damming of the Ocmulgee and Oconee Rivers may substantially alter the delivery of nutrients and OC, and is an area for further examination in this watershed.

The effects of climate change on export of nutrients and OC from watersheds are largely unknown. Declines in precipitation in the Altamaha River watershed have resulted in significant drops in water delivery from all of the major tributaries to the Altamaha River, and from the Altamaha River to the coastal zone (Fig. 2.2). Hope et al. (1994) suggest that decreased runoff

would result in lower OC delivery to rivers. It is tempting to suggest that decreasing OC at about half of the stations in the Altamaha River watershed (Table 2.7) may be due in part to lower runoff from the watersheds, especially in light of the strong hydrologic connection between OC and river discharge. However concomitant changes in land use in these same watersheds make this conclusion difficult.

Average OC export from the Altamaha River to the coastal zone was 255 kmol C km^{-2} yr^{-1} (Fig. 2.4), which is similar to the mean OC export (255.8 kmol C km^{-2} yr^{-1}) from a large number of temperate forest watersheds throughout the world, although variation between watersheds is high (Hope et al. 1994). OC export from the lower portion of the Altamaha and Ohoopee River sub-watersheds are higher than from the Oconee and Ocmulgee River sub-watersheds (Fig. 2.4), and more closely resembles the average OC export from wetlands of 556 kmol C km^{-2} yr^{-1} (Hope et al. 1994). These two sub-watersheds lie entirely within the coastal plain and drain extensive zones of freshwater wetlands, which likely contribute substantially to the overall load of OC in the Altamaha River.

SUMMARY AND MANAGEMENT IMPLICATIONS

Although the Altamaha River watershed remains undeveloped relative to other Southeastern U.S. watersheds, increasing population densities in the upper watershed are linked with increased inorganic nitrogen loading and possibly phosphorus loading. Agricultural land use is prevalent but decreasing throughout the watershed, and its role in nutrient loading to rivers is less clear but apparently minor compared with suburban and urban land use. Agriculture may, however, play a more important role in organic carbon export to rivers, along with organic carbon export from extensive wetlands in the lower portion of the watershed. Altered hydrology

in the Altamaha River watershed (lower river discharge due to climate change and lakes formed by the damming of rivers) likely plays a role in both the delivery and processing of nutrients and organic carbon in the watershed.

This study provides needed information on the status of the Altamaha River watershed, the links between land use and water quality, loading of nutrients and organic carbon from the Altamaha River to the coastal zone, and a framework for future investigations and management decisions. Although the Altamaha River and estuary appear to remain relatively undisturbed, increasing population in the past three decades has clearly made an impact. Poorly managed future population growth in the watershed, especially in the currently undeveloped coastal zone, will put the health of this important watershed and estuarine system at risk.

ACKNOWLEDGEMENTS

We thank the United States Geological Survey for making thirty years of monitoring data available. This research was supported by the National Science Foundation's Georgia Coastal Ecosystems Long Term Ecological Research Program (OCE 99-82133).

LITERATURE CITED

American Rivers. 2002. America's most endangered rivers of 2002. Washington, DC.

Cole, J.J. B.L. Peierls, N.F. Caraco and M.L. Pace. 1993. Nitrogen loading of rivers as a human-driven process. In: McDonnell, M.J. and S.T.A. Pickett (Eds). Humans as Components of Ecosystems: The Ecology of Subtle Human Effects and Populated Areas (pp 141-157). Springer Verlag, New York, NY.

Dame R., Alber, M., Allen, D., Mallin, M., Montague, C., Lewitus, A., Chalmers, A., Gardner, R., Gilman, C., Kjerfve, B., Pinckney, J., Smith, N. 2000. Estuaries of the south Atlantic coast of North America: Their geographical signatures. *Estuaries* 23: 793-819.

Fisher, D.C. and M. Oppenheimer. 1991. Atmospheric nitrogen deposition and the Chesapeake Bay estuary. Ambio 20: 102-108.

Garrow, J.S., W.P.T. James and A. Ralph. (Eds). 1999. Human nutrition and dietetics, 10th Edition. Churchill Livingstone, Edinburgh.

Groffman, P.M., G. Howard, A.J. Gold and W.M. Nelson. 1996. Microbial nitrate processing in shallow groundwater in a riparian forest. *J. Environ. Qual.* 25: 1309-1316.

Hope, D., M.F. Billett and M.S. Cresser. 1994. A review of the export of carbon in river water: Fluxes and processes. *Environmental Pollution* 84: 301-324.

Howarth, R.W., J.R. Fruci and D. Sherman. 1991. Inputs of sediment and carbon to an estuarine ecosystem: Influence of land use. 1991. *Ecological Applications* 1: 27-39.

Howarth, R.W., G. Billen, D. Swaney, A. Townsend, N. Jaworski, K. Lajtha, J. A. Downing, R. Elmgren, N. Caraco, T. Jordan, F. Berendse, J. Freney, V. Kudeyarov, P. Murdoch, and Zhu Zhao-Liang, 1996. Regional nitrogen budgets and riverine N & P fluxes for the drainages to the North Atlantic Ocean: Natural and human influences. *Biogeochemistry* 35: 75-139.

Howarth, R.W. 1998. An assessment of human influence on fluxes of nitrogen from the terrestrial landscape to the estuaries and continental shelves of the North Altantic Ocean. *Nutrient Cycling in Agroecosystems* 52: 213-233.

James, W.F. and J.W. Barko. 2004. Diffusive fluxes and equilibrium processes in relation to phosphorus dynamics in the upper Mississippi River. *River Research* 20: 473-484.

Lal, R. 2003. Soil erosion and the global carbon budget. Environment International. 29: 437-450.

Leeth, D.C., J.S. Clarke, S.D. Craigg and C.J. Wipperfurth. 2003. Ground-water conditions and studies in Georgia, 2001. United States Geological Survey, Water Resources Investigations Report 03-4032.

Litke, D.W. 1999. Review of phosphorus control measures in the United States and their effects on water quality. Water Resources Investigations Report 99-4007. U.S. Geological Survey, Denver, Colorado.

Lurry, D.L. and D.D. Dunn. 1997. Trends in nutrient concentration and load for streams in the Mississippi River Basin, 1974-94. United States Geological Survey, Water Resources Investigations Report 97-4223.

Mulholland, P.J. 2004. The importance of in-stream uptake for regulating stream concentrations and outputs of N and P from a forested watershed: evidence from long-term chemistry records for Walker Branch Watershed. *Biogeochemistry* 70: 403-426.

National Oceanic and Atmospheric Administration. 1996. NOAA's estuarine eutrophication survey. Volume 1: South Atlantic Region. Office of Ocean Resources Conservation Assessment, Silver Spring, Maryland.

Nixon, S.W. 1995. Coastal marine eutrophication: a definition, social causes, and future concerns. *Ophelia* 41:199-219.

Nixon, S.W., J.W. Ammermann, L.P. Atkinson, V.M. Berounsky, G.B Billen, W.C. Boicourt, W.R. Boynton, T.M. Church, D.M Ditoro, R. Elmgren, J.H. Garber, A.E. Giblin, R.A. Jahnke, N.J.P. Owens, M.E.Q. Pilson and S.P. Seitzinger. 1996. The fate of nitrogen and phosphorus at the land-sea margin of the North Atlantic Ocean. Biogeochemistry 35: 141-180.

Paerl, H.W., J.L. Pinckney, J.M. Fear and B.L. Peierls. 1998. Ecosystem responses to internal and watershed organic matter loading: Consequences for hypoxia in the eutrophying Neuse River Estuary, North Carolina, USA. *Marine Ecology Progress Series* 166: 17-25.

Peierls, B.L., N.F. Caraco, M.L. Pace and J.J. Cole. 1991. Human influence on river nitrogen. *Nature* 350: 386-387.

Pinckney J.L., Paerl H.W., Tester P, Richardson TL. 2001. The role of eutrophication and nutrient loading in estuarine ecology. *Environmental Health Perspectives* 109: 699-706.

Turner, R.E. and N.N. Rabalais. 1991. Changes in Mississippi River water-quality this century. Bioscience 41: 140-147.

U.S. Census Bureau. 2003. 2000 Census of Population and Housing, *Population and Housing Unit Counts* PHC-3-12, Georgia. Washington, DC.

U.S. Department of Agriculture. 1976. 1974 Census of Agriculture, *Georgia State and County Data, Volume One, Geographic Area Series, Part 10*. Washington, DC.

U.S. Department of Agriculture. 2004. 2002 Census of Agriculture, *Georgia State and County Data, Volume One, Geographic Area Series, Part 10.* Washington, DC.

Van Breemen, N., E.W. Boyer, C.L. Goodale, N.A. Jaworski, K. Paustian, S.P. Seitzinger, K. Lajtha, B. Mayer, D. Van Dam, R.W. Howarth, K.J. Nadelhoffer, M. Eve and G. Billen. 2002. Where did all the nitrogen go? Fate of nitrogen inputs to large watersheds in the northeastern U.S.A. *Biogeochemsitry* 57/58: 267-293.

Vitousek, P.M., H.A. Mooney, J. Lubchenco and J.M. Melillo. 1997. Human domination of Earth's ecosystems. Science. 277: 494-499.

Warnken, K.W. and P.H. Santschi. 2004. Biogeochemical behavior of organic carbon in the Trinity River downstream of a large reservoir lake in Texas, USA. *Science of the Total Environment* 329: 131-144.

Table 2.1. United States Geological Survey (USGS) and National Climate Data Center (NCDC) site numbers, latitude and longitude, year of record, number of records, average discharge, distance from ocean, elevation above sea level, and approximate (cumulative) drainage area of USGS water quality and discharge monitoring stations from which data was obtained for this study (see Fig. 1). (L) denotes station was used to determine sub-watershed loading rates, (Q) denotes sites for which long-term daily discharge data was obtained separately from water quality data, and (P) denotes NCDC precipitation monitoring stations.

USGS / NCDC Site Number		Longitude	Latitude	Year of Record	n	Q (m^3 sec^{-1})	Distance (km)	Elevation (m)	Drainage Area (km^2)
Upper Ocmulgee									
02208005[a]		-83.8807	33.4543	1974-2003	339	20.4	596	164.6	1,140
02210500		-83.8382	33.3079	1974-1994, 1999-2000	242	56.1	577	128.0	3,678
02212950	(L)	-83.6541	32.8699	1974-2001	291	70.6	511		5,776
092318	(P)	-83.8603	33.5967	1900-2004	33873				
Lower Ocmulgee									
02213700		-83.6030	32.6715	1970-2003	330	47.5	486	76.5	6,967
02214265		-83.5368	32.5426	1974-1994, 1999-2000	217	80.6	449		8,676
02215500	(L)	-82.6740	31.9202	1968-2003	346	150.7	232	26.7	13,416
02215500	(Q)	-82.6740	31.9202	1936-2002	24106	154.3	232	25.1	13,416
094170	(P)	-83.4722	32.2836	1900-2004	37488				
Upper Oconee									
02218000		-83.3265	33.8560	1974-2003	340	29.0	590	238.7	2,028
02223000	(L)	-83.2154	33.0896	1968-1994, 1996, 1999	275	85.3	425	70.3	7,640
090435	(P)	-83.3267	33.9483	1944-2004	21866				
Lower Oconee									
02223040		-83.1899	33.0293	1974-1996, 1999	251	72.7	411		7,640
02223600	(L)	-82.8582	32.4802	1974-2003	319	119.0	320	45.7	11,499
02223500	(Q)	-82.8946	32.5446	1900-2002	37528	136.6	313	45.7	11,499
092839	(P)	-82.9039	32.5403	1911-2002	32928				
Ohoopee									
02225500	(L)	-82.1773	32.0785	1968-1979, 1990-1994, 1999	89	32.4	194	22.5	2,875
02225500	(Q)	-82.1773	32.0785	1903-1907, 1937-2002	25522	28.1	194	22.5	2,875
Altamaha									
02225000		-82.3535	31.9391	1970-1994, 1999	258	315.7	176	18.7	30,043
02225990		-81.8384	31.6666	1974-1994, 1999	236	401.1	83		35,223
02226010		-81.7651	31.6235	1974-2003	324	392.6	79	9.1	35,223
02226160	(L)	-81.6054	31.4272	1974-1995, 1999	274	403.3	25		36,259
02226000	(Q)	-81.8279	31.6547	1931-2002	25933	382.1	83	7.5	35,223
093754	(P)	-81.9286	31.9364	1904-2004	35919				

Table 2.2. Means and ranges of temperature, discharge, ammonium, nitrate+nitrite, phosphorus, and organic carbon at USGS water quality monitoring stations. Sites that do not share the same in letter in 'Group' for each variable have statistically different means ($p > 0.05$, see text for description of statistical analyses).

USGS Site		Temp (°C)	Q (m^3 sec^{-1})	NH_4^+ (µM)	NO_x (µM)	P (µM)	OC (µM)
Upper Ocmulgee							
02208005	Mean	16.1	20.4	3.1	48.0	3.1	265
	Range	2.5 - 29.1	0.5 - 156	1.4 - 28.6	1.4 - 127.1	0.6 - 35.5	83 - 917
	Group	A	A	A	G	D	A
02210500	Mean	17.4	56.1	10.5	33.6	2.9	298
	Range	2.0 - 30.0	4.7 - 354	1.4 - 66.4	1.4 - 67.0	0.6 - 9.0	83 - 1342
	Group	AB	ABC	D	E	CD	A
02212950	Mean	19.0	70.6	3.7	33.6	2.5	296
	Range	3.2 - 36.0	3.9 - 484	0.7 - 42.9	1.4 - 71.4	0.6 - 16.1	83 - 1667
	Group	BC	ABC	A	E	BCD	A
Lower Ocmulgee							
02213700	Mean	19.2	47.5	10.3	47.8	5.0	385
	Range	3.5 - 34.0	6.6 - 102	1.4 - 109.0	1.4 - 160.0	0.7 - 45.0	83 - 1625
	Group	BC	AB	D	G	E	B
02214265	Mean	18.7	80.6	6.9	42.3	5.1	394
	Range	3.0 - 32.0	12.5 - 359	1.4 - 30.0	11.4 - 114.0	1.9 - 25.0	83 - 1000
	Group	BC	ABC	B	F	E	B
02215500	Mean	19.4	150.7	3.8	32.9	2.8	403
	Range	3.0 - 32.0	22.1 - 1121	1.4 - 64.0	1.4 - 72.0	0.7 - 8.0	83 - 1750
	Group	BC	D	A	E	BCD	B
Upper Oconee							
02218000	Mean	16.2	29	11.1	67.1	6.0	276
	Range	1.0 - 33.0	1.4 - 325	1.4 - 72.0	1.4 - 221.0	1.6 - 39.0	42 - 1208
	Group	A	AB	D	H	F	A
02223000	Mean	19.0	85.3	4.9	14.4	1.6	281
	Range	3.0 - 31.0	7.2 - 478	1.4 - 35.7	1.4 - 52.9	0.6 - 12.9	83 - 792
	Group	BC	BCD	AB	B	A	A
Lower Oconee							
02223040	Mean	18.9	72.7	7.3	16.0	2.6	311
	Range	3.0 - 31.0	5.8 - 521	1.4 - 33.0	1.4 - 56.0	0.7 - 9.0	83 - 1167
	Group	BC	ABC	BC	B	BCD	A
02223600	Mean	18.8	119	7.2	21.1	3.0	381
	Range	3.0 - 33.0	9.2 - 1157	1.4 - 50.0	4.3 - 48.0	0.7 - 7.0	83 - 1717
	Group	BC	CD	BC	CD	CD	B
Ohoopee							
02225500	Mean	17.4	32.4	9.1	7.0	2.2	799
	Range	3.0 - 30.0	0.7 - 286	1.4 - 121.0	1.4 - 36.0	0.7 - 8.0	125 - 1750
	Group	AB	AB	CD	A	AB	E
Altamaha							
02225000	Mean	19.3	315.7	3.0	24.3	2.8	429
	Range	4.0 - 31.0	42.2 - 1907	1.4 - 28.0	0.7 - 56.0	0.7 - 8.0	83 - 1500
	Group	BC	E	A	D	BCD	B
02225990	Mean	20.1	401.1	2.9	21.9	2.6	507
	Range	4.5 - 32.0	47.0 - 2496	1.4 - 16.0	1.4 - 76.0	0.7 - 9.0	83 - 1542
	Group	C	F	A	CD	BCD	C
02226010	Mean	20.4	392.6	3.8	22.4	2.7	663
	Range	5.0 - 32.0	40.2 - 2807	1.4 - 19.0	1.4 - 51.0	0.7 - 11.0	167 - 3000
	Group	C	F	A	CD	BCD	D
02226160	Mean	19.7	403.3	3.2	19.1	2.4	698
	Range	5.0 - 32.0	47.0 - 2541	0.7 - 16.0	1.4 - 49.0	0.7 - 11.0	83 - 1750
	Group	C	F	A	BC	BC	D

Table 2.3. Average concentrations of nutrients and organic carbon from all stations in each sub-watershed of the Altamaha River (data from Table 2). Sites that do not share the same in letter in 'Group' for each variable have statistically different means ($p > 0.05$).

Watershed		NH_4^+ (µM)	NO_x (µM)	P (µM)	OC (µM)
Upper Ocmulgee	Mean	5.35	39.20	2.83	284.28
	Group	B	C	B	A
Lower Ocmulgee	Mean	6.95	40.83	4.18	393.88
	Group	BC	CD	C	B
Upper Oconee	Mean	8.32	44.30	4.11	278.31
	Group	CD	D	C	A
Lower Oconee	Mean	7.22	18.89	2.85	350.45
	Group	C	B	B	B
Ohoopee	Mean	9.08	7.01	2.20	798.96
	Group	D	A	A	D
Altamaha	Mean	3.25	21.94	2.63	580.96
	Group	A	B	AB	C

Table 2.4. Multivariate regression coefficients and statistical significance of NH_4^+ concentration versus date, water temperature and the natural log of river discharge at several USGS water quality monitoring stations in four sub-watersheds of the Altamaha River. Average river discharge (Q) and number of observations included in the multivariate regression (n) are given for reference.

Watershed	USGS Site	Q (m^3 sec^{-1})	n	Date (μM yr^{-1})		Temperature (μM $°C^{-1}$)		Discharge [μM (m^3 sec^{-1})$^{-1}$]		Intercept		Overall Equation	
				coef.	p-value	coef.	p-value	coef.	p-value	coef.	p-value	R2	p-value
Upper Ocmulgee	02208005	20.4	337										
	02210500	56.1	232	-0.394	<0.001			-2.405	<0.001	33.147	<0.001	0.164	<0.001
	02212950	70.6	286	-0.105	0.001					7.715	<0.001	0.036	0.001
Lower Ocmulgee	02213700	47.5	257	-0.810	<0.001			-5.283	<0.001	63.382	<0.001	0.325	<0.001
	02214265	80.6	209	-0.283	<0.001	-0.254	<0.001	-3.862	<0.001	37.648	<0.001	0.328	<0.001
	02215500	150.7	321					-0.545	0.021	5.713	<0.001	0.017	0.021
Upper Oconee	02218000	29	327	0.183	<0.001	-0.646	<0.001	-4.398	<0.001	27.650	<0.001	0.294	<0.001
	02223000	85.3	244										
Lower Oconee	02223040	72.7	247	-0.182	<0.001			-1.537	<0.001	19.218	<0.001	0.223	<0.001
	02223600	119	313	-0.087	0.017	-0.150	0.001	-3.366	<0.001	27.654	<0.001	0.274	<0.001
Ohoopee	02225500	32.4	81	-0.580	0.001					27.502	<0.001	0.125	0.001
Altamaha	02225000	315.7	255	0.056	0.019					1.033	0.222	0.022	0.019
	02225990	401.1	235										
	02226010	392.6	320					-0.932	<0.001	8.873	<0.001	0.094	<0.001
	02226160	403.3	261					-0.655	<0.001	6.835	<0.001	0.068	<0.001

Table 2.5. Multivariate regression coefficients and statistical significance of NO_x concentration versus date, water temperature and the natural log of river discharge at several USGS water quality monitoring stations in four sub-watersheds of the Altamaha River. Average river discharge (Q) and number of observations included in the multivariate regression (n) are given for reference.

Watershed	USGS Site	Q (m^3 sec^{-1})	n	Date (μM yr^{-1})		Temperature (μM $°C^{-1}$)		Discharge [μM (m^3 sec^{-1})$^{-1}$]		Intercept		Overall Equation	
				coef.	p-value	coef.	p-value	coef.	p-value	coef.	p-value	R2	p-value
Upper Ocmulgee	02208005	20.4	338	1.309	<0.001	-0.365	0.003	-11.934	<0.001	33.595	<0.001	0.559	<0.001
	02210500	56.1	231			-1.138	<0.001	-1.934	0.030	60.341	<0.001	0.295	<0.001
	02212950	70.6	288			-0.583	<0.001	-3.063	<0.001	56.442	<0.001	0.151	<0.001
Lower Ocmulgee	02213700	47.5	257	1.034	<0.001					10.995	0.075	0.157	<0.001
	02214265	80.6	211	1.276	<0.001			-13.939	<0.001	55.021	<0.001	0.607	<0.001
	02215500	150.7	320	0.459	<0.001	-0.301	0.002	-12.740	<0.001	80.082	<0.001	0.488	<0.001
Upper Oconee	02218000	29	327	1.273	<0.001	0.406	0.004	-19.448	<0.001	69.260	<0.001	0.571	<0.001
	02223000	85.3	244			-0.527	<0.001	1.386	0.004	19.242	<0.001	0.256	<0.001
Lower Oconee	02223040	72.7	247			-0.514	<0.001			25.795	<0.001	0.152	<0.001
	02223600	119	314	0.197	<0.001			-2.349	<0.001	23.255	<0.001	0.129	<0.001
Ohoopee	02225500	32.4	67					-2.008	<0.001	12.076	<0.001	0.264	<0.001
Altamaha	02225000	315.7	254	0.402	<0.001	-0.176	0.029	-8.009	<0.001	56.599	<0.001	0.461	<0.001
	02225990	401.1	234	0.254	0.007	-0.299	0.002	-7.442	<0.001	59.808	<0.001	0.362	<0.001
	02226010	392.6	323	0.232	<0.001	-0.323	<0.001	-7.152	<0.001	59.067	<0.001	0.375	<0.001
	02226160	403.3	261	0.209	0.007	-0.316	<0.001	-8.345	<0.001	64.116	<0.001	0.456	<0.001

Table 2.6. Multivariate regression coefficients and statistical significance of P concentration versus date, water temperature and the natural log of river discharge at several USGS water quality monitoring stations in four sub-watersheds of the Altamaha River. Average river discharge (Q) and number of observations included in the multivariate regression (n) are given for reference.

Watershed	USGS Site	Q (m^3 sec^{-1})	n	Date (μM yr^{-1})		Temperature (μM $°C^{-1}$)		Discharge [μM (m^3 sec^{-1})$^{-1}$]		Intercept		Overall Equation	
				coef.	p-value	coef.	p-value	coef.	p-value	coef.	p-value	R2	p-value
Upper Ocmulgee	02208005	20.4	338	-0.151	<0.001			0.458	0.005	7.778	<0.001	0.199	<0.001
	02210500	56.1	230	-0.136	<0.001	-0.047	<0.001	0.285	0.005	7.556	<0.001	0.432	<0.001
	02212950	70.6	288	-0.060	<0.001			0.694	<0.001	2.107	0.008	0.178	<0.001
Lower Ocmulgee	02213700	47.5	257	-0.213	<0.001			-1.283	<0.001	18.364	<0.001	0.290	<0.001
	02214265	80.6	210	-0.105	<0.001			-1.895	<0.001	16.622	<0.001	0.361	<0.001
	02215500	150.7	320	-0.035	<0.001					4.235	<0.001	0.049	<0.001
Upper Oconee	02218000	29	327	0.077	<0.001			-1.979	<0.001	8.895	<0.001	0.188	<0.001
	02223000	85.3	245			-0.027	0.049	0.160	0.028	1.534	0.001	0.068	<0.001
Lower Oconee	02223040	72.7	244	-0.029	0.019	-0.028	0.044	-0.327	<0.001	5.350	<0.001	0.088	<0.001
	02223600	119	314										
Ohoopee	02225500	32.4	88	-0.040	0.006					3.407	<0.001	0.086	0.006
Altamaha	02225000	315.7	255										
	02225990	401.1	234	0.038	0.009					1.213	0.020	0.029	0.009
	02226010	392.6	323					-0.356	<0.001	4.688	<0.001	0.101	<0.001
	02226160	403.3	273					-0.362	<0.001	4.437	<0.001	0.100	<0.001

Table 2.7. Multivariate regression coefficients and statistical significance of OC concentration versus date, water temperature and the natural log of river discharge at several USGS water quality monitoring stations in four sub-watersheds of the Altamaha River. Average river discharge (Q) and number of observations included in the multivariate regression (n) are given for reference.

Watershed	USGS Site	Q (m^3 sec^{-1})	n	Date (μM yr^{-1})		Temperature (μM $°C^{-1}$)		Discharge [μM (m^3 sec^{-1})$^{-1}$]		Intercept		Overall Equation	
				coef.	p-value	coef.	p-value	coef.	p-value	coef.	p-value	R2	p-value
Upper Ocmulgee	02208005	20.4	331	-2.759	0.003	4.532	<0.001	63.564	<0.001	136.053	0.009	0.152	<0.001
	02210500	56.1	226										
	02212950	70.6	281	-5.847	<0.001	3.335	0.042	43.315	0.004	291.561	0.006	0.102	<0.001
Lower Ocmulgee	02213700	47.5	252	-10.180	<0.001	3.513	0.021			714.927	<0.001	0.206	<0.001
	02214265	80.6	204	-5.536	0.003					585.679	<0.001	0.042	0.003
	02215500	150.7	315					152.930	<0.001	-306.879	<0.001	0.282	<0.001
Upper Oconee	02218000	29	321	-3.208	0.002			34.892	0.002	290.892	<0.001	0.057	<0.001
	02223000	85.3	240	-2.594	0.024			19.729	0.002	298.998	<0.001	0.061	<0.001
Lower Oconee	02223040	72.7	241					16.267	0.029	256.066	<0.001	0.020	0.029
	02223600	119	305					26.441	0.002	270.933	<0.001	0.030	0.002
Ohoopee	02225500	32.4	64			18.294	<0.001	163.563	<0.001	80.444	0.560	0.402	<0.001
Altamaha	02225000	315.7	248					144.369	<0.001	-343.034	<0.001	0.281	<0.001
	02225990	401.1	231			4.462	0.035	182.930	<0.001	-591.449	<0.001	0.406	<0.001
	02226010	392.6	319	-4.675	0.010			46.356	0.003	593.603	<0.001	0.052	<0.001
	02226160	403.3	246					80.857	<0.001	249.697	0.008	0.087	<0.001

Table 2.8. Average nutrient and organic carbon export, discharge and drainage area for six major sub-watersheds of the in the Altamaha River watershed, and the corresponding fraction of the total Altamaha River export, discharge and area. The sum of the Ocmulgee, Oconee and Ohoopee Rivers [Σ(Ocmulgee Oconee Ohoopee)] is also shown.

	USGS Site	Q	Area	Average Export (kmol d^{-1})				Fraction of Altamaha					
Watershed	Number	(m^3 s^{-1})	(km^2)	NH_4^+	NO_x	P	OC	Q	Area	NH_4^+	NO_x	P	OC
Upper Ocmulgee	02212950	70.6	5,776	22.8	193.6	19.3	2,102	0.18	0.16	0.21	0.36	0.24	0.09
Lower Ocmulgee	02215500	150.7	13,416	37.1	305.7	35.5	6,768	0.38	0.38	0.35	0.57	0.43	0.28
Upper Oconee	02223000	91.1	7,640	33.5	132.9	14.1	2,335	0.23	0.22	0.31	0.25	0.17	0.09
Lower Oconee	02223600	119.0	11,499	46.0	191.3	30.1	4,216	0.30	0.33	0.43	0.36	0.37	0.17
Ohoopee	02225500	32.4	2,875	21.1	10.7	4.8	2,975	0.08	0.08	0.20	0.02	0.06	0.12
Altamaha	02226010	392.6	35,223	107.1	536.3	81.7	24,608						
Σ(Ocmulgee Oconee Ohoopee)		302.1	27,790	104.1	507.8	70.3	13,959	0.77	0.79	0.97	0.95	0.86	0.57

FIGURE LEGENDS

Figure 2.1. Map of the USGS water quality, river discharge (Q), and NCDC meteorological monitoring (P) stations, major dams, and cities with populations exceeding 50,000 (U.S. Census Bureau 2003) in the Altamaha River watershed. The Altamaha, Oconee, Ocmulgee, Ohoopee and Little Ocmulgee River sub-watersheds are shown on the inset with the outline of the state of Georgia. Sites 02225990 and 02226000(Q) are not distinguishable at this scale.

Figure 2.2. Mean daily discharge (natural log transformed) from the Oconee, Ocmulgee, Ohoopee and Altamaha Rivers and estimated mean daily precipitation for the Altamaha River watershed (natural log transformed) from 1970 to 2002. Best-fit linear regressions and the calculated change (per year) in river discharge and estimated total watershed precipitation for the period are shown.

Figure 2.3. Relationship between mean river discharge, temperature and nutrient concentrations in the Altamaha River watershed USGS water quality monitoring stations and distance upriver from the ocean.

Figure 2.4. Estimated sub-watershed specific and total Altamaha watershed population density and agricultural land use at the beginning and end of the study period and average sub-watershed specific and total watershed nutrient and organic carbon loading rates per area of watershed. Note that population density increased while agricultural land use decreased during the study period.

Figure 2.5. 1970 and 2000 population density and population growth from 1970 to 2000 by county in the Altamaha River sub-watersheds (U.S. Census Bureau 2003).

Figure 2.6. 1969 and 2002 agricultural land use (percent farm acreage by county) and percent change in agricultural land use from 1969 to 2002 in the Altamaha River watershed (United States Department of Agriculture 1974, 2004).

Figure 2.7. Relationship between sub-watershed specific population densities (average of 1970 and 2000) and average riverine inorganic nitrogen ($NO_x + NH_4^+$) export per area of watershed. The total Altamaha River watershed value is also shown, but not included in the regression.

Figure 2.1

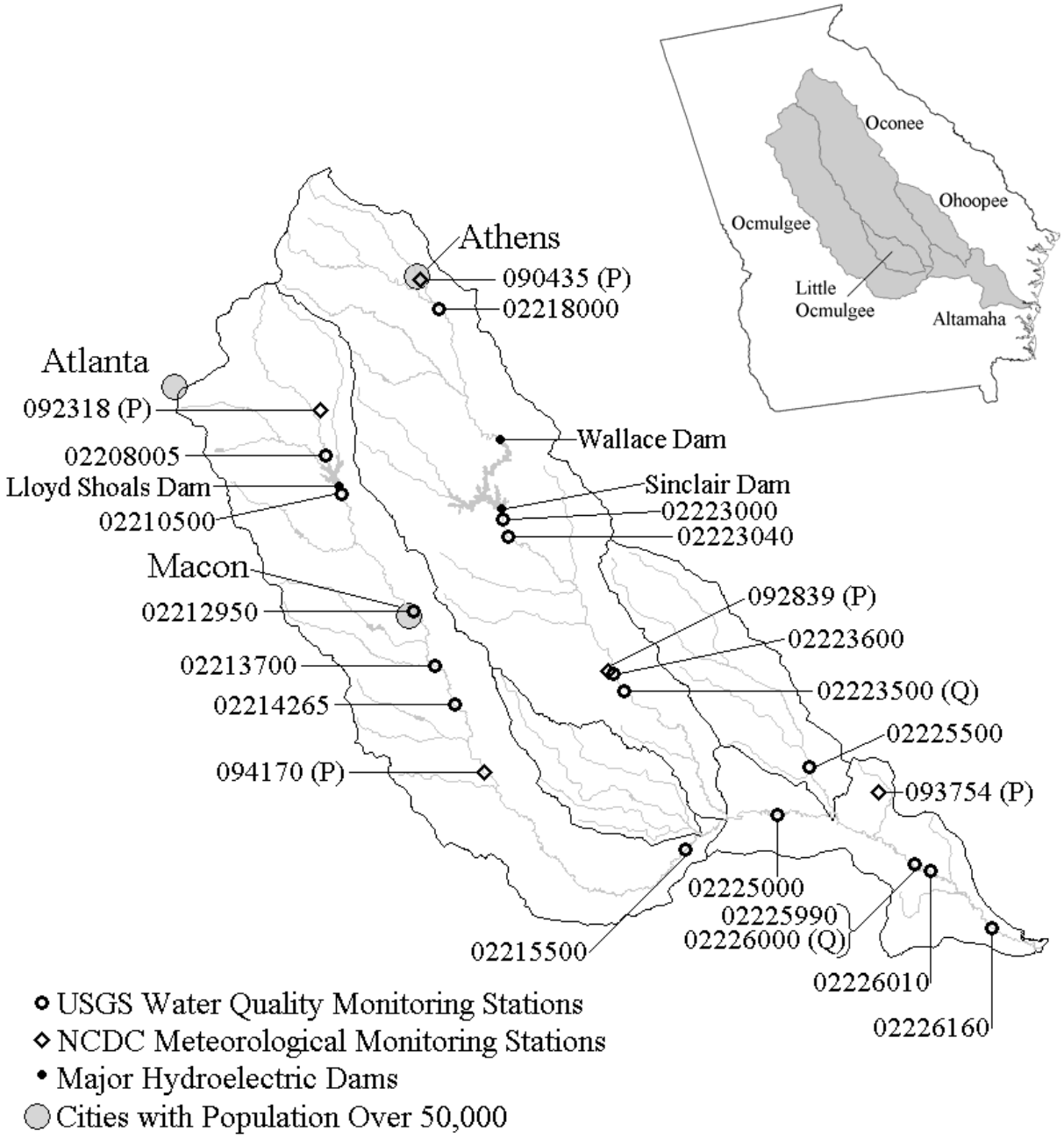
Oconee
Ohoopee
Ocmulgee
Little Ocmulgee
Altamaha
Athens
090435 (P)
02218000
Atlanta
092318 (P)
02208005
Lloyd Shoals Dam
02210500
Wallace Dam
Sinclair Dam
02223000
02223040
Macon
02212950
02213700
02214265
094170 (P)
092839 (P)
02223600
02223500 (Q)
02225500
093754 (P)
02225000
02225990
02226000 (Q)
02226010
02226160
02215500
USGS Water Quality Monitoring Stations
NCDC Meteorological Monitoring Stations
Major Hydroelectric Dams
Cities with Population Over 50,000

Figure 2.2

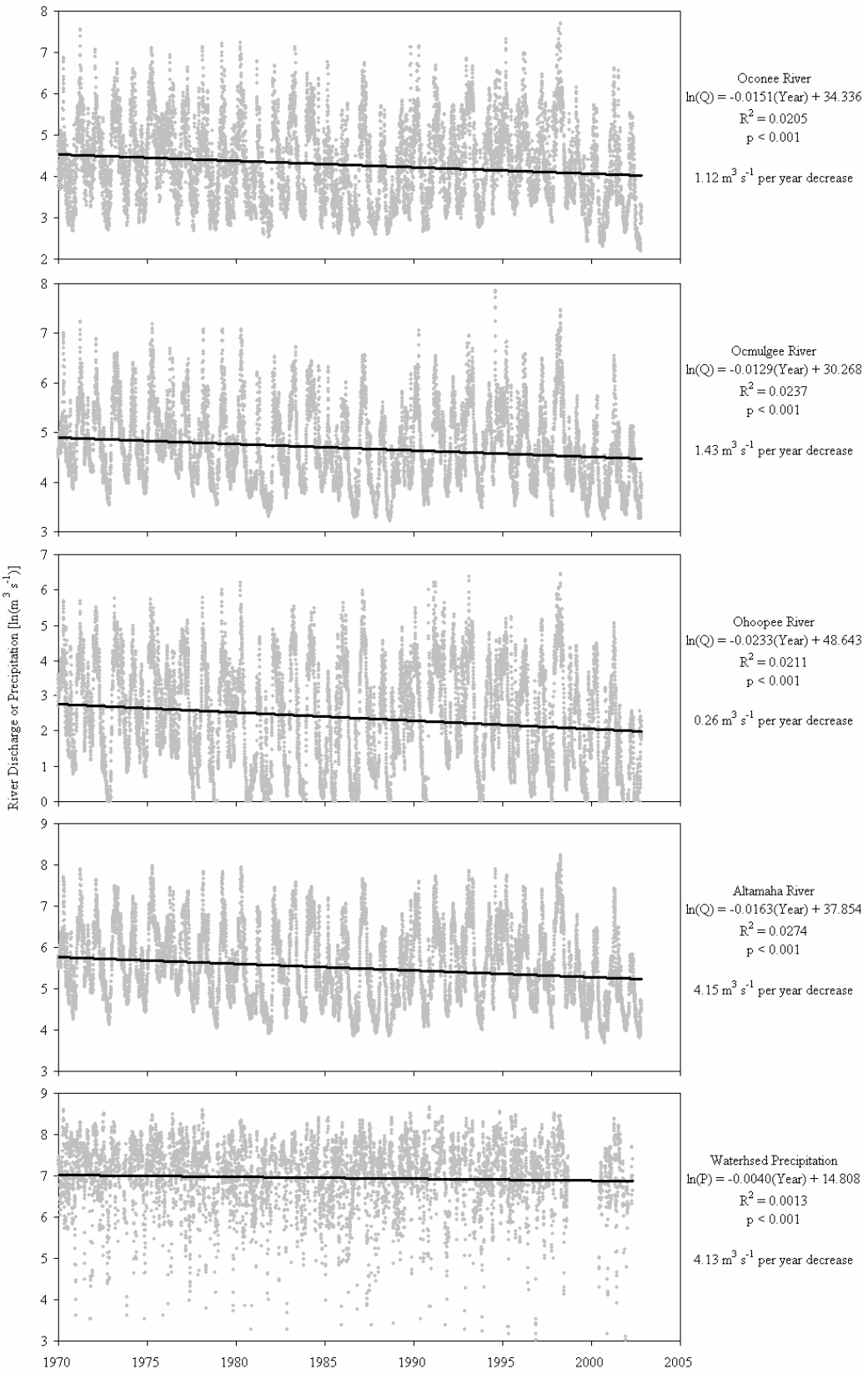
River Discharge or Precipitation [ln(m3 s-1)]
Oconee River
ln(Q) = -0.0151(Year) + 34.336
R2 = 0.0205
p < 0.001
1.12 m3 s-1 per year decrease
Ocmulgee River
ln(Q) = -0.0129(Year) + 30.268
R2 = 0.0237
p < 0.001
1.43 m3 s-1 per year decrease
Ohoopee River
ln(Q) = -0.0233(Year) + 48.643
R2 = 0.0211
p < 0.001
0.26 m3 s-1 per year decrease
Altamaha River
ln(Q) = -0.0163(Year) + 37.854
R2 = 0.0274
p < 0.001
4.15 m3 s-1 per year decrease
Waterhsed Precipitation
ln(P) = -0.0040(Year) + 14.808
R2 = 0.0013
p < 0.001
4.13 m3 s-1 per year decrease
1970
1975
1980
1985
1990
1995
2000
2005

Figure 2.3

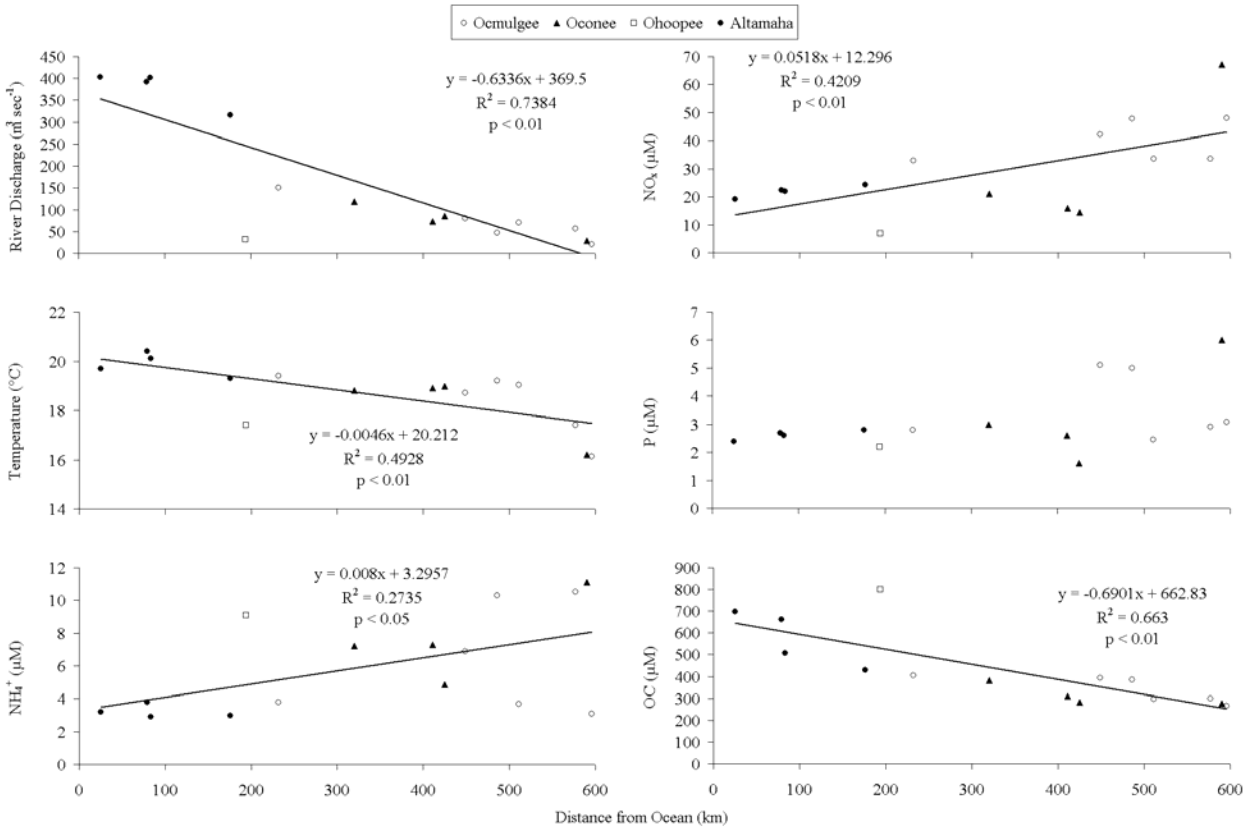
Ocmulgee
Oconee
Ohoopee
Altamaha
River Discharge (m³ sec⁻¹)
y = -0.6336x + 369.5
R² = 0.7384
p < 0.01
NOx (µM)
y = 0.0518x + 12.296
R² = 0.4209
p < 0.01
Temperature (°C)
y = -0.0046x + 20.212
R² = 0.4928
p < 0.01
P (µM)
NH4+ (µM)
y = 0.008x + 3.2957
R² = 0.2735
p < 0.05
OC (µM)
y = -0.6901x + 662.83
R² = 0.663
p < 0.01
Distance from Ocean (km)

Figure 2.4

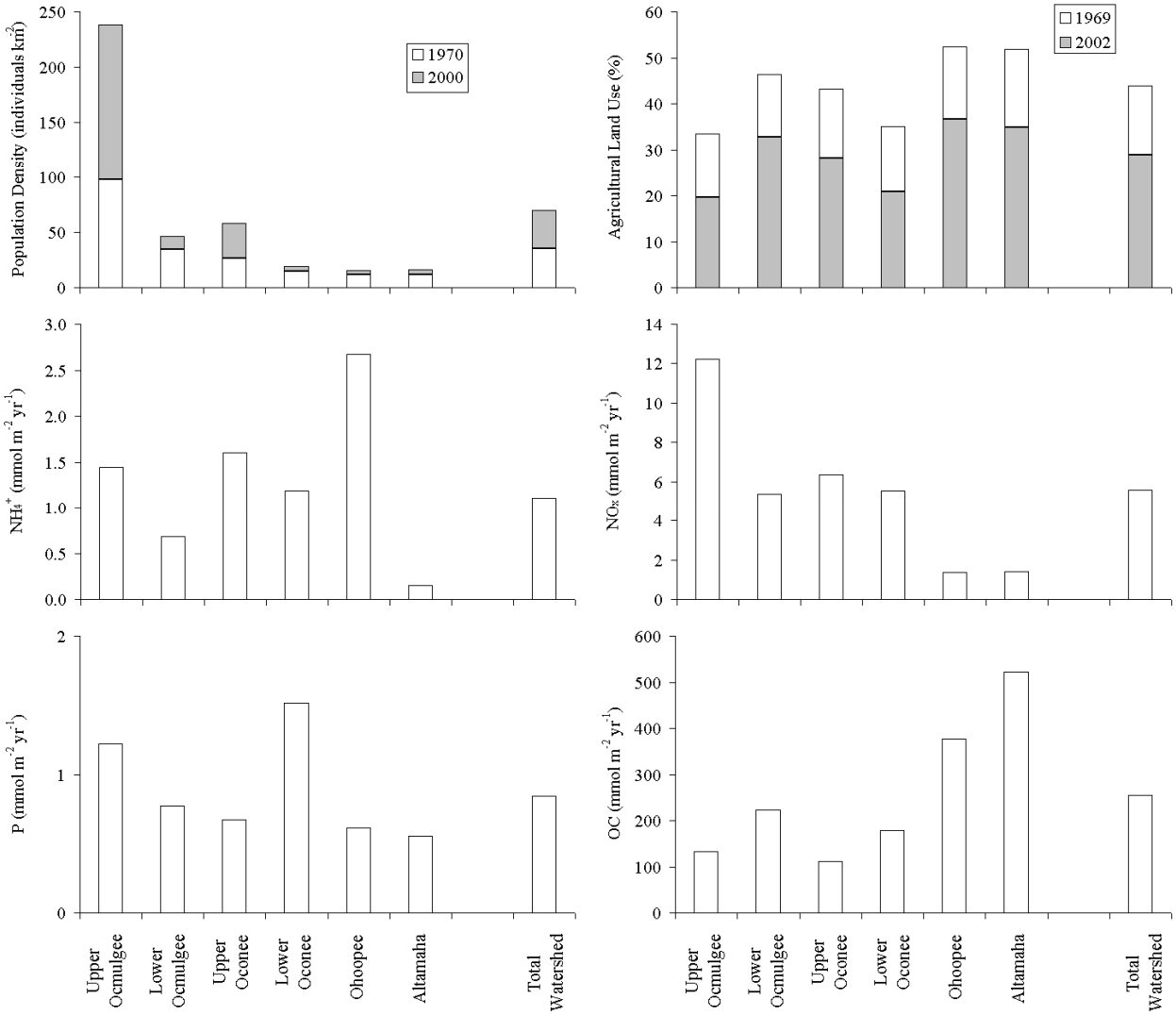
Population Density (individuals km^{-2})
1970
2000
Agricultural Land Use (%)
1969
2002
NH_4^+ (mmol m^{-2} yr^{-1})
NO_3 (mmol m^{-2} yr^{-1})
P (mmol m^{-2} yr^{-1})
OC (mmol m^{-2} yr^{-1})
Upper Ocmulgee
Lower Ocmulgee
Upper Oconee
Lower Oconee
Ohoopee
Altamaha
Total Watershed

Figure 2.5

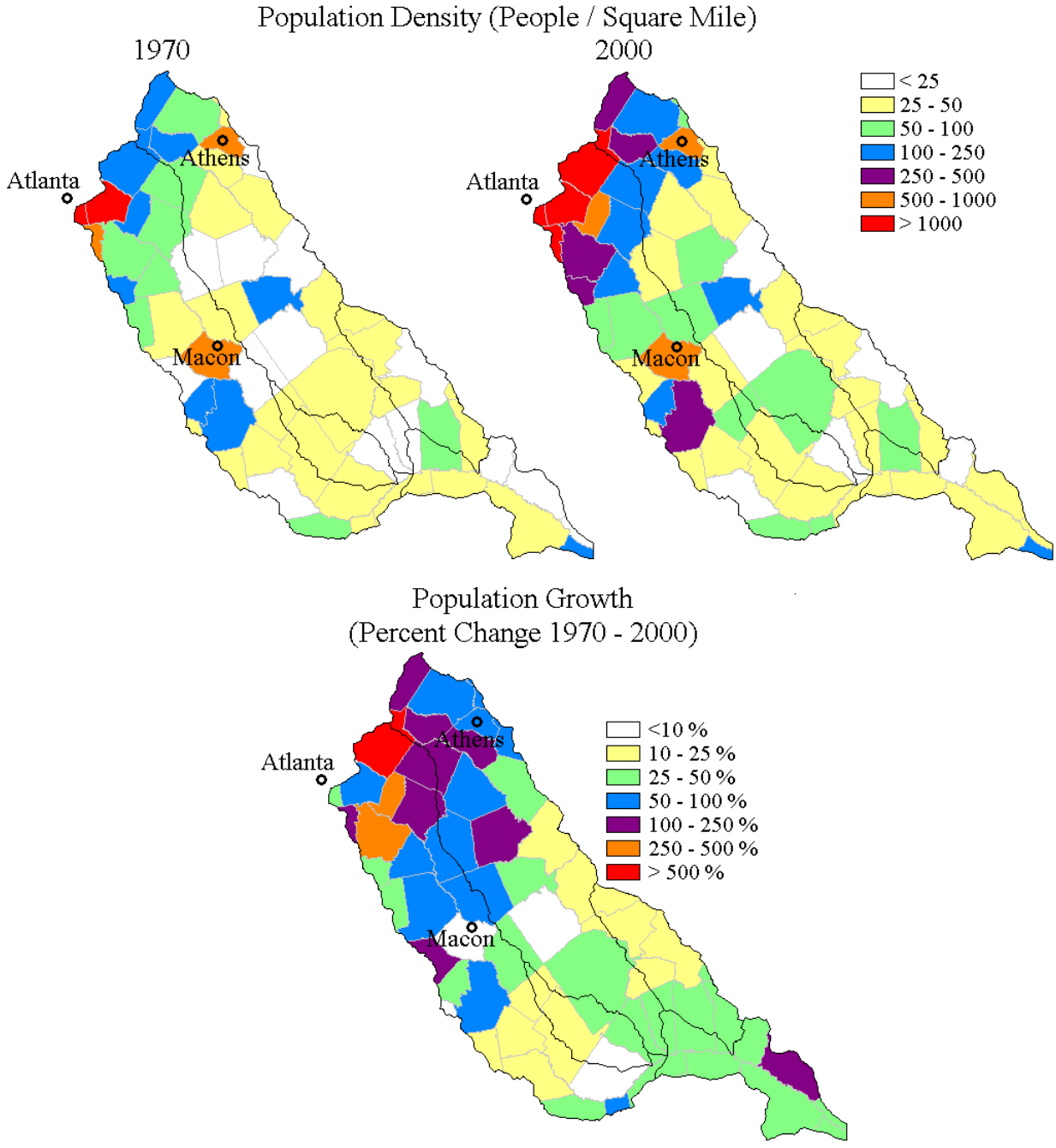
Population Density (People / Square Mile)
1970
2000
Atlanta
Athens
Macon
< 25
25 - 50
50 - 100
100 - 250
250 - 500
500 - 1000
> 1000
Population Growth
(Percent Change 1970 - 2000)
<10 %
10 - 25 %
25 - 50 %
50 - 100 %
100 - 250 %
250 - 500 %
> 500 %

Figure 2.6

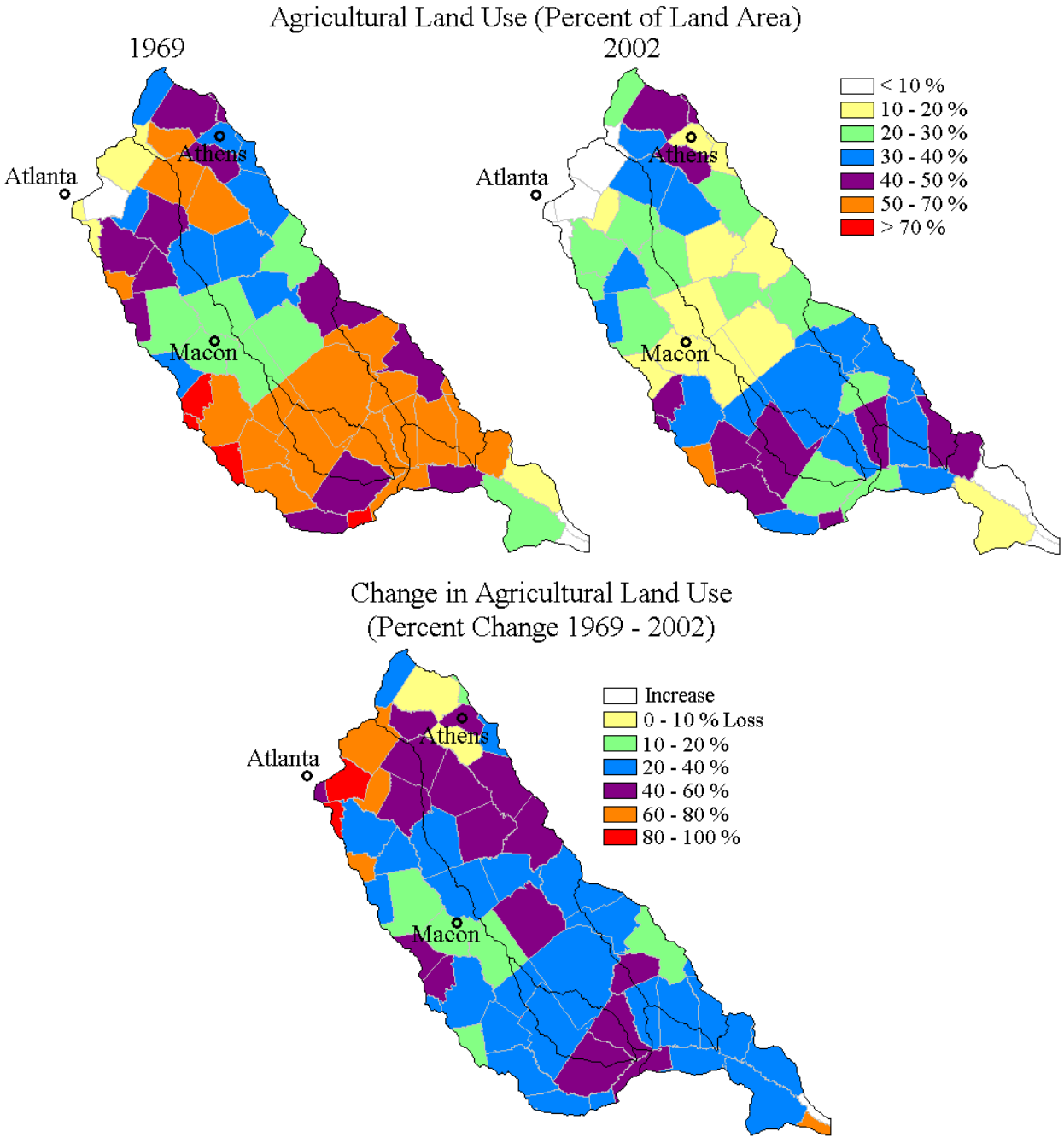
Agricultural Land Use (Percent of Land Area)
1969
2002
Atlanta
Athens
Macon
< 10 %
10 - 20 %
20 - 30 %
30 - 40 %
40 - 50 %
50 - 70 %
> 70 %
Change in Agricultural Land Use
(Percent Change 1969 - 2002)
Increase
0 - 10 % Loss
10 - 20 %
20 - 40 %
40 - 60 %
60 - 80 %
80 - 100 %

Figure 2.7

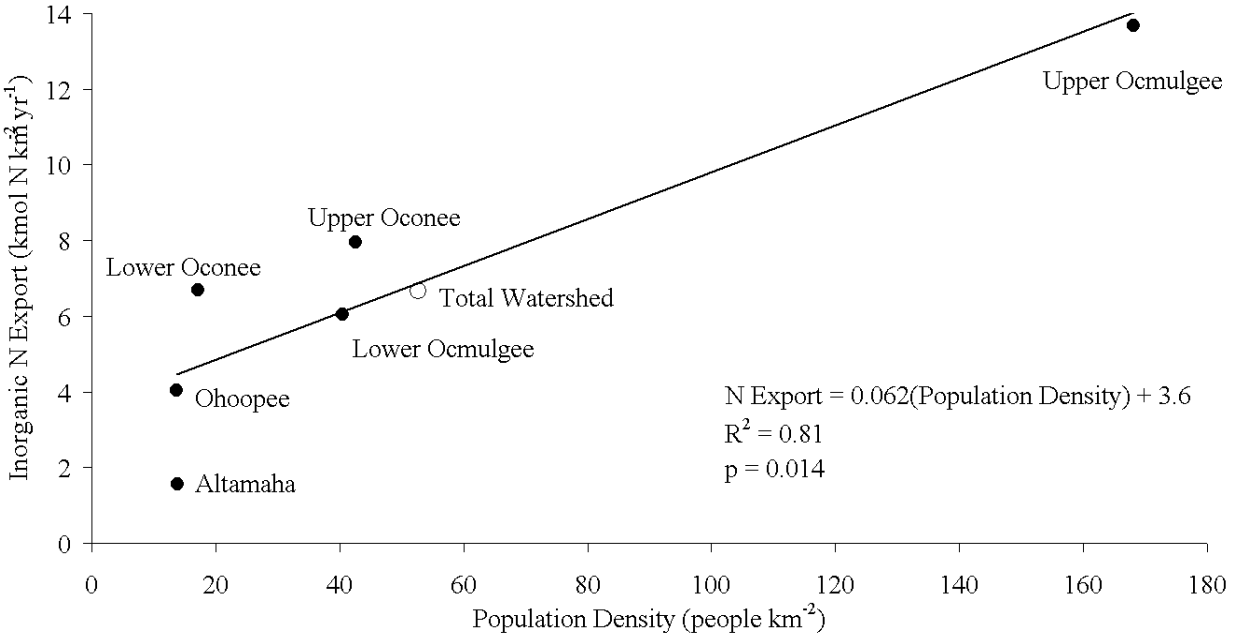
Inorganic N Export (kmol N km-2 yr-1)
Population Density (people km-2)
Upper Ocmulgee
Upper Oconee
Lower Oconee
Total Watershed
Lower Ocmulgee
Ohoopee
Altamaha
N Export = 0.062(Population Density) + 3.6
R2 = 0.81
p = 0.014
0
2
4
6
8
10
12
14
0
20
40
60
80
100
120
140
160
180

CHAPTER 3

MICROBIAL AND GEOCHEMICAL RAMIFICATIONS OF SALINITY INTRUSION INTO TIDAL FRESHWATER SEDIMENTS[1]

[1] Weston, N.B., S.B. Joye, and R. Dixon. Prepared for submission to *Global Biogeochemical Cycles*

ABSTRACT

Upriver salinity intrusion may occur in rivers where watershed water withdrawals, sea-level rise and climate change are occurring. To determine the effects of salinity intrusion on the biogeochemistry of freshwater sediments in the tidal portion of the Altamaha River, GA, we conducted an anaerobic salinity-amendment experiment on sediments in which salinity was increased slowly over a 2 week period to 10‰ and was then held constant for an additional 3 weeks. Concentrations of ammonium, nitrate+nitrite, phosphate, silicate, sulfate, dissolved organic carbon and nitrogen, chloride, sodium, potassium, magnesium, calcium, reduced iron and manganese, methane, nitrous oxide, hydrogen sulfide, dissolved inorganic carbon and the pH of water exiting control and salinity-amended reactors were monitored during the experiment, and sediment solid phase organic carbon, nitrogen, total sulfur and sediment phosphorus and iron fractions were measured three times during the experiment.

Salinity-driven desorption of ammonium and dissolution of silicate and phosphorus minerals resulted in increased porewater concentrations and export of these nutrients following salinity intrusion. In freshwater control sediments, terminal oxidation of organic matter was dominated by methanogenesis (62%), followed by sulfate reduction (18%), denitrification (10%) and iron reduction (10%). Methanogenesis declined to <10% of total organic matter mineralization within two weeks of initial salinity intrusion, and <5% by the end of the 5 week experiment. Sulfate reducers were able to respond to increased sulfate concentrations quickly despite the increasing ionic strength of the porewater. Sulfate reduction was the dominant (>50%) organic matter oxidation pathway within two weeks of salinity intrusion, and >95% of the total organic matter mineralized was oxidized

by sulfate after 4 weeks. Total *in situ* sediment organic matter mineralization more than doubled by the end of the experiment in the salinity-amended sediments, likely due to the greater thermodynamic energy yield of sulfate reduction versus methanogenesis. During initial salinity intrusion, decreasing pH and increasing ionic strength appeared to have altered the availability of the large pool of iron-oxides in these sediments, and microbial Fe reduction was responsible for >60% of organic matter oxidation for a short period. Salinity intrusion resulted in dramatic geochemical and microbial shifts in freshwater sediments in this experiment. This work indicates that increased nutrient (ammonium, phosphate and silicate) flux, decreased methanogenesis and methane emissions, and a rapid shift to sulfate reduction and increased overall organic matter mineralization and carbon dioxide release will accompany salinity intrusion into previously freshwater riverine sediments.

INTRODUCTION

Climate change and water diversions within the watersheds of rivers can reduce the volume of freshwater delivered by rivers to the coastal zone. As freshwater discharge decreases and the freshwater-saltwater mixing zone moves upriver, saline waters intrude into previously freshwater regions (Hamilton 1990; Knowles 2002). Rising sea-levels (Wigley 2005), the potential for lower precipitation in watersheds of rivers (Smith et al. 2005) and global increases in riverine water withdrawals (Gleick 2003) may result in widespread salinity intrusion in mid-latitude coastal ecosystems. The increase in ionic strength and change in concentrations of many substances during the transition from freshwater to saltwater exerts a powerful influence on plant (Crain et al. 2004), animal (Kupschus and Tremain 2001) and microbial communities in aquatic

systems (Rysgaard 1999; Mondrup 1999; Dincer and Kargi 1999; Pattnaik et al. 2000; Mishra et al. 2003).

Riverine sediments are important zones of biogeochemical transformation, yet we know little about the biogeochemical and microbial response of freshwater sediments to salinity intrusion. In freshwater sediments microbial methanogenesis (Capone & Kiene 1988) and iron (Fe) reduction (Roden & Wetzel 1996) are the dominant pathways of anaerobic organic matter mineralization. Methane (CH_4) produced from methanogenesis is a major trace greenhouse gas, and freshwater wetlands are the major natural source of CH_4 to the atmosphere (Wuebbles and Hayhoe 2002). Due to the availability of sulfate (SO_4^{2-}) in seawater, sulfate reduction replaces methanogenesis as the dominant microbial terminal electron accepting process in marine sediments (Jørgensen 1982; Capone & Kiene 1988; Howarth 1993).

Anaerobic microbial process in sediments are thought to largely control the shift in the limiting nutrient for primary production in freshwater (phosphorus; Schindler 1977) to marine waters (nitrogen; Nixon et al. 1996). Phosphorus (P) is precipitated with Fe and stored in sediments, creating P limitation of primary production in freshwater aquatic ecosystems. Hydrogen sulfide (HS^-) produced from sulfate reduction reacts with and sequesters Fe in marine sediments, resulting in higher P availability and nitrogen (N) limitation of primary production in marine systems (Caraco et al. 1989; Harris 1999; Blomqvist et al. 2004). The pathways of anaerobic microbial metabolism and the degradation of organic matter in sediments therefore influence the global cycling of carbon, nutrients, and greenhouse gasses.

Salinity intrusion is likely to have multiple profound effects on the microbial community and biogeochemistry of freshwater sediments, and alter the fluxes of nutrients and greenhouse gasses from the sediments. The shift from methanogenesis to sulfate reduction may reduce

emissions of CH_4. However, nutrient fluxes may increase following salinity intrusion, stimulating excess productivity and adversely effecting water quality in coastal systems. Little is known about how quickly the microbial community in the tidal freshwater portion of an estuary is able to adapt to changes in salinity associated with up-river salinity intrusion or how the biogeochemistry of the sediments responds to the increase in salinity.

In this study, we simulate and monitor the effects of salinity intrusion into anaerobic sediments from the tidal freshwater portion of the Altamaha River, GA, using sediment flow-through reactors. Changes in concentrations of nutrients [ammonium (NH_4^+), nitrate+nitrite (NO_x), phosphate (HPO_4^{2-}), silicate (SiO_2)], SO_4^{2-}, dissolved organic carbon and nitrogen (DOC and DON), major ions [chloride (Cl^-), sodium (Na^+), potassium (K^+), magnesium (Mg^{2+}), calcium (Ca^{2+})], reduced iron (Fe^{2+}) and manganese (Mn^{2+}), CH_4, nitrous oxide (N_2O), HS^- and dissolved inorganic carbon (DIC) and pH of water exiting the reactors was measured during and for several weeks after salinity intrusion. Changes in sediment solid-phase C, N, P, S and Fe concentrations were also determined. Shifts in the major pathways of microbial organic matter mineralization in freshwater sediments following salinity intrusion were estimated.

METHODS

Study Site

The Altamaha River drains the third largest watersheds on the East coast of the United States (approximately 36,000 km^2). The watershed lies entirely within the state of Georgia, and land use within the watershed is a mixture of pristine, agricultural and residential/urban. The watershed remains relatively undeveloped compared with other East coast watersheds, although development pressure is increasing (Chapter 2). Inorganic nitrogen concentrations in the

Altamaha River have increased from the 1970s through 2000, largely due to residential and urban development in the upper portions of the watershed near metropolitan Atlanta. NO_3^- concentrations average about 20 μM (Chapter 2). Discharge from the Altamaha River averages about 400 $m^3\ s^{-1}$, but has declined by about 4 $m^3\ s^{-1}$ per year over the past three decades (Chapter 2). Although water-withdrawal within the watershed has increased since 1950 (Fanning 2003), precipitation within the Altamaha River watershed has also significantly decreased in the past thirty years and can account for the decreased river discharge (Chapter 2).

Sediments from the in the tidal freshwater portion of the Altamaha River 26 km upriver from the mouth of the estuary were sampled on July 12, 2004. Intact sediment cores (8.8 cm inner diameter) were obtained from an unvegetated, intertidal mud-bank in the estuarine channel at low tide. Cores were transported to the laboratory, stored at *in situ* temperatures overnight, and sectioned for porewater and solid-phase sampling and for flow-through reactor experiments the following day.

Porewater Profiles

Duplicate sediment cores were sectioned anaerobically (1 cm intervals to 4 cm, and 2 cm intervals to 20 cm) for porewater and solid-phase analyses. Sediment was centrifuged to obtain porewater, which was split into several vials for analysis of NH_4^+, NO_x, HPO_4^{2-}, SiO_2, SO_4^{2-}, DOC, DON, Cl^-, Na^+, K^+, Mg^{2+}, Ca^{2+}, Fe^{2+}, HS^-, DIC and pH (Table 3.1). CH_4 and N_2O concentrations were determined by subsampling 2 cm^{-3} of sediment from intact cores directly into a headspace vial which was immediately sealed and shaken with 2 ml of 1 N NaOH. Separate sediment samples of a known volume were also dried (80°C) for later solid-phase analysis.

Flow-through Reactors

Sediment flow-through reactor experiments (Roychoudhury 1997, 2003; Brüchert and Arnosti 2003) were initiated one day after sampling. Sediment from the 3-5 cm depth of twelve sediment cores was extruded into twelve separate flow-through reactors (8.8 cm^2 inner diameter). Sediments were not homogenized, and care was taken to preserve the natural sediment structure. Sediment flow-through reactors were constructed of polycarbonate plastic and consisted of a 2 cm section of sediment, capped on either end with a 15 μm frit and held in place with an upper and lower housing. The polycarbonate housings had an inlet/outlet in the center, and spiral grooves on the inner surface to promote diffuse flow across the surface of the frit. The assembly was bolted lightly together and sealed with viton o-rings between the core, frit and housing. A peristaltic pump was used to pump anaerobic artificial freshwater (AFW; Table 3.2) from a reservoir through all of the reactors at a slow flow rate (~10 ml hr^{-1}). The entire experimental assembly (reservoir, pump and reactors) was placed in a nitrogen-flushed anaerobic chamber (Coy Labs).

After a five day equilibration and porewater flushing period in which all flow-through reactors received AFW, the salinity of the inflow water was gradually increased in six of the reactors. Artificial seawater (ASW) was mixed with AFW (Table 3.2) in increasing ratios to simulate a 10‰ increase in salinity over a two-week period. Salinity was then held constant at 10‰ for an additional three weeks. Control reactors received AFW for the duration of the experiment. ASW and AFW both contained 200 μM carbon as dextran, a polysaccharide of dextrose as a carbon source. Duplicate reactors from both the control and salinity treatments were sacrificed for sediment solid-phase measurements on days 9, 15, and upon termination of

the experiment (day 35). Reactors were disassembled and a known volume of sediment was dried (80°C) for later solid-phase analysis.

Water exiting the flow-through reactors was sampled daily (until day 20) or every few days (from day 20 to 35) for NH_4^+, NO_x, HPO_4^{2-}, SiO_2, SO_4^{2-}, DOC, DON, Cl^-, Na^+, K^+, Mg^{2+}, Ca^{2+}, Fe^{2+}, Mn^{2+}, HS^-, CH_4, N_2O, DIC and pH (Table 3.1). Outflow tubing was placed in a 20ml glass vial, which was allowed to fill and overflow for several volumes before subsampling for the various analyses (Table 3.1). In addition, flow rate through the reactors was monitored for the duration of the experiment. Aqueous speciation and mineral solubility were determined using the PHREEQC geochemical program with standard databases (Parkhurst 1995) and concentrations of aqueous solutes in the flow-through reactor outflow.

Solid-phase Analyses

Porosity and bulk density were determined after drying a known volume of wet sediment. Sediment total carbon, nitrogen and sulfur were measured on dried, ground sediment using a ThermoFinnigan Flash EA 1112 CNS analyzer. Carbonate content was determined on a Shimadzu TOC-5000 infra-red gas analyzer following in-line acidification of sediment. Dried, ground sediment was extracted sequentially to determine sediment Fe and P fractions. Sediment P fractions were extracted following the SEDEX extraction procedure (Ruttenberg 1992), and sequentially extracted for reactive Fe fractions (Poulton and Canfield 2005).

RESULTS

Porewater Profiles

Porewater Cl^- concentrations in the Altamaha River sediments increased slightly with depth, from about 0.5 at the surface to 1.5 mM at 10 cm (Fig. 3.1). SO_4^{2-} concentrations increased with depth until 5 cm, and then decreased to about 50 μM at depth (Fig. 3.1). SO_4^{2-}/Cl^- molar ratios decreased in the 3 to 10 cm depth from 0.1 in the surface sediments to 0.04 in deeper sediments. Ca^{2+} and DIC concentrations decreased significantly with depth ($p < 0.05$), while NH_4^+ and SiO_2 increased with depth ($p < 0.05$, Fig. 3.1). HPO_4^{2-} concentrations were constant below 5 cm, but exhibited shallow (3-5 cm) concentration maxima, as did NH_4^+ and SiO_2 concentrations (Fig. 3.1). NO_x concentrations decreased with depth until 9 cm, below which NO_x increased slightly. Inorganic nitrogen was dominated by NH_4^+ (~0.8 mM), as porewater NO_x concentrations were low (~2 μM). CH_4 concentrations were above 1 mM except in the surface sediment, and DOC concentrations exceeded 5 mM (Fig. 3.1).

Flow-through Reactors

Increased major ion concentrations [Na^+, SO_4^{2-} (Fig. 3.2), Cl^-, K^+, Mg^{2+}, Ca^{2+}, (not shown)] were measured in response to increasing salinity in the salinity-amended flow-through reactors. Differences in major ion concentration exiting the control and salinity-amended reactors were small but significant ($p < 0.001$) on the day following the initial increase. Major ion concentrations increased smoothly until day 15, and were then constant until the termination of the experiment (Fig. 3.2). SO_4^{2-} uptake during flow through the reactors was estimated using Na^+ concentrations to calculate an expected SO_4^{2-} [$(SO_4^{2-})_E$] concentration by assuming Na was unreactive:

(3.1) $(SO_4^{2-})_E = [(Na^+ - Na^+_{AFW}) / (Na^+_{ASW} - Na^+_{AFW})] * (SO_4^{2-}_{ASW} - SO_4^{2-}_{AFW}) + SO_4^{2-}_{AFW}$

where Na^+, Na^+_{AFW} and Na^+_{ASW} are the sodium concentrations measured in the water exiting the reactors, and in the AFW and ASW inflow solutions, respectively, and $SO_4^{2-}_{AFW}$ and $SO_4^{2-}_{ASW}$ are the AFW and ASW inflow sulfate concentrations, respectively. The change in sulfate concentration was then obtained by subtracting the SO_4^{2-} measured exiting the reactors from $(SO_4^{2-})_E$. There was a net uptake in sulfate in both control and salinity-amended reactors (Fig. 3.3). SO_4^{2-} consumption averaged about 25 μM in the control reactors for the entire experiment, while uptake in the salinity-amended flow-through reactors increased as SO_4^{2-} concentrations increased during the initial salinity increase (Fig. 3.3). SO_4^{2-} uptake then decreased again to levels equivalent to control SO_4^{2-} uptake on day 9, and then increased again for the duration of the experiment, reaching about 300 μM by the termination of the experiment (Fig. 3.3).

There were significant ($p < 0.05$) enduring [SiO_2, CH_4, DIC, HS^-] or transient (Fe^{2+}, HPO_4^{2-}, NH_4^+, pH) differences in the concentration of a number of dissolved species exiting the control and salinity-amended flow-through reactors during the salinity intrusion experiment (Fig. 3.2). Concentrations of SiO_2 exiting the control reactors dropped slightly during the experiment, but remained between 150 and 200 μM after the initial flushing of porewater (Fig. 3.2). SiO_2 concentrations in the salinity-amended reactors increased above control concentrations ($p < 0.05$) on day 7 and remained elevated (> 250 μM) for the duration of the experiment (Fig. 3.2). CH_4 concentrations decreased in the salinity-amended reactors, becoming significantly lower than control reactor concentrations on day 5 ($p < 0.01$), and remained lower than control concentrations for the duration of the experiment. CH_4 in the control reactors was relatively

constant at about 100 μM, while CH_4 concentrations remained below 20 μM after day 7 in the salinity-amended reactors (Fig. 3.2).

DIC concentrations were similar in the control and salinity-amended reactors until day 15, after which DIC concentrations in the salinity-amended reactors became significantly higher ($p < 0.05$, Fig. 3.2). DIC concentrations increased during flow through both the control and salinity-amended experiments (Fig. 3.3). Net DIC production (correcting for inflow concentrations) was relatively constant in the control reactors, averaging about 150 μM for the total experiment (Fig. 3.3). Net DIC production in the salinity-amended reactors paralleled that of the control reactors until day 15, after which DIC production increased to a maximum of about 400 μM at the termination of the experiment (Fig. 3.3). HS^- in the salinity-amended reactors increased above concentrations in the control reactors on day 4 ($p < 0.05$), reaching concentrations of about 30 μM by the end of the experiment.

Fe^{2+} and NH_4^+ concentrations both increased during the initial period of increasing salinity, and decreased again to match levels in the control reactors shortly after the salinity stabilized at 10‰. Fe^{2+} was significantly ($p < 0.05$) higher in the salinity-amended reactors from day 3 until day 16, and concentrations exceeded 500 μM at the peak (days 7-9, Fig. 3.2). NH_4^+ concentrations in the salinity-amended reactors exceeded those in the control reactors on day 1 and remained significantly higher through day 11 ($p < 0.05$, Fig.2). HPO_4^{2-} concentrations initially decreased in the salinity-amended reactors, becoming significantly lower than control concentrations on day 2, and remaining lower through day 9 ($p < 0.05$, Fig.2). HPO_4^{2-} concentrations then increased in the salinity-amended reactors, becoming significantly higher than concentrations exiting control reactors on day 15 ($p < 0.05$, Fig. 3.2). pH levels in the salinity-amended reactors decreased during the ramp in salinity, becoming significantly different

from control reactors on day 1 and remained significantly lower (by about 0.4 pH units at peak difference) through day 18 ($p < 0.05$, Fig. 3.2).

NO_x and Mn^{2+} were undetectable in water exiting the reactors for both control and salinity-amended reactors for the duration of the experiment (data not shown). The change in NO_x concentration during flow through the sediment reactors (Fig. 3.3) was calculated from the change in inflow water concentration over time in the salinity-amended reactors. NO_x uptake was a constant 20 μM in the control reactors, and decreased with decreasing NO_x in the inflow water to 0.2 μM in the salinity-amended reactors (Fig. 3.3). There were no significant differences in concentrations of DOC or DON between control and salinity-amended reactors (Fig. 3.2).

Solid Phase

Sediment carbonate, organic nitrogen, organic carbon and total sulfur all significantly decreased with depth in the sediment cores ($p < 0.05$), and the C:N ratio was constant with depth (Fig. 3.1). Carbonate content of the sediment was low (< 0.01% by weight), and organic carbon was several orders of magnitude higher (about 5% by weight, Fig. 3.1). Carbonate may have reflected the DIC in solution when the sediment was dried, as the concentrations are similar and the sediment was not rinsed before carbonate analysis. Sediment organic nitrogen was also about two orders of magnitude higher than porewater inorganic nitrogen (Fig. 3.1).

Sediment total P was dominated largely by organic P, and the inorganic P fractions (adsorbed, acetate and HCl extractable) contributed to only about 20% of the total (Table 3.3). The inorganic P was composed mostly of HCl extractable detrital fluorapatite, and authigenic fluorapatite and carbonate and Fe bound P contributed to about 5% of total P (Table 3.3).

Dithionite-reducible Fe (Poulton and Canfield 2005) content in the sediment was relatively high, and accounted for about half of the total Fe (Table 3.3). Adsorbed Fe (1 M $MgCl_2$ extractable; Poulton and Canfield 2005) was low and did not change during the experiment (Table 3.3).

There were no significant changes in sediment solid phase organic carbon, organic nitrogen, total sulfur or P fractions (Table 3.3). Reducible Fe content in salinity-amended sediments at the end of the flow-through experiment (51.6 μmol cm^{-3}) was significantly ($p < 0.05$) lower than in the control reactors or initial sediments (Table 3.3). Other fractions of Fe did not change during the flow-through experiment.

Mineral Solubility

Water flowing out of both the control and salinity-amended reactors was undersaturated with respect to calcite ($CaCO_3$) and amorphous iron ($Fe(OH)_3$), and supersaturated with goethite (FeOOH), iron monosulfide (FeS), and quartz (SiO_2) for the duration of the experiment (Fig. 3.4). Other SiO_2 minerals (i.e. amorphous SiO_2 and chalcedony) were undersaturated (data not shown). The reactors were supersaturated with respect to vivianite ($Fe_3(PO_4)_2$) and siderite ($FeCO_3$) until about day 24, after which the salinity-amended reactors were undersaturated (Fig. 3.4). Water exiting the reactors was undersaturated with respect to hydroxyapatite ($Ca_5(PO_4)_3OH$) in both treatments until about day 19, after which Ca^{2+} and HPO_4^{2-} were saturated in the salinity amended reactors (Fig. 3.4).

DISCUSSION

Salinity intrusion into tidal freshwater sediments of the Altamaha River resulted in changes in the concentrations of carbon, nitrogen, phosphorus, silica, iron, and sulfur exiting the

salinity-amended flow-through reactors (Figs. 3.2 and 3.3). The changes are the result of both abiotic geochemical reactions associated with the higher ionic strength of the porewater, as well as shifts in microbial pathways of organic matter mineralization.

Abiotic Geochemical Shifts

Changes in SiO_2, NH_4^+ and HPO_4^{2-} concentrations were likely driven largely by the increasing ionic strength of porewater during salinity intrusion, rather than by microbial processes. The presence of cations in solution promotes the hydrolysis of Si-O bonds and the dissolution of quartz minerals (Dove 1999). SiO_2 concentrations in water exiting the salinity-amended bioreactors increased shortly after the initial breakthrough of saline waters and remained elevated (Fig. 3.2), indicating greater dissolution rates of silica minerals due to salinity intrusion was not a transient process, at least on the timescales of this experiment.

Concentrations of NH_4^+ and HPO_4^{2-} were several orders of magnitude higher in the sediment porewater at the outset of the flow-through experiment (Fig. 3.1) than in the inflow water (Table 3.2). Although the volume of the flow-through reactors was replaced about twice per day, concentrations of NH_4^+ and HPO_4^{2-} in the reactor outflows remained above inflow concentrations for the duration of the experiment (Fig. 3.2), likely due to exchange of adsorbed ions, mineral dissolution, and organic N and P mineralization. The salinity breakthrough was accompanied by an increase in NH_4^+ and a decrease in HPO_4^{2-} concentrations exiting the salinity-amended reactors (Fig. 3.2).

Competition for sediment exchange sites by ions in saline waters (Seitzinger et al. 1991), as well as ion pairing of NH_4^+ and anions in saline water (Gardner et al. 1991), reduces adsorption of NH_4^+ in saline sediments. As salinities increased, NH_4^+ adsorbed to sediment

exchange sites was desorbed, and porewater NH_4^+ concentrations increased. However, unlike SiO_2 export from these sediments, the increased NH_4^+ export was relatively short, lasting for about 12 days (Fig. 3.2). Desorption of NH_4^+ is a rapid process, taking only hours to reach equilibrium (Rosenfeld 1979). Concentrations of NH_4^+ exiting the salinity-amended reactors responded to even the initial small increase in salinity (from 0.063 in the AFW to 0.161‰ on the first day of amendment), and adsorbed NH_4^+ was exchanged largely at the lower salinities below about 7‰. There was little difference between the control and salinity-amended reactors on day 10, although the salinity was still increasing. This suggests that the initial intrusion of salinity in freshwater sediments will result in the largest changes in sediment NH_4^+ sorption.

The decrease in HPO_4^{2-} concentrations during the salinity breakthrough was unexpected. As with NH_4^+, adsorption and desorption of HPO_4^{2-} in sediments can control dissolved concentrations of HPO_4^{2-} (Sundareshwar and Morris 1999), and increasing ionic strength would be expected to desorb exchangeable HPO_4^{2-}. However, HPO_4^{2-} sorption is more closely coupled with Fe and aluminum geochemistry in sediments (Sundareshwar and Morris 1999). The high Fe^{2+} concentrations in the reactor outflows during this period (Fig. 3.2) and the supersaturation of viviante (Fig. 3.3) suggest that iron-phosphate binding and possibly mineral precipitation may have lowered HPO_4^{2-} concentrations during salinity intrusion. Following the initial decrease in HPO_4^{2-} concentrations in the reactor outflow during the salinity breakthrough, HPO_4^{2-} concentrations increased in the salinity-amended reactors (Fig. 3.2), in parallel with a decrease in viviante saturation and an increase in hydroxyapatite saturation (Fig. 3.2). It appears that HPO_4^{2-} concentrations were largely regulated by mineral solubilities. Total export of HPO_4^{2-} was small relative to solid-phase P (Table 3.3). Therefore, no significant change in sediment P content

(total or sequential extraction) over time or between the control and salinity-amended reactors was measured (Table 3.3).

The increase in Fe^{2+} concentrations during the salinity intrusion (Fig. 3.2) do not appear to be due to simple desorption of Fe adsorbed to sediment particles. Exchangeable Fe^{2+} was low (< 0.5 μmol cm^{-3}; Table 3.3) and, even if exchanged and exported from the reactors on a single day, would account for only a change in concentration of about 300 μM. The peak in Fe^{2+} concentrations during the salinity breakthrough is accompanied by a decrease in pH. The decrease in pH and increase in Fe^{2+} during and following the breakthrough of saline water in the sediment reactors parallels the stability isopleths of amorphous Fe ($Fe(OH)_3$) and goethite (FeOOH) minerals (Fig. 3.5; Stumm and Morgan 1996). Although amorphous Fe remained undersaturated and goethite remained supersaturated for the duration of the experiment (Figs. 3.4 and 3.5), sediments contain a heterogeneous mixture of Fe-oxides with a range of reactivities (Lovley 1991). The reactivity of metal oxides in sediments is controlled by many factors, including the available metal oxide surface area, sorption of inorganic and organic species on the metal oxide surface, temperature, and the pH and ionic strength of the porewater (Brown et al. 1999). It is difficult to determine with certainty in this experiment whether the apparent Fe-oxide dissolution was an abiotic reaction, or a microbially-mediated reduction coupled to the oxidation of organic matter (see the *Microbial Processes* section for further discussion).

The decrease in pH during the salinity breakthrough (Fig. 3.2) is likely due to surface chemistry and exchange in the sediments, and decreases in pH with increasing salinity have been observed by others (Mahrous et al. 1983; Lu et al. 2004). As the ionic strength of the solution entering the sediments increases, protons bound to negatively charged sediments are replaced by Na^+ and other ions, decreasing the pH of the porewater. It does not appear to be carbonate

mineral precipitation (i.e. $Ca^{2+} + HCO_3^- \rightarrow CaCO_3 + H^+$), as the sediment carbonate content was low and did not change during the experiment ($p > 0.05$, Table 3.3). Carbonate mineral precipitation would decrease carbonate alkalinity by twice the decrease in total DIC, and the slope of the carbonate alkalinity (calculated from DIC and pH, Stumm and Morgan 1996) to total DIC was 0.99 ($r^2 = 0.88$).

Microbial Pathways

Rates of metabolic pathways in the flow-through reactors were estimated using a simple model of C production, on a per mol carbon basis:

$$\Sigma C = DNF + FeR + SR + MG \quad (3.2)$$

where ΣC is the total carbon production (DIC and CH_4) and DNF, FeR, SR and MG are estimated rates of microbial denitrification, iron reduction, sulfate reduction and methanogenesis, respectively. Net rates (nmol cm^{-3} d^{-1}) of CH_4 and Fe(II) production (Fig. 3.2) and NO_x and SO_4^{2-} consumption (Fig. 3.3) were calculated from changes in concentration (Figs. 3.2 and 3.3, Table 3.3) and the flow rate (10 ml hr^{-1}) in the flow-through reactors. FeR, DNF and SR were estimated from Fe(II) production and NO_3^- and SO_4^{2-} consumption using ratios of 0.25, 1.125 and 2 carbon to Fe(II), NO_3^- and SO_4^{2-}, respectively (Stumm and Morgan 1996). MG was estimated by

$$(2f)\Delta CH_4 + (1-f)\Delta CH_4 \quad (3.3)$$

where f is the ratio of CH_4 produced from organic matter to CH_4 produced by hydrogenotrophic CO_2 reduction and ΔCH_4 is the production rate of CH_4.

Modeled ΣC production was then compared with measured ΣC production from the control and salinity-amended flow-through reactors. An f value of 0 (i.e. H_2 is electron donor for all of MG) resulted in modeled net ΣC that did not agree with measured values, and an f value of 1.0 produced ΣC that were too high (Fig. 3.6). Modeled ΣC production matched the measured ΣC production reasonably well when an f value of 0.5 was used in the control reactors (Fig. 3.6). Modeled ΣC in the salinity-amended reactors, using an f of 0.5, matched measured ΣC production from about day 12 on, but did not adequately estimate ΣC production during the initial period of salinity change (Fig. 3.6). There were changes in both Fe^{2+} production (Fig. 3.2) and SO_4^{2-} uptake (Fig. 3.3) during this period, which may have been due to geochemical changes (see *Abiotic Geochemical Processes* section above) or errors in calculation rather than changes in microbial respiration.

ΣC production estimated without contributions of FeR, SR or both FeR and SR were calculated (Fig. 3.6). When ΣC production was estimated without FeR (Model– FeR, Fig. 3.6), modeled DIC production remained overestimated during the salinity breakthrough. ΣC modeled without SR (Model – SR) matched measured ΣC production rates quite well until day 11, after which measured ΣC production became larger than modeled estimates in the absence of SR. Modeled ΣC production without both FeR and SR (Model-SR-FeR, Fig. 3.6) underestimated measured ΣC production during the salinity breakthrough. We suspect that this reflects an error in the SO_4^{2-} uptake calculation (equation 3.1) due to variable transport of the Na^+ and SO_4^{2-} ions through the flow-through reactors during this period. SO_4^{2-} sorption in soils, mainly to aluminum and Fe-oxyhydroxides, is inversely related to pH (Nodvin et al. 1986). Although

usually a minor process at pH > 5, SO_4^{2-} sorption does occur at higher pHs (Arbestain et al. 1999). Retardation of SO_4^{2-} relative to Na^+ in the flow-through reactors during the initial salinity breakthrough (Fig. 3), perhaps enhanced by the decrease in pH during this period (Fig. 2), may have resulted in apparent ΔSO_4^{2-} (equation 3.1; Fig. 3.3) that did not reflect microbial SR. SR was therefore estimated to remain at levels measured in the control reactors during this period (shaded area in Fig. 3.6).

Although the increase in ionic strength and decrease in pH associated with the salinity intrusion may have caused abiotic dissolution of Fe-oxides (see *Abiotic Geochemical Processes* section above), the modeled ΣC production suggests that microbial FeR during the salinity breakthrough is required to produce the measured terminal carbon exiting the salinity-amended reactors (Fig. 3.6). We therefore suspect that shifts in ionic strength and pH during the salinity intrusion increased the availability of Fe-oxides to the microbial iron-reducing community. Concentrations of reducible (dithionite reducible, Poulton and Canfield 2005) Fe-oxides were high in these sediments (Table 3.3), and a large fraction of these Fe-oxides were apparently not available for microbial reduction. Although some portion of this Fe-oxide pool was reduced during salinity intrusion, the majority of reducible Fe-oxides were not reduced (Table 3.3). We suspect that decreasing pH and/or increasing ionic strength increased the available surface area of Fe-oxides for microbial iron reducers during salinity intrusion.

The fraction of total organic matter mineralization in the control and salinity-amended reactors during the course of the 5 week experiment was estimated using results from the models of ΣC production (Fig. 3.7). In the control reactors, the importance of the terminal electron accepting processes was relatively constant over time and was dominated by MG (62%). SR contributed a further 18% to organic carbon oxidation, and contributions of DNF and FeR were

similar at about 10%. The importance of FeR declined to about 5% at the end of the experiment, likely due to consumption of available iron-oxides in the freshwater sediment (Fig. 3.7).

In the salinity-amended reactors, organic matter oxidation shifted from MG dominated to SR dominated, with greater than 95 % of organic matter oxidized by SO_4^{2-} at the end of the experiment (Fig. 3.7). Carbon flow through DNF dropped to negligible levels during the salinity breakthrough, as did MG by complete breakthrough of 10‰ seawater. FeR appeared to peak in the middle of the salinity breakthrough, oxidizing up to 60% of the total carbon mineralized for a short period of time. Note, however, that estimates of organic carbon oxidation during the breakthrough are not well constrained. Nevertheless, this experiment demonstrates the ability of sulfate reducing bacteria to rapidly adapt to increased ionic strength and sulfate concentrations in sediment porewater. SR became the dominant process (> 50% organic carbon oxidized) 12 days after initial salinity intrusion (Fig. 3.7).

Rates of DNF in the flow-through reactors appeared to be controlled solely by concentrations of available NO_x, as no NO_x was detected in the water exiting either the control or salinity-amended reactors at any time. There is some evidence that denitrifying bacteria are inhibited by changes in salinity, especially when freshwater sediments are exposed to saline water, and by HS^- produced by sulfate reducers in marine systems (Rysgaard et al. 1999; Mondrup 1999, An and Gardner 2002). N_2O concentrations were low (<0.1 μM) and did not change during salinity intrusion (data not shown). Some fraction of the NO_3^- entering the flow-through reactors may have been converted to NH_4^+ via dissimilatory nitrate reduction to ammonium (DNRA) rather than to N_2 gas by denitrification. However, all NO_x was reduced in both control and salinity-amended sediments.

Concentrations of CH_4 and rates of MG dropped soon after salinity intrusion (Figs. 3.2 and 3.7). Changes in salinity (Mishra et al 2003; Pattnaik et al. 2000), competition between methanogens and Fe reducers (Roden and Wetzel 1996) or SO_4^{2-} reducers (Capone & Kiene 1988; Mishra et al. 2003) for reduced substrates, the lower energy yield of MG as compared to FeR and SR (Stumm and Morgan 1996), and inhibition of methanogens by HS^- produced by sulfate reduction (Visser et al. 1993; O'Flaherty et al. 1998) can all decrease CH_4 production in sediments. Due to these inhibitory effects on methanogenesis, rates of CH_4 production and emission from saline sediments are often lower than from freshwater sediments (Bartlett et al. 1987; Capone and Kiene 1988). Inhibition of methanogenesis and a reduction in CH_4 concentrations was apparent at salinities of less than 2‰ during salinity intrusion into freshwater sediments of the Altamaha River (Figs. 3.2 and 3.7). Even small changes in salinity associated with upriver migration of the freshwater-seawater mixing zone are therefore likely to shift the dominant pathway of organic matter mineralization away from methanogenesis.

Total organic matter mineralization appears to have increased following salinity intrusion. ΣC production was significantly higher ($p < 0.05$) in the salinity-amended reactors from day 15 on (Fig. 3.7). Increasing ionic strength may have leached labile dissolved organic carbon from sediments (in a manner similar to NH_4^+ exchange) that was then available for microbial utilization. However, DOC and DON concentrations did not change following salinity intrusion (Fig. 3.2). Although dissolved organic matter sorbed to mineral surfaces and subsequently leached can be highly bioavailable (Hedges and Keil 1995), presumably some fraction would have been unavailable to microbes and detectable as increased DOC and DON concentrations in the water exiting the reactors. Further, the increase in ΣC production is largely measured towards the end of the salinity breakthrough, and appears to reflect the increase in SR

(Fig. 3.7). The higher thermodynamic yield of SR as compared to MG (Stumm and Morgan 1996) and the shift in dominance to SR following salinity intrusion suggests that SO_4^{2-} reducers were able to take advantage of *in situ* organic matter that was not available to methanogens.

Although not often the dominant pathway of organic matter oxidation in the freshwater sediments, SO_4^{2-} reduction does occur in freshwater systems (Holmer and Storkholm 2001). The decrease in SO_4^{2-}/Cl^- ratios in the Altamaha River sediment (Fig. 3.1) suggests that the 3-5 cm depth was a zone of active SR in the unmanipulated sediment cores. It appears that the freshwater sulfate reducing community in these tidal freshwater sediments was able to adapt relatively quickly to increased ionic strength and SO_4^{2-} concentrations. Considerable increase in rates of SR was evident within 2 weeks of salinity intrusion (Fig. 3.7), and HS^- production indicated a SR response in under a week (Fig. 3.2).

Implications of Salinity Intrusion

Overall export of NH_4^+, HPO_4^{2-}, SiO_2, Fe^{2+}, CH_4 export and total mineralization (ΣC) from freshwater and salinity intrusion impacted sediments were estimated for the 35 days during and following salinity intrusion (Table 3.4). Export of nutrients (NH4+, HPO_4^{2-}, SiO_2) was 20 to 40% higher from salinity-amended sediments than from freshwater sediments (Table 3.4). Despite the initial drop in HPO_4^{2-} concentrations during the initial salinity intrusion (Fig. 3.2), total HPO_4^{2-} flux from these sediments was higher following salinity intrusion (Table 3.4). The salinity-driven desorption of NH_4^+, enhancement of SiO_2 and HPO_4^{2-} mineral dissolution may be sources of these nutrients to coastal waters during up-river salinity intrusion. Excess loading of nutrients has resulted in the eutrophication of many coastal waters (Nixon 1995; Howarth 1996; Vitousek et al. 1997; Paerl et al. 1998), and salinity intrusion may provide yet another

mechanism of nutrient delivery to fuel excess productivity in the coastal zone. It is interesting to note that the timing of salinity intrusion is likely to coincide with lowest rates of nutrient delivery from the watershed (during low river discharge) amplifying the effects of higher rates of nutrient release from the sediments.

Lower rates of methanogenesis (Fig. 3.7) resulted in decreased CH_4 export from salinity-impacted sediments (Table 3.4). The inhibition of methanogenesis following salinity intrusion would reduce emissions of this greenhouse gas to the atmosphere, although due to the limited geographical extent of salinity intrusion, this reduction would likely be minor on a global scale. ΣC export was higher in the salinity-amended sediments (Table 3.4), but much of this C was derived from the added dextran polysaccharide. The *in situ* sediment organic carbon mineralized can be estimated by subtracting the added dextran (assuming all of the dextran was mineralized). Mineralization of *in situ* sediment organic matter appears to have more than doubled following salinity intrusion (Table 3.4). Lower CH_4 emissions would then be at least partially offset by lower organic matter burial rates and higher CO_2 release from salinity intrusion impacted sediments due to the ability of sulfate reducers to more efficiently oxidize sediment organic carbon.

The shift in dominant microbial pathways of organic mineralization from MG to SR during salinity intrusion occurred relatively rapidly (Fig. 3.7). This transition was marked by a period of several days when FeR was apparently the principle pathway of organic C oxidation. The effects of changing salinity on the availability of Fe-oxides, FeR, and their relationship with P geochemistry in sediments warrant further investigation. The impact of salinity intrusion on freshwater estuarine sediments is dramatic. This experiment demonstrates that a combination of

geochemical and microbial shifts alters the biogeochemistry of many elements (C, N, P, S, Si, Fe) important to the productivity of coastal waters.

ACKNOWLEDGMENTS

We thank M. Erickson and W. Porubsky for assistance in the field and laboratory, and J. Edmonds and M. Moran for discussion of the experiment. This research was supported by the National Science Foundation's Georgia Coastal Ecosystems Long Term Ecological Research Program (OCE 99-82133).

LITERATURE CITED

Armstrong, J. 1979. Application of the formaldoxime colorimetric method for the determination of manganese in the pore water of anoxic estuarine sediments. Estuaries. 3: 198-201.

Bartlett, K.B., D.S. Bartlett, R.C. Harriss and D.I. Sebacher. 1987. Methane emissions along a salt-marsh salinity gradient. Biogeochemistry. 4: 183-202.

Battle, M., M. Bender, T. Sowers, P.P. Tans, J.H. Butler, J.W. Elkins, J.T. Ellis, T. Conway, N. Zhang, P. Lang and A.D. Clarke. Atmospheric gas concentrations over the past century measured in air from firn at the South Pole. Nature 383: 231-235.

Blomqvist, S., G. Anneli and R. Elmgren. 2004. Why the limiting nutrient differs between temperate coastal seas and freshwater lakes: A matter of salt. Limnol. Oceanogr. 49: 2236-2241.

Brown, G.E., V.E. Henrich, W.H. Casey, D.L. Clark, C. Eggleston, A. Felmy, D.W. Goodman, M. Grätzel, G. Maciel, M.I. McCarthy, K.H. Nealson, D.A. Sverjensky, M.F. Toney, J.M.

Zachara. Metal oxide surfaces and their interactions with aqueous solutions and microbial organisms. Chemical Reviews 99: 77-174.

Brüchert, V. and C. Arnosti. 2003. Anaerobic carbon transformation: Experimental studies with flow-through cells. Marine Chemistry 80: 171-183.

Camps Arbestain, M.C., M.E. Barreal and F. Macías. 1999. Relating sulfate sorption in forest soils to lithological classes, as defined to calculate Critical Loads of Acidity. The Science of the Total Environment. 241: 181-195.

Capone, D.G. and R.P. Kiene. 1988. Comparison of microbial dynamics in marine and fresh-water sediments - contrasts in anaerobic carbon catabolism. Limnol. Oceanogr. 33: 725-749.

Caraco, N.F., J.J. Cole and G.E. Likens. Evidence for sulfate-controlled phosphorus release from sediments of aquatic systems. Nature 341: 316-318.

Cline, J. D. 1969. Spectrophotometric determination of hydrogen sulfide in natural waters. Limnol. Oceanogr. 14:454-458.

Crain, C.M., B.R. Silliman, S.L. Bertness and M.D. Bertness. 2004. Physical and biotic drivers of plant distribution across estuarine salinity gradients. Ecology 85: 2539-2549.

Dincer, A.R., F. Kargi. 1999. Salt inhibition of nitrification and denitrification in saline wastewater. Environ. Technol. 20: 1147-1153.

Dove, P.M. 1999. The dissolution kinetics of quartz in aqueous mixed cation solutions. *Geochim. Cosmochim. Acta* 63: 3715-3727.

Fanning, J.L. 2003. Water use in Georgia, 2000; and trends, 1950-2000. Proceedings of the 2003 Georgia Water Resources Conference.

Froelich P.N., G.P. Klinkhammer, M.L. Bender, N.A. Luedtke, G.R. Heath, D. Cullen, P. Dauphin, D. Hammond, B. Hartman and V. Maynard. 1979. Early oxidation of organic-

matter in pelagic sediments of the eastern equatorial Atlantic - suboxic diagenesis. Geochim. Cosmochim. Acta 43: 1075-1090.

Gardner, W.S., S.P. Seitzinger and J.M. Malczyk. 1991. The effects of sea salts on the forms of nitrogen released from estuarine and freshwater sediments: Does ion pairing affect ammonium flux? Estuaries 14: 157-166.

Gleick, P.H. 2003. Water use. Annual Review of Environment and Resources 28: 275-314.

Hamilton, P. 1990. Modeling salinity and circulation for the Columbia River Estuary. Progress in Oceanography 25: 113-156.

Harris, G.P. 1999. Comparison of the biogeochemistry of lakes and estuaries: Ecosystem processes, functional groups, hysteresis effects and interactions between marco- and microbiology. Mar. Freshwater Res. 50: 791-811.

Hedges, J.I., and R.G. Keil. 1995. Sedimentary organic matter preservation: An assessment and speculative synthesis. Marine Chemistry. 49: 81-115.

Holmer, M. and P. Storkholm. 2001. Sulphate reduction and sulphur cycling in lake sediments: A review. Freshwater Biology 46: 431-451.

Howarth, R.W. 1993. Microbial processes in salt-marsh sediments. In: Ford, T.E. (ed) Aquatic microbiology: an ecological approach. Blackwell, Cambridge, p 239-259.

Howarth, R.W., G. Billen, D. Swaney, A. Townsend, N. Jaworski, K. Lajtha, J. A. Downing, R. Elmgren, N. Caraco, T. Jordan, F. Berendse, J. Freney, V. Kudeyarov, P. Murdoch, and Zhu Zhao-Liang, 1996. Regional nitrogen budgets and riverine N & P fluxes for the drainages to the North Atlantic Ocean: Natural and human influences. *Biogeochemistry* 35: 75-139.

Jørgensen, B.B. 1982. Mineralization of organic-matter in the sea bed - the role of sulfate reduction. Nature 296: 643-645.

Keeling, C.D., T.P. Whorf, M. Wahlen and J. Vanderplicht. 1995. Interannual extremes in the rate of rise of atmospheric carbon-dioxide since 1980. Nature 375:666-670.

Knowles, N. 2002. Natural and management influences on freshwater inflows and salinity in the San Francisco Estuary at monthly to interannual scales. Water Resources Research 38: 1289.

Kostka, J.E., B. Gribsholt, E. Petrie, D. Dalton, H. Skelton and E. Kristensen. 2002. The rates and pathways of carbon oxidation in bioturbated saltmarsh sediments. Limnol. Oceanogr. 47: 230-240.

Kupschus, S. and D. Tremain. Associations between fish assemblages and environmental factors in nearshore habitats of a subtropical estuary. Journal of Fish Biology. 58: 1383-1403.

Lovley, D.R. 1991. Dissimilatory Fe(III) and Mn(IV) reduction. Microbiological Reviews 55: 259-287.

Lu S.G., C. Tang and Z. Rengel. 2004. Combined effects of waterlogging and salinity on electrochemistry, water-soluble cations and water dispersible clay in soils with various salinity levels. Plant and Soil. 264: 231-245.

Mahrous, F.N., D.S. Mikkelson and A.A. Hafez. 1983. Effect of soil-salinity on the electro-chemical and chemical-kinetics of some plant nutrients in submerged soils. Plant and Soil 75: 455-472.

Mishra, S.R., P. Pattnaik, N. Sethenathan and T.K. Adhya. 2003. Anion-mediated salinity affecting methane production in a flooded alluvial soil. Geomicrobiol. J. 20: 579-586.

Mondrup, T. 1999. Salinity effects on nitrogen dynamics in estuarine sediment investigated by a plug-flux method. Biol. Bull. 197: 287-288.

Nixon, S.W., J.W. Ammermann, L.P. Atkinson, V.M. Berounsky, G.B Billen, W.C. Boicourt, W.R. Boynton, T.M. Church, D.M Ditoro, R. Elmgren, J.H. Garber, A.E. Giblin, R.A.

Jahnke, N.J.P. Owens, M.E.Q. Pilson and S.P. Seitzinger. 1996. The fate of nitrogen and phosphorus at the land-sea margin of the North Atlantic Ocean. Biogeochemistry 35: 141-180.

Nodvin, S.C., C.T. Driscoll and G.E. Likens. The effect of pH on sulfate adsorption by a forest soil. Soil Science 142: 69-75.

O'Flaherty, V., T. Mahoney, R. O'Kennedy and E. Colleran. 1998. Effect of pH on growth kinetics and sulphide toxicity thresholds of a range of methanogenic, syntrophic and sulphate-reducing bacteria. Process Biochemistry 33: 555-569.

Paerl, H.W., J.L. Pinckney, J.M. Fear and B.L. Peierls. 1998. Ecosystem responses to internal and watershed organic matter loading: Consequences for hypoxia in the eutrophying Neuse River Estuary, North Carolina, USA. *Marine Ecology Progress Series* 166: 17-25.

Parkhurst, D.L. 1995. User's guide to PHREEQC – a computer program for speciation, reaction-path, advective-transport, and inverse geochemical calculations. U.S. Geol. Surv. Water Resour. Inv. 95-4227.

Pattnaik, P. S.R. Mishra, K. Bharati, S.R. Mohanty, N. Sethunathan and T.K. Adhya. 2000. Influence of salinity on methanogenesis and associated micrflora in tropical rice soils. Microbiological Res. 155: 215-220.

Poulton, S.W. and D.E. Canfield. 2005. Development of a sequential extraction procedure for iron: Implications for iron partitioning in continentally derived particulates. Chem. Geol. 214: 209-221.

Roden, E.E. and R.G. Wetzel. 1996. Organic carbon oxidation and suppression of methane production by microbial Fe(III) oxide reduction in vegetated and unvegetated freshwater wetland sediments. Limnol. Oceanogr. 41: 1733-1748.

Roychoudhury, A.N., E. Vollier and P. Van Cappellen. 1998. A plug flow-through reactor for studying biogeochemical reactions in undisturbed aquatic sediments. Applied Geochemistry 13: 26-280.

Roychoudhury, A.N., P. Van Cappellen, J.E. Kostka, E. Vollier. 2003. Kinetics of microbially mediated reactions: dissimilatory sulfate reduction in saltmarsh sediments (Sapelo Island, Georgia, USA). Estuarine, Coastal and Shelf Science 56: 1001-1010.

Ruttenberg K.C. 1992. Development of a sequential extraction method for different forms of phosphorus in marine sediment. *Limnol. Oceanogr.* 37: 1460-1482.

Rysgaard, S., P. Thastum, T. Dalsgaard, P.B. Christensen and N.P. Sloth. 1999. Effects of salinity on NH_4^+ adsorption capacity, nitrification, and denitrification in Danish estuarine sediments. Estuaries 22: 21-30.

Schindler, D.W. 1977. Evolution of phosphorus limitation in lakes. Science. 195: 260-262.

Seitzinger, S. P., W.S. Gardner and A.K. Spratt. 1991. The effect of salinity on ammonium sorption in aquatic sediments: implications for benthic nutrient cycling. Estuaries 14: 167-174.

Smith, S.J., A.M. Thomson, N.J. Rosenberg, R.C. Izaurralde, R.A. Brown and T.M.L. Wigley. 2005. Climate change impacts for the conterminous USA: An integrated assessment. Part 1. Scenarios and context. Climatic Change 69: 7-25.

Solorzano L. 1969. Determination of ammonia in natural waters by the phenolhypochlorite method. *Limnol. Oceanogr.* 14: 799-801.

Stookey, L.L. 1970. Ferrozine – A new spectrophotometric reagent for iron. Analytical Chemistry. 42: 779-781.

Stumm, W. and J.J. Morgan. 1996. Aquatic Chemistry, Third Edition. Wiley, New York.

Sundareshwar, P.V. and J.T. Morris. Phosphorus sorption characteristics of intertidal marsh sediments along an estuarine salinity gradient. Limnology and Oceanography 44: 1693-1701.

Visser, A., A.N. Nozhevnikova and G. Lettinga. 1993. Sulfide inhibition of methanogenic activity at various pH levels at 55°C. Journal of Chemical Technology and Biotechnology 57: 9-13.

Vitousek, P.M., H.A. Mooney, J. Lubchenco and J.M. Melillo. 1997. Human domination of Earth's ecosystems. Science. 277: 494-499.

Wuebbles, D.J. and K. Hayhoe. 2002. Atmospheric methane and global change. Earth-Science Reviews 57: 177-210.

Wigley, T.M.L. 2005. The climate change commitment. Science 307: 1766-1769.

Table 3.1. Sampling, preservation and analytical methods for aqueous samples from porewater profiles and flow-through reactors.

Analyte	Sample	Preservation	Analytical Method
CH_4	Unfiltered in He purged headspace vial	4.4 N phosphoric acid	Shimadzu GC 14A flame ionization detector gas chromatograph
DIC	Unfiltered	Run immediately	Shimadzu TOC 5000 infra-red gas analyzer
pH	Unfiltered	Run immediately	Accumet AP62 pH meter and Sensorex 450C pH probe
HS^-	Unfiltered	0.1 M zinc acetate	Colorimetric (Cline 1969)
Cl^-, SO_4^{2-}, Na^+, K^+, Mg^{2+}, Ca^{2+}	0.2 µm filtered	0.2 N nitric acid, refrigerated	Dionex ion chromatograph
Fe^{2+}	0.2 µm filtered	0.2 N nitric acid, refrigerated	Colorimetric (Stookey 1970)
Mn^{2+}	0.2 µm filtered	0.2 N nitric acid, refrigerated	Colorimetric (Armstrong 1979)
HPO_4^{2-}	0.2 µm filtered	0.2 N nitric acid, refrigerated	Lachat Quikchem 8000 autoanalyzer (Method 31-115-01-1G)
DOC	0.2 µm filtered	0.2 N nitric acid, refrigerated	Shimadzu TOC 5000 high-temperature combustion infra-red gas analyzer after sparging with CO_2-free air
NOx ($NO_3^- + NO_2^-$)	0.2 µm filtered	Refrigerated	Antek Instruments model 745 vanadium reduction manifold followed by a model 7050 nitric oxide detector
DON	0.2 µm filtered	Refrigerated	Shimadzu TOC 5000 high-temperature combustion and Antek 7020 nitric oxide detection for total dissolved nitrogen (TDN). DON = TDN – NH4+ - NOx
SiO_2	0.2 µm filtered	Refrigerated	Lachat Quikchem 8000 autoanalyzer (Method 31-114-27-1-B)
NH_4^+	0.2 µm filtered	0.4% phenol	Colorimetric (Solorzano 1969)

Table 3.2. Composition of artificial fresh water (AFW) and artificial seawater (ASW) flow-through reactor inflow solutions.

Component	AFW	ASW
Salinity (‰)	0.063	9.9
pH	7.9	7.9
Dextran (μM C)	200	200
Major Ions		
Cl^- (μM)	980	155,132
Na^+ (μM)	910	148,794
Mg^{2+} (μM)	98	7,169
Ca^{2+} (μM)	323	2,897
K^+ (μM)	87	2,813
SO_4^{2-} (μM)	35	7,969
HCO_3^- (μM)	669	669
Nutrients		
NH_4^+ (μM)	0.94	0.94
HPO_4^{2-} (μM)	0.15	0.15
NO_3^- (μM)	19.78	0.20

Table 3.3. Sediment solid-phase measurements (mean ± standard deviation) from initial core (3-5 cm depths, n = 2) and control and salinity-amended flow-through reactors sampled at the end of the experiment (day 35, n = 2 each). All units in μmol (of C, N, S, P or Fe) cm^{-3} of wet sediment. Statistical differences ($p < 0.05$, pair wise) between reactors and initial sediment (I) and between control and salinity-amended reactors (S) are noted.

	Initial	Control	Salinity
Carbonate	3.72 ± 0.15	3.83 ± 1.17	3.54 ± 0.15
Organic Nitrogen	121.2 ± 4.2	122.1 ± 8.7	112.8 ± 7.5
Organic Carbon	1534 ± 37	1584 ± 76	1603 ± 88
Total Sulfur	62.5 ± 1.0	74.1 ± 8.6	71.7 ± 7.2
Phosphorus			
Exchangeable	0.035 ± 0.008	0.023 ± 0.010	0.063 ± 0.046
Authigenic Apatite	0.81 ± 0.06	0.75 ± 0.05	0.70 ± 0.03
Total Inorganic	2.31 ± 0.07	2.24 ± 0.10	2.35 ± 0.22
Organic	11.89 ± 1.47	11.74 ± 2.35	8.68 ± 1.45
Total	14.2 ± 1.4	14.0 ± 2.2	11.0 ± 1.2
Iron			
Exchangeable	0.33 ± 0.26	0.26 ± 0.11	0.52 ± 0.30
Reducible Fe(III)	61.8 ± 1.7	**71.0** ± 6.4 ^{S}	**51.6** ± 1.8 ^{I,S}
Total	115.6 ± 5.2	121.4 ± 18.7	112.4 ± 10.7

Table 3.4. Total export (μmol cm^{-3}) from freshwater and salinity-amended sediments from the Altamaha River (for 35 days), and the percent change due to salinity intrusion. ΣC is the total carbon (DIC and CH_4) flux, and *in situ* C is ΣC corrected for carbon (dextran) addition (12.5 μmol cm^{-3}).

	Freshwater	Salinity-Intrusion	Percent Change
NH_4^+	2.84	3.71	30.7
HPO_4^{2-}	1.58	1.90	20.7
SiO_2	11.54	15.96	38.3
Fe^{2+}	4.86	12.08	148.6
CH_4	6.93	1.61	-76.8
ΣC	16.21	20.29	25.2
in situ C	3.72	7.80	109.7

FIGURE LEGENDS

Figure 3.1. Porewater chloride (Cl^-), sulfate (SO_4^{2-}), sulfate to chloride ratio (SO_4^{2-}/Cl^-), calcium (Ca^{2+}), phosphate (HPO_4^{2-}), ammonium (NH_4^+), nitrate+nitrite (NO_x), silicate (SiO_2), dissolved inorganic carbon (DIC), dissolved organic carbon (DOC) and methane (CH_4), and sediment solid-phase carbonate, organic nitrogen, organic carbon, total sulfur and organic carbon to nitrogen molar ratio. The depth of sediment used in the flow-through reactor experiments (3-5 cm) is indicated by dashed lines.

Figure 3.2. Concentrations (mean ± standard deviation) of sodium (Na^+), sulfate (SO_4^{2-}), silicate (SiO_2), reduced iron (Fe^{2+}), methane (CH_4), dissolved organic carbon (DOC), phosphate (HPO_4^{2-}), ammonium (NH_4^+), hydrogen sulfide (HS^-), dissolved inorganic carbon (DIC), pH and dissolved organic nitrogen (DON) of water exiting control and salinity-amended flow-through reactors.

Figure 3.3. Net change in concentrations (± standard deviation, see text for description) of sulfate (ΔSO_4^{2-}), nitrate+nitrite (ΔNO_x) and dissolved inorganic carbon (ΔDIC) during flow through control and salinity-amended sediment reactors.

Figure 3.4. Mineral saturation indices [log(IAP) – log (K_T), where IAP is the ion activity product and K_T is the reaction equilibrium constant] for selected iron, phosphorus, silica, calcium and carbonate minerals calculated using the PHREEQC geochemical program for water exiting the control and salinity-amended flow-through reactors.

Figure 3.5. Diagram of pH and log[Fe^{2+}] concentrations of water exiting control and salinity-amended flow-through reactors. The stability isopleths for goethite (FeOOH) and amorphous iron oxides [$Fe(OH)_3$] are indicated.

Figure 3.6. Measured and modeled rates of dissolved inorganic carbon (DIC) production in (top) control flow-through reactors [with estimates calculated using different fractions (f) of methanogenesis from organic matter] and (bottom) salinity-amended reactors (including estimates without FeR or SR). The shaded area in the salinity-amended reactors denotes the period for which modeled SR appears to be overestimated. See text for further description.

Figure 3.7. Terminal carbon (ΣC) production (DIC + CH_4) in the control and salinity-amended reactors and salinity in the salinity-amended reactors (top). The dashed line indicates the amount of the dextran polysaccharide added to both control and salinity-amended reactors (nmol C cm^{-3} d^{-1}). Estimated contribution of denitrification (DNF), methanogenesis (MG), sulfate reduction (SR) and iron reduction (FeR) terminal electron accepting processes (TEAPs) to total organic carbon oxidation in (middle) control and (bottom) salinity-amended flow-through reactors. The period for which SR was estimated to remain constant in the salinity-amended reactors is indicated by vertical dashed lines.

Figure 3.1

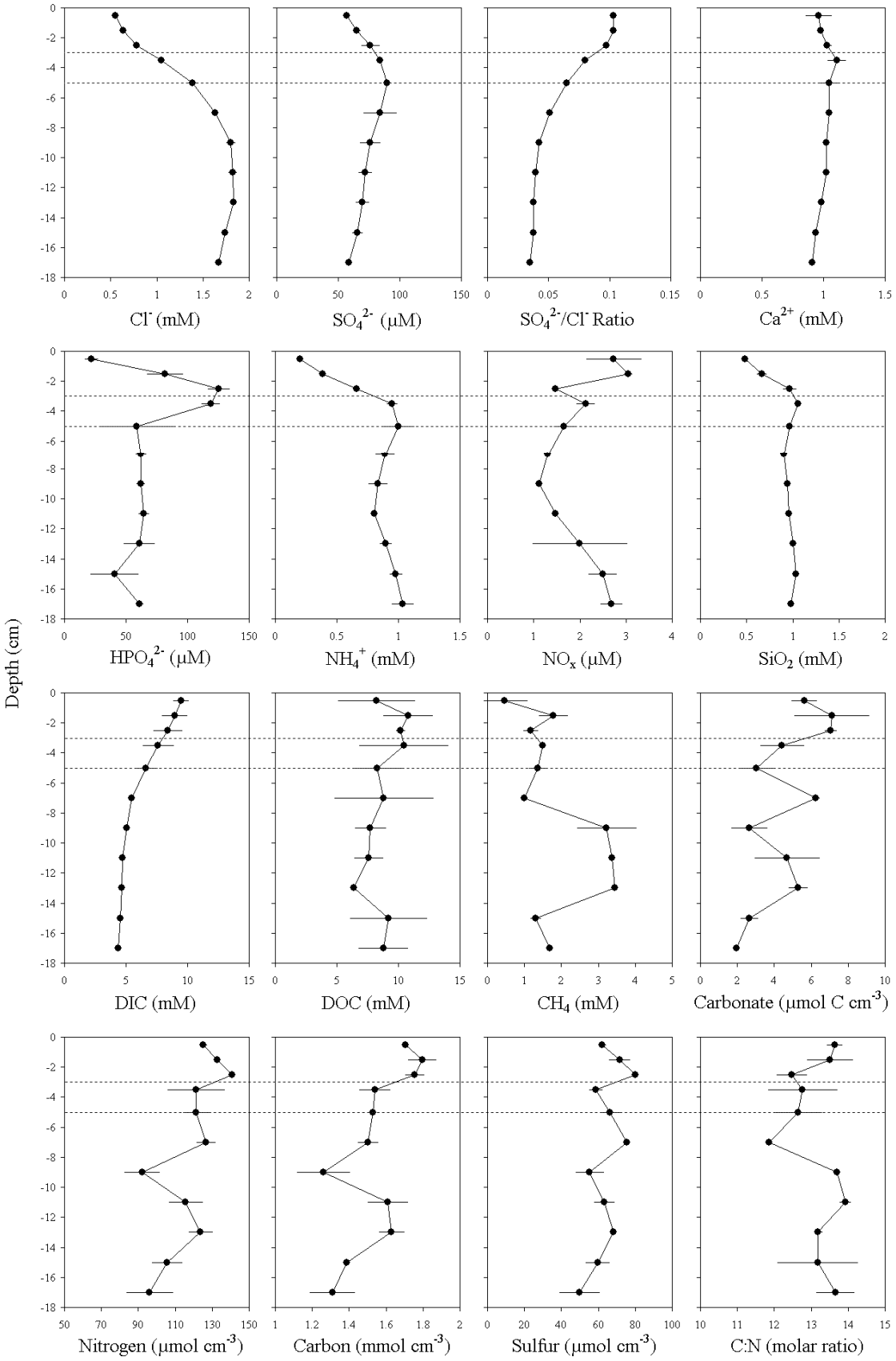
Depth (cm)
Cl⁻ (mM)
SO4 2- (µM)
SO4 2-/Cl⁻ Ratio
Ca2+ (mM)
HPO4 2- (µM)
NH4 + (mM)
NOx (µM)
SiO2 (mM)
DIC (mM)
DOC (mM)
CH4 (mM)
Carbonate (µmol C cm-3)
Nitrogen (µmol cm-3)
Carbon (mmol cm-3)
Sulfur (µmol cm-3)
C:N (molar ratio)

Figure 3.2

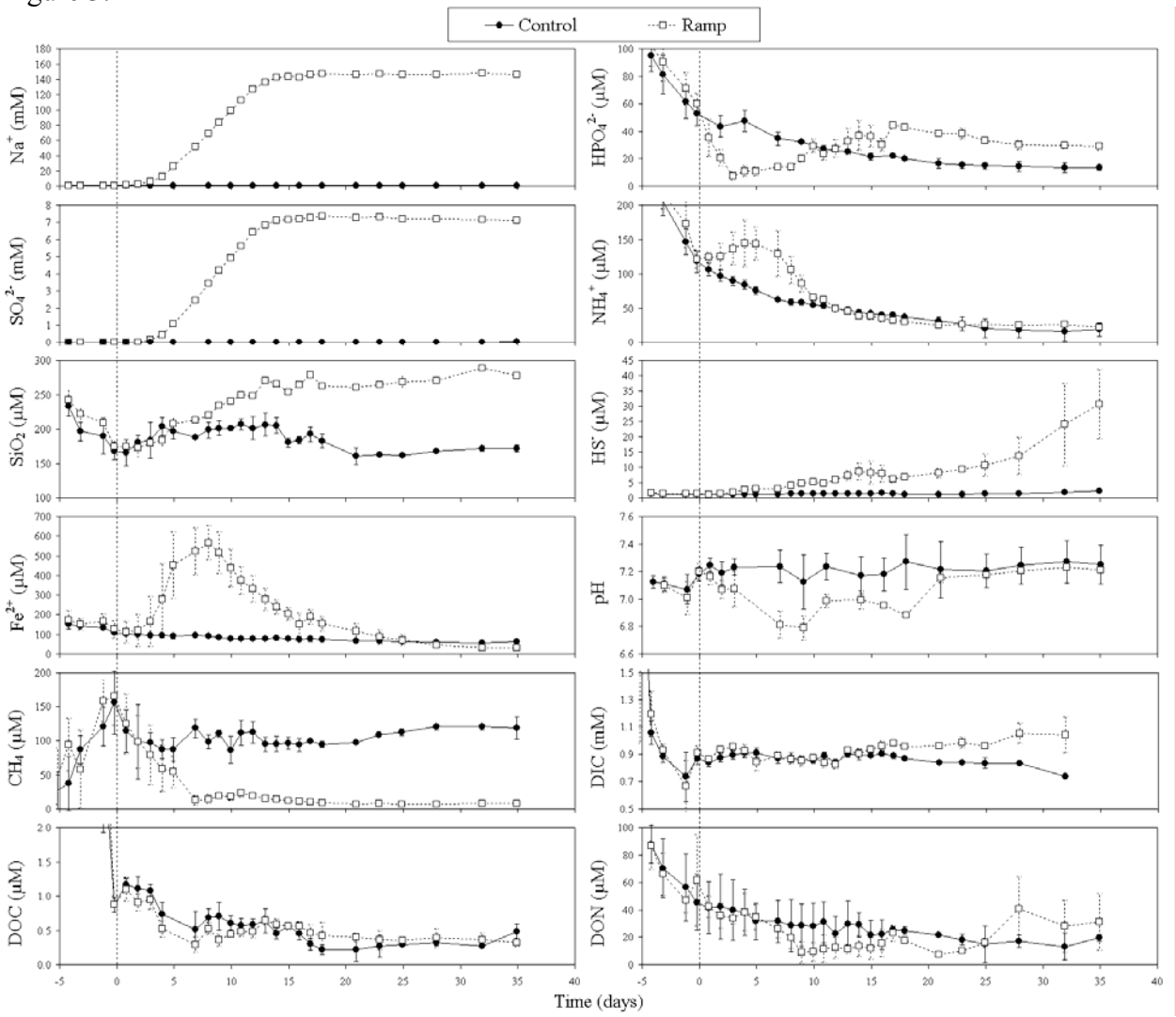
Control
Ramp
Na+ (mM)
HPO4 2- (µM)
SO4 2- (mM)
NH4 + (µM)
SiO2 (µM)
HS- (µM)
Fe2+ (µM)
pH
CH4 (µM)
DIC (mM)
DOC (µM)
DON (µM)
Time (days)

Figure 3.3

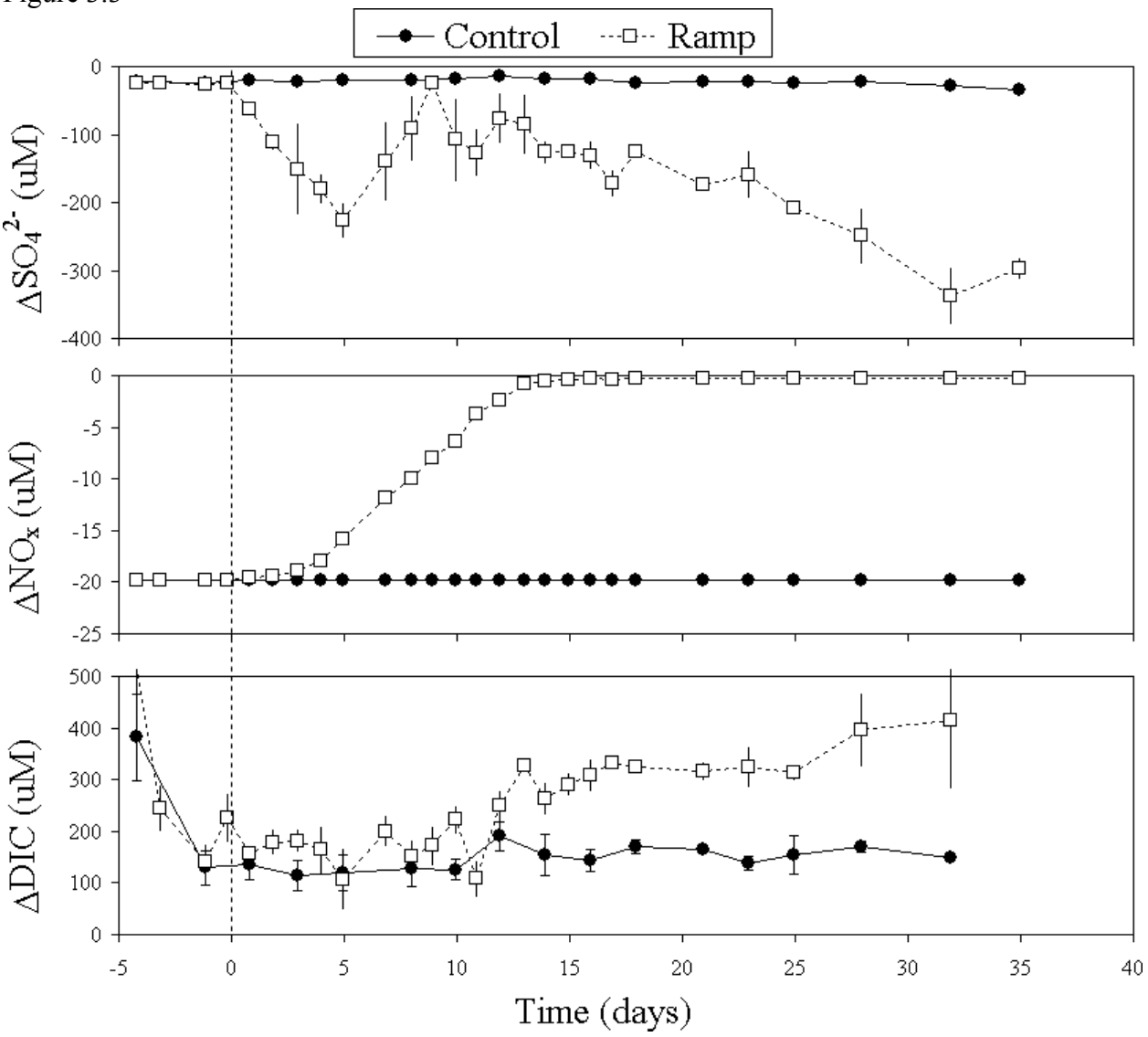
Control
Ramp
ΔSO_4^{2-} (uM)
0
-100
-200
-300
-400
ΔNO_x (uM)
0
-5
-10
-15
-20
-25
ΔDIC (uM)
500
400
300
200
100
0
-5
0
5
10
15
20
25
30
35
40
Time (days)

Figure 3.4

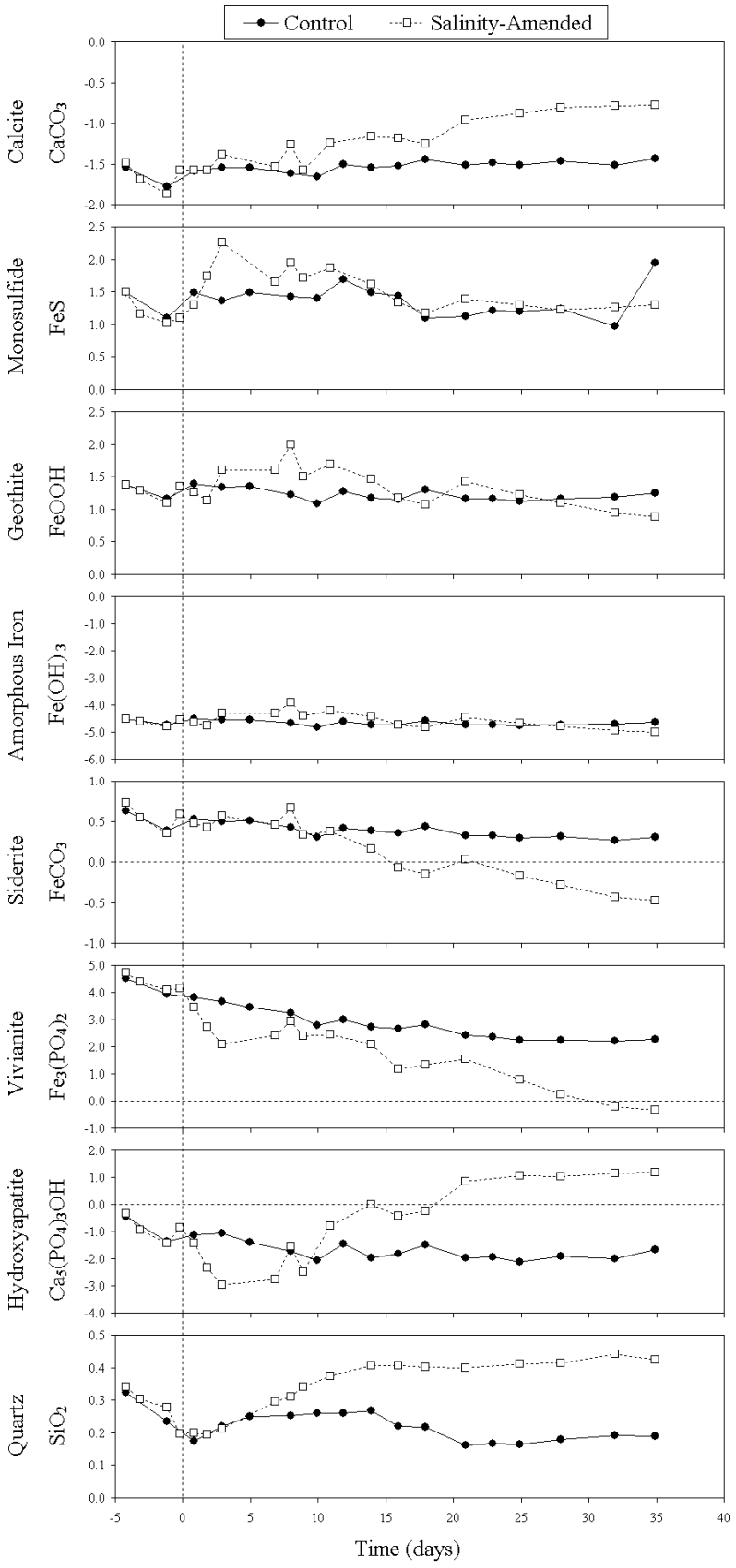
Control
Salinity-Amended
Calcite
$CaCO_3$
Monosulfide
FeS
Geothite
FeOOH
Amorphous Iron
$Fe(OH)_3$
Siderite
$FeCO_3$
Vivianite
$Fe_3(PO_4)_2$
Hydroxyapatite
$Ca_5(PO_4)_3OH$
Quartz
SiO_2
Time (days)

Figure 3.5

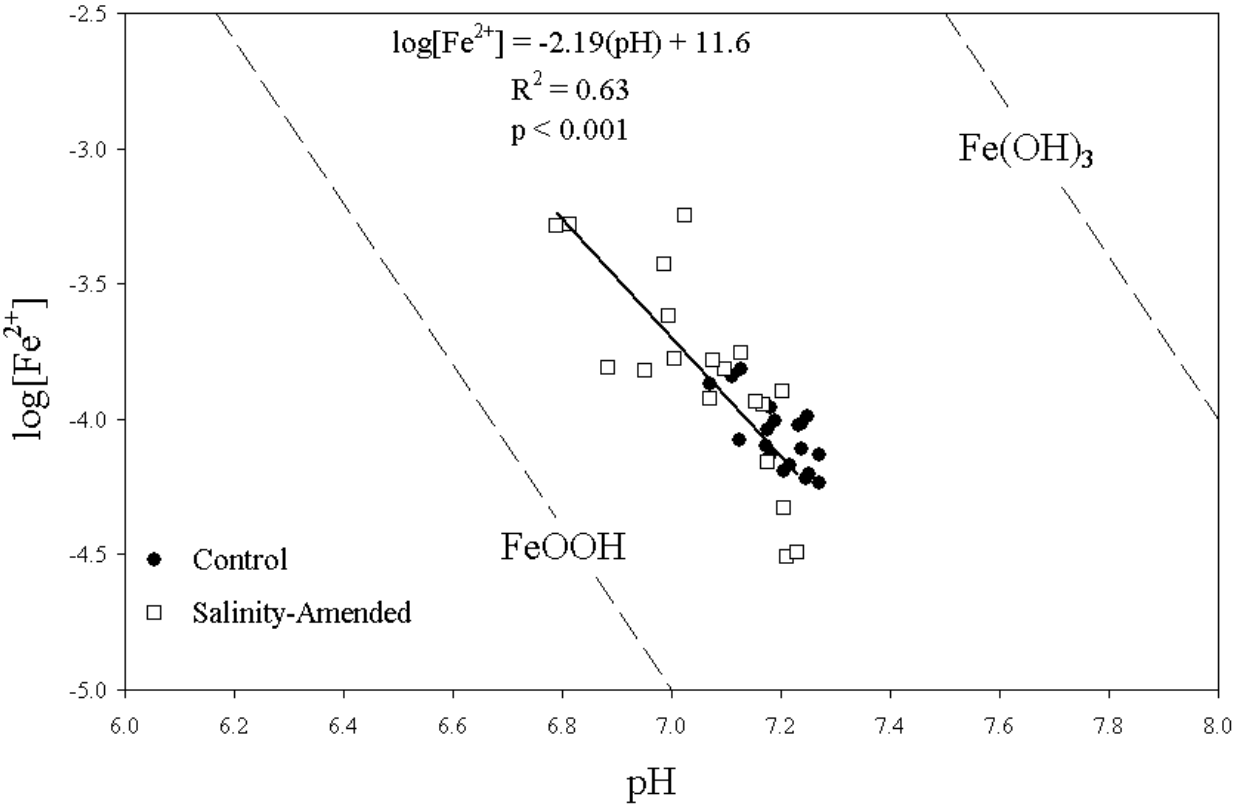
log[Fe2+] = -2.19(pH) + 11.6
R2 = 0.63
p < 0.001
Fe(OH)3
FeOOH
Control
Salinity-Amended
log[Fe2+]
pH
-2.5
-3.0
-3.5
-4.0
-4.5
-5.0
6.0
6.2
6.4
6.6
6.8
7.0
7.2
7.4
7.6
7.8
8.0

Figure 3.6

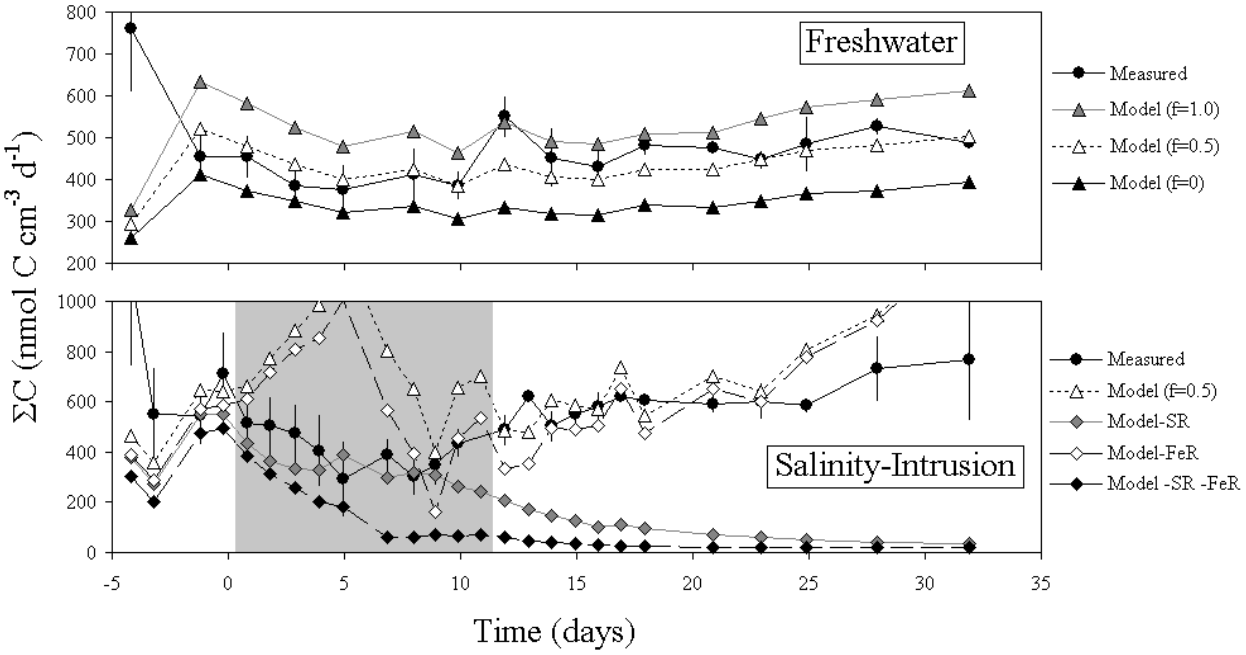
Freshwater
Measured
Model (f=1.0)
Model (f=0.5)
Model (f=0)
Salinity-Intrusion
Measured
Model (f=0.5)
Model-SR
Model-FeR
Model -SR -FeR
ΣC (nmol C cm-3 d-1)
Time (days)

Figure 3.7

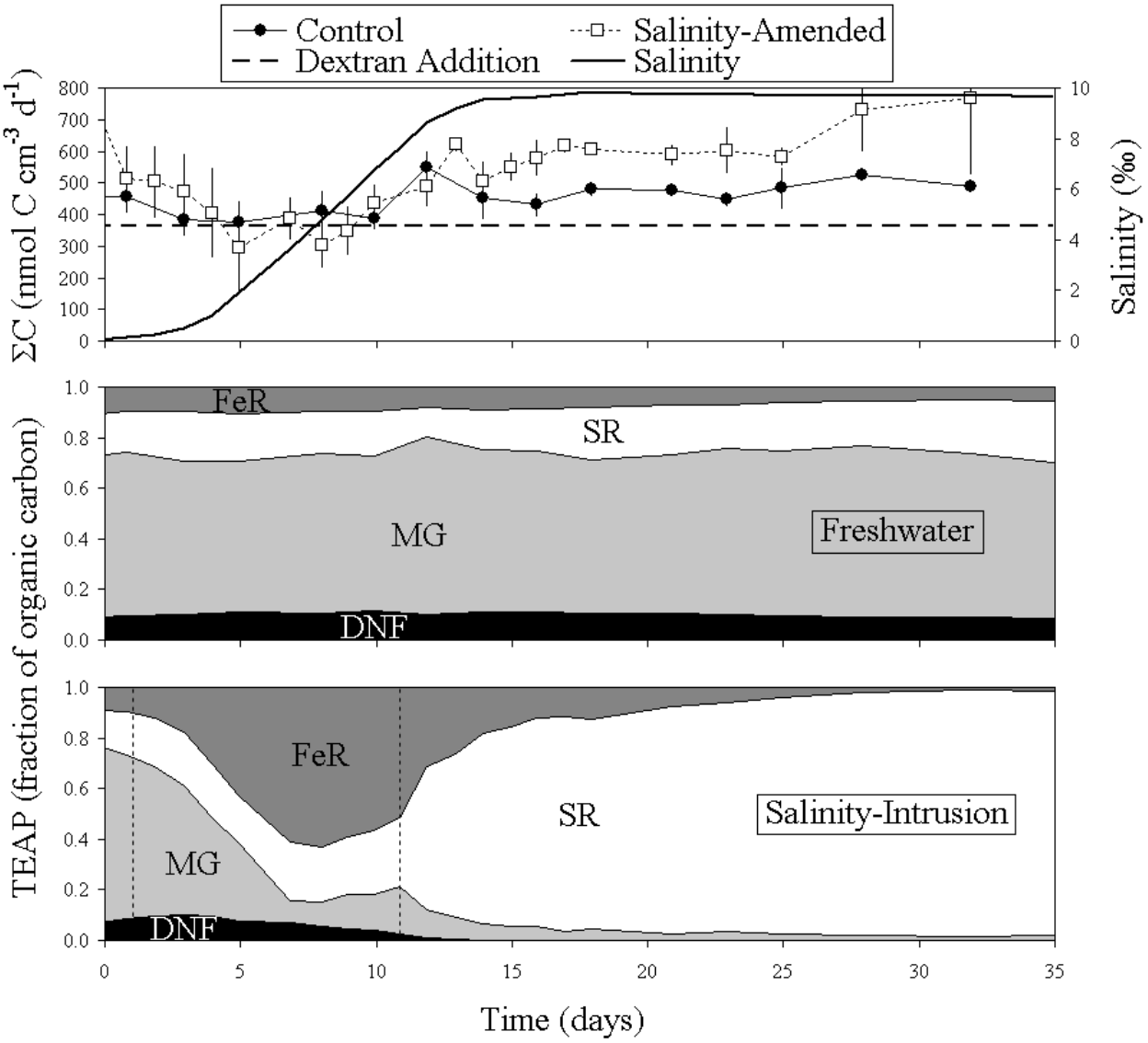
Control
Salinity-Amended
Dextran Addition
Salinity
ΣC (nmol C cm-3 d-1)
Salinity (‰)
FeR
SR
MG
DNF
Freshwater
TEAP (fraction of organic carbon)
Salinity-Intrusion
Time (days)

CHAPTER 4

POREWATER STOICHIOMETRY OF TERMINAL METABOLIC PRODUCTS, SULFATE, AND DISSOLVED ORGANIC CARBON AND NITROGEN IN ESTUARINE INTERTIDAL CREEK-BANK SEDIMENTS[1]

[1] Weston, N.B., S.B. Joye, W.P. Porubsky, V. Samarkin, M. Erickson and S.E. MacAvoy. Accepted to *Biogeochemistry* 05/26/2005.

ABSTRACT

Porewater equilibration samplers were used to obtain porewater inventories of inorganic nutrients (NH_4^+, NO_x, PO_4^{3-}), dissolved organic carbon (DOC) and nitrogen (DON), sulfate (SO_4^{2-}), dissolved inorganic carbon (DIC), hydrogen sulfide (H_2S), chloride (Cl^-), methane (CH_4) and reduced iron (Fe^{2+}) in intertidal creek-bank sediments at eight sites in three estuarine systems over a range of salinities and seasons. Sulfate reduction (SR) rates and sediment particulate organic carbon (POC) and nitrogen (PON) were also determined at several of the sites. Four sites in the Okatee River estuary in South Carolina, two sites on Sapelo Island, Georgia and one site in White Oak Creek, Georgia appeared to be relatively pristine. The eighth site in Umbrella Creek, Georgia was directly adjacent to a small residential development employing septic systems to handle waste. The large data set (> 700 porewater profiles) offers an opportunity to assess system-scale patterns of porewater biogeochemical dynamics with an emphasis on DOC and DON distributions. SO_4^{2-} depletion $(SO_4^{2-})_{Dep}$ was used as a proxy for SR, and $(SO_4^{2-})_{Dep}$ patterns agreed with measured (^{35}S) patterns of SR. There were significant system-scale correlations between the inorganic products of terminal metabolism (DIC, NH_4^+ and PO_4^{3-}) and $(SO_4^{2-})_{Dep}$, and SR appeared to be the dominant terminal carbon oxidation pathway in these sediments. The data suggest that septic-derived dissolved organic matter fueled microbial metabolism and SR at a site with development in the upland. Seasonality was observed in the porewater inventories, but temperature alone did not adequately describe the patterns of $(SO_4^{2-})_{Dep}$, terminal metabolic products (DIC, NH_4^+, PO_4^{3-}), dissolved organic carbon and nitrogen, and SR observed in this study. It appears that production and consumption of DOC are tightly coupled in these sediments, and that bulk DOC is likely a recalcitrant

pool. Preferential hydrolysis of PON relative to POC when overall organic matter mineralization rates were high appears to drive the observed patterns in POC:PON, DOC:DON and DIC:DIN ratios. These data, along with the weak seasonal patterns of SR and organic and inorganic porewater inventories, suggest that the rate of hydrolysis limits organic matter mineralization in the intertidal creek-bank sediments of this study.

INTRODUCTION

Coastal regions account for the majority of organic matter mineralization in marine sedimentary environments (Middelburg et al. 1997). Benthic-pelagic processes are tightly coupled in shallow coastal systems (Rowe et al. 1976), and sediment remineralization of organic matter provides a significant fraction of the inorganic nutrients required to support benthic and water-column primary production (Boynton & Kemp 1985, Hopkinson et al. 1999). The mineralization of particulate organic matter (POM) in anaerobic sediments is achieved largely by the coupling of hydrolytic, fermentative and terminal metabolic processes (Fenchel & Findlay 1995). Dissolved organic matter (DOM) formed by the initial hydrolysis of POM is subsequently oxidized to inorganic end products by fermenters and terminal metabolizers.

Despite the importance of DOM as an intermediate in the degradation of organic matter, relatively little is known about DOM dynamics in estuarine sediments. Seasonal concentrations of porewater dissolved organic carbon (DOC) in Chesapeake Bay and Cape Lookout Bight sediments were similar and, in general, concentrations were positively correlated with temperature (Alperin et al. 1994, Burdige 2001). Molecular size determination studies of sediment DOC suggest that a small pool of polymeric low molecular weight DOC is produced in sediments and is recalcitrant to further remineralization (Amon & Benner 1996, Burdige &

Gardner 1998). The bulk of labile DOM, however, is degraded to monomeric low molecular weight DOM that is then mineralized via terminal metabolic processes.

Much less is known about dissolved organic nitrogen (DON) dynamics in estuarine sediments. Due to the importance of nitrogen in regulating coastal system productivity (Howarth 1988), the concentrations and fate of DON in coastal sediments is relevant and potentially significant. Sediment cycling of specific fractions of DON such as amino acids (Burdige & Martens 1988) and urea (Lomstein et al. 1989) have been investigated, as have sediment DON flux rates (Hopkinson 1987, Enoksson 1993, Burdige & Zheng 1998). However, porewater profiles of total DON are sparse (Enoksson 1993, Burdige & Zheng 1998, Yamamuro & Koike 1998).

In the current study, we document seasonal and spatial patterns of DOC and DON along with, and in relation to, several other biogeochemical variables in shallow intertidal estuarine sediments at eight sites in coastal South Carolina and Georgia. Sediment porewater profiles were measured in porewater equilibration samplers to obtain seasonal steady-state inventories of DOC, DON, ammonium (NH_4^+), nitrate+nitrite (NO_x), phosphate (PO_4^{3-}), dissolved inorganic carbon (DIC), reduced iron (Fe^{2+}), chloride (Cl^-), sulfate (SO_4^{2-}), hydrogen sulfide (H_2S) and methane (CH_4) at sites across gradients in salinity in several estuarine systems. A large data set of over 700 individual profiles was obtained. A more limited amount of sediment solid phase particulate organic carbon (POC) and nitrogen (PON) pool size determinations and SO_4^{2-} reduction (SR) rate measurements were also made.

This study provides a comprehensive description of system-scale patterns of sediment biogeochemistry with emphasis on DOC and DON in intertidal creek-bank environments. Rather than focus on metabolic pathways and nutrient and organic matter dynamics at any one

site, we chose to evaluate patterns at the system-scale level. A site that appears to receive septic inputs from the adjacent residential community is discussed in more detail.

METHODS

Study Site

Eight sites in coastal Georgia and South Carolina, USA, were used to investigate shallow estuarine sediment processes (Fig. 4.1). We chose to investigate porewater biogeochemistry of intertidal creek-bank sediment in relatively small tidal creeks. These intertidal sites were macrophyte free, but benthic microalgae were present on the sediment surface at most sites. The salt marsh vegetation adjacent to the creek-bank was dominated by *Spartina alterniflora* at all sites.

Sites on the Duplin River (SAP1) and Dean Creek (SAP2) were sampled on Sapelo Island, Georgia. These pristine marsh sites are saline, but can be influenced by freshwater discharge from the Altamaha River. Two sites in the Satilla River estuarine system were also sampled. Site STL1 is in the White Oak Creek tributary to the Satilla River, and site STL2 is adjacent to the Dover Bluff residential community, and may receive septic inputs from the developed upland. The STL2, SAP1 and SAP2 sites were sampled between September 2000 and August 2003 (Table 4.1). STL1, sampled in 2002 and 2003, is an oligohaline site upstream from site STL2.

Four sites in the Okatee River Estuary system (Fig. 4.1) in South Carolina, a mid-sized tidal creek draining into the Colleton River Estuary, were sampled between 2001 and 2003 (Table 4.1). Sites OKT1, OKT3 and OKT4 were sampled along a salinity gradient in the Okatee Estuary. Salinity in the Okatee is highly dependent on freshwater discharge. Site OKT1 in the

upper reaches of the Okatee can have salinities ranging from 0 to 20 ppt. The OKT4 site further downstream in the Okatee is less influenced by freshwater discharge, with salinities typically near seawater levels. The OKT2 site on Malind Creek, a small tidal creek feeding the Okatee, typically has salinities comparable to the OKT1 site. In January 2003, an additional five sites between the OKT3 and OKT4 sites were sampled to evaluate spatial variability in porewater biogeochemistry (Table 4.1).

Experimental Design

Porewater was sampled using porewater diffusion equilibration samplers (hereafter referred to as 'peepers', Hesslein 1976), constructed from ultra high molecular weight polyethylene. Thirty 18 ml volume chambers (12 cm wide x 1 cm in height x 1.5 cm in depth) were machined at 1.5 or 2.0 cm intervals into a back-plate (14 x 60 x 2 cm), over which a 0.2 μm nylon membrane (Biotrans® Nylon Membrane) and a 0.5 cm thick cover-plate (with openings corresponding to the chambers) were placed and secured with natural nylon screws. Assembly was conducted with the sampler submerged in deionized water, with care taken to ensure the chambers were bubble free. Samplers were stored for at least five days in He purged deionized water prior to deployment.

Peepers were transported to the field sites in He purged deionized water, and duplicate peepers were deployed vertically in the unvegetated, intertidal creek-bank sediment at each site (with the exception of August 2001 and the survey sites when single peepers were deployed). At the OKT sites, peepers were deployed at two heights on the creek-bank; one approximately 0.5 m below vegetation and the other at approximately mean low water. At the SAP and STL sites, peepers were deployed parallel to the creek at approximately 0.5 m below vegetation. Peepers

were allowed to equilibrate for 6 to 8 weeks before collection. Peepers were deployed on seven dates at Georgia sites, and on three dates at South Carolina sites (Table 4.1). A total of 72 peepers were sampled at the eight sites (Table 4.1).

Ammonium (NH_4^+), nitrate+nitrite (NO_x), phosphate (PO_4^{3-}), dissolved organic carbon (DOC) and nitrogen (DON), dissolved inorganic carbon (DIC), hydrogen sulfide (H_2S), sulfate (SO_4^{2-}), chloride (Cl^-), reduced iron (Fe^{2+}), and methane gas (CH_4) were measured on the porewater inside the equilibration meter chambers.

Additionally, intact sediment cores were obtained from the STL2 and OKT4 sites in April, June and August 2002 and January 2003 for particulate organic carbon (POC) and nitrogen (PON) analysis and *ex situ* SO_4^{2-} reduction rate assays using $^{35}SO_4^{2-}$ tracer.

Porewater Analyses

Upon collection, peepers were immediately placed in thick (0.15 mm) polypropylene He purged bags and transported to the laboratory. In the lab, the peepers were placed in a He purged glove-bag (Aldrich® AtmosBag), and porewater in the chambers extracted into a gas-tight glass syringe after piercing the membrane with a needle (Becton-Dickinson® 18G) attached to the syringe and split into several containers for various analyses (Table 4.2).

All sample vials were acid-washed, rinsed with ultrapure water (Barnstead® NANOpure UV) and combusted at 500 ^oC prior to use. In the glove-bag, 1 ml of sample was injected into a He purged and crimp-sealed 6 ml headspace vial, which was then acidified with 0.1 ml of concentrated phosphoric acid. Unfiltered sample was pipetted into vials for alkalinity and H_2S determination. The remaining sample was then filtered through a 0.2 μm filter (Gelman® Acrodisk or Target® cellulose) into an 8 ml glass vial. Sample for NH_4^+ (0.1 to 0.5 ml) and for

acidification (4 ml + 0.1 ml of concentrated nitric acid) were then pipetted from this filtered sample (Table 4.2). The filtered sample remaining was saved for NO_x and TDN analysis. All vials were capped (teflon lined caps on NO_x/TDN and acidified samples) prior to removal from the glovebag. The reagents for NH_4^+, H_2S, and alkalinity were added to sample vials prior to sampling (Table 4.2).

Total alkalinity was measured immediately upon removal of vials from the glove-bag (Sarazin et al. 1999). NH_4^+ was analyzed within 2 d by standard colorimetric techniques (Solorazano 1969). NO_x (nitrate + nitrite) samples were refrigerated and analyzed within 2 weeks colorimetrically on an autoanalyzer (September 2000, January and April 2001 samples) by cadmium reduction, or vanadium reduction and nitric oxide (NO) detection on an Antek® chemiluminescent detector (745 NO_3^-/ NO_2^- reduction and 7050 NO analyzer, August 2001 and subsequent sampling dates). PO_4^{3-} was measured colorimetrically by autoanalyzer on acidified samples (Murphy & Riley 1962). SO_4^{2-} and Cl^- was determined by ion chromatography on a Dionex® DX 500 system on acidified samples. Fe^{2+} was determined on acidified samples using standard colorimetric techniques (Stookey 1970).

DIC (April 2001 and subsequent sampling dates) and CH_4 were analyzed on the gas phase of the acidified headspace vial after vigorous shaking. CH_4 and DIC were measured on a gas chromatograph equipped with a flame ionization detector (Shimadzu® GC 14A with 2 m Carbosphere column [Alltech® Instruments]) and a methanizer (Shimadzu®) to convert carbon dioxide to CH_4 for precise quantification. In September 2000 and January 2001, DIC was calculated from total alkalinity and pH, after correction for the contribution of H_2S to the alkalinity (Stumm & Morgan 1996). Comparison between the two methods for determining DIC

using a suite of sodium bicarbonate standards and porewater samples showed good agreement (<5% difference).

DOC was measured on a Shimadzu total organic carbon analyzer (TOC-5000®) on acidified (pH < 2) samples after sparging with CO_2 free air for 15 minutes. Total dissolved nitrogen (TDN), and by difference the dissolved organic nitrogen (DON = TDN - [NH_4^+ + NO_x]), was analyzed by high-temperature catalytic oxidation of unacidified samples on a Shimadzu TOC machine coupled to an Antek® NO analyzer (Álvarez-Salgado & Miller 1998). As NH_3 is volatile and was lost from the TDN samples during storage, we found it necessary to re-measure the NH_4^+ concentration on these samples to correct for the change in NH_4^+ concentration. Filter (Gelman Acrodisk® and Target® cellulose filters) blanks for the dissolved organics were determined and corrected for. DOC filter blanks were significant when using the Gelman Acrodisk® filters, but were reproducible and thus easily corrected for. DON did not have measurable filter blanks.

Porewater profiles of each constituent were obtained, and the total sediment inventory was determined by integrating profiles by depth (correcting for porosity). Total inventory per cm^2 of sediment area was calculated to a depth of 40 cm, and for depths of 0 to 10 cm and from 10 to 40 cm. SO_4^{2-} depletion of the porewater inventories was calculated as

$$(4.1) \quad (SO_4^{2-})_{Dep} = [(Cl^-_{inv}) \bullet (R_{SW})^{-1}] - SO_4^{2-}{}_{inv}$$

where $(SO_4^{2-})_{Dep}$ is the SO_4^{2-} depletion of the inventory in μmol cm^{-2}, Cl^-_{inv} and $SO_4^{2-}{}_{inv}$ are the measured Cl^- and SO_4^{2-} inventories in μmol cm^{-2}, respectively, and R_{SW} is the molar ratio of Cl^- to SO_4^{2-} in surface seawater (R_{SW} = 19.33).

$(SO_4^{2-})_{Dep}$ reflects the net amount of SO_4^{2-} consumption, presumably via SO_4^{2-} reduction, in the sediments. Cl^-, an unreactive anion is seawater, reflects the contribution of fresh versus saline waters in the porewater. As the concentrations of both Cl^- and SO_4^{2-} are orders of magnitude higher in seawater than in freshwater, the contribution of freshwater Cl^- and SO_4^{2-} to the inventories in the porewater is negligible, and freshwater dilutes seawater Cl^- and SO_4^{2-} concentrations. As the Cl^- to SO_4^{2-} ratio of seawater is constant (Pilson 1988), the 'expected' inventory of SO_4^{2-} can be calculated from the measured inventory of Cl^-. The observed (measured) SO_4^{2-} inventory is then subtracted from the 'expected' inventory, providing an estimate of SO_4^{2-} depletion, and thus net patterns of sulfate reduction, in the sediment column. DIC inventories were corrected for background overlying water DIC concentrations.

Solid Phase and Sulfate Reduction Rate Measurements

POC and PON were measured at the STL2 and OKT4 sites on four dates (Table 4.1). Additionally, particulates were measured at the SAP1, SAP2, OKT1 and OKT3 sites in April 2002, and at the SAP2 site in August 2002. In January 2003, triplicate cores were obtained at the STL2 and OKT4 sites for POC and PON analysis to evaluate spatial variability. Intact sediment cores (7.8 cm inner diameter) were sectioned within two days of collection, and sediment samples dried at 80 ºC and ground. Both acidified (1 N HCl) and unacidified samples were analyzed on a ThermoFinnigan Flash EA 1112 Series NC analyzer to determine carbon and nitrogen content. Sediment POC content was determined for acidified samples (after removal of carbonates).

Sulfate reduction (SR) rates were determined on four dates at the STL2 and OKT4 sites, and on two dates at the SAP2 site (Table 4.1). Triplicate sub-cores (0.8 cm inner diameter) were

collected at 7 depths from intact sediment cores, capped with a rubber stoppers, and injected with 50 µl (about 2 µCi) of a $Na_2{}^{35}SO_4$ solution. Samples were incubated for 12 to 24 hours at *in situ* temperatures and then transferred to 50 ml centrifuge tubes containing 10 ml of 20% zinc acetate solution to halt microbial activity and fix $H_2{}^{35}S$ as $Zn^{35}S$ and frozen. Samples were then centrifuged, and rinsed with N_2 purged distilled water and centrifuged several times to remove surplus $^{35}SO_4{}^{2-}$. The rinse water was saved to determine $^{35}SO_4{}^{2-}$ activity. The rinsed sediment was then subjected to a one-step hot chromous acid distillation to recover reduced ^{35}S (Canfield et al. 1986). The H_2S produced during the distillation was trapped in two in-line 5 ml zinc acetate traps. The activity of both the reduced sulfur and $SO_4{}^{2-}$ fractions was determined by scintillation counting (Beckman® LS 6500 scintillation system) of sample in ScintiSafe® Gel LSC Cocktail. The $SO_4{}^{2-}$ reduction rate was calculated as:

$$(4.2) \quad SR = ([{}^{35}S_{reduced}] \bullet [{}^{35}SO_4{}^{2-}]^{-1}) \bullet [SO_4{}^{2-}] \bullet ø \bullet \alpha SO_4{}^{2-} \bullet t^{-1}$$

where the $SO_4{}^{2-}$ reduction rate (SR) rate is expressed as µmol $SO_4{}^{2-}$ reduced per cm^{-3} of sediment per d^{-1}, $[{}^{35}S_{reduced}]$ is the activity of the reduced sulfur pool, $[{}^{35}SO_4{}^{2-}]$ is the activity of the substrate pool added at the beginning of the experiment, $[SO_4{}^{2-}]$ is the pore water $SO_4{}^{2-}$ concentration (mM), ø is the sediment porosity, $\alpha SO_4{}^{2-}$ is the isotope fractionation factor for $SO_4{}^{2-}$ reduction (1.06; Jørgensen, 1978), and t is incubation time (days). Total sediment rates (µmol cm^{-2} d^{-1}) were obtained by integrating the rate profile over depth, taking into account the porosity.

RESULTS

A total of 72 sets of porewater profiles of NH_4^+, NO_x, PO_4^{3-}, DIC, DOC, DON, Fe^{2+}, Cl^-, SO_4^{2-}, H_2S and CH_4 were obtained at eight sites on several different dates (Table 4.1). Two profiles, from the STL2 and SAP1 sites in August 2002, are shown in Figure 4.2 as examples of the data obtained in this study. A subset of detailed data [Cl^-, DIC, $(SO_4^{2-})_{Dep}$ and NH_4^+] from duplicate porewater profiles at sites STL2 and OKT3 are shown in Figure 4.3. Due to the large number of individual profiles, seasonal and system-scale patterns are illustrated by the trends observed in depth-integrated porewater inventories.

Between-Site Comparisons

Comparison between sites was conducted on average porewater inventory data. The salinity gradients of the Georgia and South Carolina estuarine sites can be observed in the porewater Cl^- inventories. The seasonally averaged porewater inventories of Cl^- were lowest at the STL1 and OKT1 sites in Georgia and South Carolina, respectively, while the SAP2 and OKT4 sites had porewater Cl^- pools that approached full-strength seawater (Fig. 4.4).

The STL2 site had significantly higher average porewater inventories of NH_4^+, PO_4^{3-}, DON, DIC and $(SO_4^{2-})_{Dep}$ (Equation 4.1) than any of the other sites ($p < 0.05$, ANOVA and Tukey pairwise comparison, Fig. 4.4). Fe^{2+} inventories were higher at the SAP2 site than all sites except OKT2 ($p < 0.05$). There was no significant difference in the NO_x, DOC, H_2S, and CH_4 inventories between sites ($p > 0.05$), although the less saline sites (STL1, OKT1, OKT2) and the STL2 site did tend to have higher CH_4 (Fig. 4.4).

System-Scale Patterns

Regressions between porewater inventories (0 - 10 cm and 10 - 40 cm) and average air temperature during the peeper deployment period, porewater inventories of Cl^-, and inventories of $(SO_4^{2-})_{Dep}$ were made to determine seasonality of and correlations between the various geochemical variables (Table 4.3, excluding the STL1 site and 'survey' sites due to small sample sizes). These regressions were also performed on data pooled from all sites with the exception of the STL2 site, due to the markedly different biogeochemical signature of this site (Fig. 4.4).

$(SO_4^{2-})_{Dep}$ inventories from 0 to 40 cm were positively correlated with temperature at the SAP1, OKT3 and OKT2 sites, and in surface 10 cm at the STL2 and SAP1 sites. H_2S, NH_4^+ and PO_4^{3-} inventories also increased with warmer temperatures at several of the sites (Table 4.3). However, there was no significant correlation between DIC or CH_4 and temperature, and correlations between Fe^{2+} or DON and temperature at only one site. DOC decreased with higher temperatures in the surface 10 cm at the SAP1 site only. When data were pooled for all sites excluding STL2, inventories of NH_4^+, $(SO_4^{2-})_{Dep}$, and H_2S in both surface (0-10 cm) and deep (10-40 cm) porewater was positively correlated with temperature (Table 4.3).

Seasonality was observed in the Cl^- pools, and this variability correlated with freshwater discharge to the coastal zone (Fig. 4.5). Cl^- inventories were negatively correlated with the deployment period river discharge (data obtained from the United States Geological Survey) at the STL2, SAP1 and SAP2 sites in Georgia ($p < 0.05$, Altamaha River) and the OKT1 and OKT4 sites in South Carolina ($p < 0.05$, Savannah River, data not shown). There was little correlation between other measured variables and porewater inventories of Cl^- (Table 4.3).

Higher inventories of DOC were measured at several OKT sites when porewater inventories of Cl^- were higher, while DON inventories decreased with Cl^- at the SAP1 site (Table

4.3). $(SO_4^{2-})_{Dep}$ to 40 cm was correlated with Cl^- inventories at the SAP2 site. At the SAP1 site, higher salinity sampling dates exhibited lower DIC and DON inventories, but increased $(SO_4^{2-})_{Dep}$ to 10 cm. CH_4 was negatively correlated with Cl^- inventories when data from all sites (excluding STL2) was pooled, and Fe^{2+} inventories were higher in 10-40 cm porewater (Table 4.3).

Porewater inventories of the measured biogeochemical variables were compared with $(SO_4^{2-})_{Dep}$ inventories at each site (Table 4.3). Surface and deep inventories of DIC, NH_4^+ and PO_4^{3-} were positively correlated with $(SO_4^{2-})_{Dep}$ at several of the sites ($p < 0.05$). A number of the other measured variables were significantly correlated with $(SO_4^{2-})_{Dep}$ inventories in these porewaters (Table 4.3).

Data pooled from all sites (except STL2) and from site STL2 alone was regressed against $(SO_4^{2-})_{Dep}$ inventories (Table 4.3, Figs. 4.6 and 4.7). Pools of DIC, NH_4^+ and PO_4^{3-} were significantly correlated with $(SO_4^{2-})_{Dep}$ inventories (Fig. 4.6). The slopes of NH_4^+ and PO_4^{3-} versus $(SO_4^{2-})_{Dep}$ were greater at the STL2 site compared to the 'all sites', although the DIC to $(SO_4^{2-})_{Dep}$ slopes were similar (Fig. 4.6).

DOC was not significantly correlated with $(SO_4^{2-})_{Dep}$ ratios when data was pooled for all sites, but DOC decreased with $(SO_4^{2-})_{Dep}$ at the STL2 site (Fig. 4.7). DON inventories were positively correlated with $(SO_4^{2-})_{Dep}$ for 'all sites' and, although DON at the STL2 site was not correlated with $(SO_4^{2-})_{Dep}$, the STL2 values fall in-line with the 'all sites' values (Fig. 4.7).

Inventories of NH_4^+, PO_4^{3-}, DIC, H_2S and DON in both surface and deep porewaters were positively correlated with $(SO_4^{2-})_{Dep}$ inventories for data from 'all sites' (Fig. 4.6, Table 4.3, $p < 0.05$), while NO_x pools in both the 0-10 and 10-40 cm depths declined slightly with increasing

$(SO_4^{2-})_{Dep}$ ($p < 0.05$, Table 4.3). Fe^{2+}, CH_4 and DOC inventories were not correlated with $(SO_4^{2-})_{Dep}$ for pooled data (Table 4.3, $p > 0.05$).

Molar ratios of DIN (NH_4^+) to DIP (PO_4^{3-}) inventories, when two outlying points were removed, were positively correlated with $(SO_4^{2-})_{Dep}$ ($p < 0.05$, Fig. 4.8) for data pooled from all sites. A similar relationship was found at the STL2 site ($p < 0.05$, Fig. 4.8), although the increase in the DIN:DIP ratio with increasing $(SO_4^{2-})_{Dep}$ was slightly greater. DIC:DIN and DOC:DON ratios were highest at low $(SO_4^{2-})_{Dep}$, and decreased with increasing $(SO_4^{2-})_{Dep}$ [$p < 0.01$, log transformed $(SO_4^{2-})_{Dep}$, Fig. 4.8]. These relationships were significant for all data pooled as well as when data from site STL2 was removed ($p < 0.01$).

Sediment Solid-phase and Sulfate Reduction Rates

POC content ranged from 0.1 to 5.0 weight % and PON content from 0.05 to 0.8 weight % in these sediments. Sediment POM content was integrated with depth to 40 cm to obtain inventories of POC and PON (Table 4.4). There was not a clear difference in POM content between sites, although the SAP2 site had lower POC than the OKT4 and STL2 sites on two of the measurement dates. Molar ratios of POC:PON followed a very similar seasonal trend at the OKT4 and STL2 sites (Fig. 4.9), increasing from April to a maximum in August, and subsequently decreasing into January.

Sulfate reduction rates generally decreased with depth in the sediment, although a shallow subsurface (5-10 cm) peak in activity was occasionally observed (data not shown). Integrated SR rates (to 40 cm) ranged from 0.3 to over 5 μmol cm^{-2} d^{-1} (Table 4.4). The STL2 site had higher rates of SO_4^{2-} reduction than the OKT4 and SAP2 sites, except in June 2002 (Table 4.4).

DISCUSSION

Over 70 sets of porewater profiles of nutrients (NH_4^+, NO_x and PO_4^{3-}), dissolved organics (DOC and DON), DIC, CH_4, Fe^{2+}, H_2S, Cl^- and SO_4^{2-} were integrated by depth to obtain porewater inventories at eights sites on several sampling dates (Table 4.1). The data discussed here offer a unique opportunity to assess spatial and temporal patterns of intertidal creek-bank sediment porewater stoichiometry and biogeochemistry in several estuarine systems.

Terminal Metabolic Pathways

Terminal oxidation of organic matter in sediments is coupled to the reduction of electron acceptors, the use of which depends on thermodynamic (relative energy yield) and kinetic (reactivity and availability) constraints (Froelich et al. 1979). Generally, aerobic respiration (O_2 reduction) is followed by denitrification (NO_3^-), metal reduction (manganese and iron oxides), SO_4^{2-} reduction, and finally methanogenesis (largely, acetate fermentation or CO_2 reduction). The variation in the net rates of terminal electron accepting processes over depth creates a biogeochemical zonation in sediments (Froelich et al. 1979). In coastal marine sediments and salt marshes, the availability of SO_4^{2-} relative to other terminal electron acceptors makes SO_4^{2-} reduction account for the majority of anaerobic carbon oxidation (Jørgensen 1982; Howarth 1993), although iron reduction can be an important pathway as well (Kostka 2002*a*). In freshwater sediments, the low concentration of SO_4^{2-} results in the increased importance of methanogenesis (Capone & Kiene 1988) and iron reduction (Roden & Wetzel 1996).

Porewater inventories as measured in this study (Fig. 4.4) were used to evaluate patterns and pathways of organic matter mineralization in intertidal estuarine sediments. The spatial scale of porewater inventories using data from equilibration samplers, which provide a quasi steady-

state profile, must be considered. Non-diffusive transport processes have the largest effect near the sediment-water interface in muddy sediments (bioturbation) or at depth along sedimentological discontinuities (e.g. deeper sand layers). Intertidal creek-bank sediments in the study area are often populated by burrowing macrofauna (Teal 1958), which can enhance solute exchange between porewater and the overlying water (Meile et al. 2001). However, bioturbation affects mainly porewater concentrations in the upper 5 cm of sediment in intertidal estuarine sites (Meile et al. 2001), and very few burrows were observed on intertidal creekbank sediments during field sampling trips, with the exception of the SAP2 site.

The muddy estuarine sites we studied are largely diffusion-dominated even near the sediment-water interface. A detailed examination of the profiles obtained in this study suggested that the majority (>90%) exhibited classical diffusive patterns (e.g. Fig. 4.2 and site STL2, Fig. 4.3). It is difficult to state with confidence that profiles are largely diffusive in nature and not influenced by bioturbation or advection. However, at the OKT sites, where peepers were placed perpendicular to the creek at different heights on the bank, the importance of advection in controlling profiles may be more readily apparent. A small subset of equilibration profiles did exhibit what appear to be advective signals (e.g. site OKT3, Fig. 4.3), in which the upper and lower peepers had variable chloride profiles, corresponding to variable profiles in other measured variables [DIC, $(SO_4^{2-})_{Dep}$ and NH_4^+]. These patterns were observed in relatively few peeper profiles, however, and we argue that the porewater equilibration inventories as presented in this paper represent the net metabolic processes occurring in the largely diffusion-dominated sediment column.

Porewater inventories reflect the balance between production/consumption and transport processes. Rapid turnover of substrates and products complicates the use of integrated

inventories to identify dominant terminal electron accepting processes. Concentrations of substrates and/or products of several terminal electron-accepting processes are maintained at low concentrations in porewaters because of close coupling between processes. For instance, nitrification-denitrification may be closely coupled in the sediments, keeping NO_3^- concentrations low (Seitzinger 1988) and making NO_3^- inventories an unsuitable proxy for denitrification. CH_4 produced during methanogenesis may be subsequently oxidized anaerobically (Iversen & Jørgensen 1985) or aerobically (Sansone & Martens 1978), making CH_4 inventories a poor indicator of gross methanogenesis rates. Similarly, Fe^{2+} produced by iron reduction may be re-oxidized and/or precipitated, resulting in underestimates of iron reduction rates from Fe^{2+} inventories. In contrast, SO_4^{2-} concentrations in seawater are relatively high (millimolar levels), and although reoxidation of H_2S occurs in the sediment, sufficient drawdown of the SO_4^{2-} pool in sediments leads to significant change in SO_4^{2-} concentration with depth, and this depletion can be used to infer patterns of net SO_4^{2-} reduction.

We consider porewater inventories of $(SO_4^{2-})_{Dep}$ to be a proxy for patterns of net integrated SO_4^{2-} reduction rates in the estuarine sediments we studied. Patterns of sulfate reduction measured with radiotracer methods agreed with patterns of $(SO_4^{2-})_{Dep}$ at the three sites where SO_4^{2-} reduction rate measurements were made (Fig. 4.10), suggesting that variability in $(SO_4^{2-})_{Dep}$ reflected rates of net SO_4^{2-} reduction at the sites rather than variability in transport or other processes. The slopes of the regressions between $(SO_4^{2-})_{Dep}$ and DIC at several of the sites and for pooled data was around 2 in the deeper porewaters (Tables 4.3 and 4.5, Fig. 4.6). The theoretical stoichiometry of SO_4^{2-} reduction coupled to the oxidation of organic matter:

$$(4.3) \quad 2\,CH_2O + SO_4^{2-} \rightarrow 2\,HCO_3^- + H_2S$$

yields a SO_4^{2-} uptake to DIC release ratio of 2 (Jørgensen 2000), providing further evidence that sulfate reduction was the dominant pathway of anaerobic organic matter mineralization at these sites.

Depth-integrated sulfate reduction rate measurements (Table 4.4) are similar in magnitude to the benthic oxygen demand at several of the same sites, while measured rates of denitrification are orders of magnitude smaller (Porubsky et al. *In Preparation*). Because oxidation of reduced sulfur can account for a large fraction of the sediment oxygen demand (Jørgensen 1977), sediment SO_4^{2-} reduction may be as or more important than aerobic respiration in the intertidal creekbank sediments we studied.

As mentioned previously, observations at the SAP2 site indicated a higher density of burrow networks than at other sites. Bioturbation can promote reoxidation of reduced compounds at depth in the sediment (Aller & Aller 1998), and may increase iron oxides available to iron reducing bacteria (Kostka et al. 2000*a*, Nielsen et al. 2003). Lowe et al. (2000) found large populations of iron reducing bacteria in surficial sediments at a site near the SAP2 site on Sapelo Island, and Kostka et al. (2000*b*) measured high rates of iron reduction in similar sediments. The SAP2 site inventories of Fe^{2+} were higher than at other sites (Fig. 4.4) suggesting that rates of microbial iron reduction may have been greater at this site than the other sites we studied.

The relationships between the porewater inventories of several metabolic products (DIC, NH_4^+, PO_4^{3-}, H_2S) and inventories of $(SO_4^{2-})_{Dep}$ from sites across a range of salinities (Fig. 4.4) and several different estuarine systems (Fig. 4.1) are noteworthy (Table 4.3, Fig. 4.6). The magnitude of the inventories of $(SO_4^{2-})_{Dep}$ compared with NO_3^-, CH_4 and Fe^{2+} inventories (Fig. 4.4) and the apparent coupling of the products of organic matter mineralization (DIC, NH_4^+,

PO_4^{3-}, H_2S) with $(SO_4^{2-})_{Dep}$ (Fig. 4.4, Table 4.3) suggests that SO_4^{2-} reduction was the dominant pathway of anaerobic organic matter oxidation, but the regulation of SO_4^{2-} reduction is complex.

Spatial and Temporal Patterns

Temperature

There was seasonal temperature-driven variation in $(SO_4^{2-})_{Dep}$, NH_4^+, and H_2S inventories (Table 3). Rates of SO_4^{2-} reduction often follow a seasonal pattern similar to that of temperature in estuarine sediments and salt marshes (Jørgensen & Sørensen 1985, King 1988, Westrich & Berner 1988). The relationship between temperature and $(SO_4^{2-})_{Dep}$, H_2S and NH_4^+ suggests that temperature does contribute to the regulation of SO_4^{2-} reduction rates in these sediments. However, measured SO_4^{2-} reduction rates (Table 4.4) do not follow the expected seasonal pattern, and the agreement between temperature and porewater inventories is not generally very strong (Table 4.3). In short, temperature alone cannot explain the patterns we have documented. Variation in the relative importance of pathways of organic matter oxidation (Kostka et al. 2002*b*), inherent small-scale variation in the estuarine creek-bank environment, and organic carbon availability to sulfate reducers (Westrich & Berner 1988, Marvin-DiPasquale & Capone 2003; V. Samarkin unpublished data) may contribute to the observed patterns. Controls on organic matter mineralization will be discussed further in the "*System-Scale Patterns of DOM*" section.

Salinity

Salinity at these estuarine sites changed on seasonal timescales, corresponding to spring discharge events and increased river discharge to the coastal zone (Fig. 4.5). Changes in

porewater Cl^- did not appear to effect porewater pools of inorganic components (Table 4.3). Salinity influences the adsorption of NH_4^+ (Rosenfeld 1979) and PO_4^{3-} (Sundareshwar & Morris 1999) to sediment particles. The magnitude of seasonal salinity changes at any one site, however, may not be sufficient to influence porewater NH_4^+ and PO_4^{3-} concentrations relative to other factors. Additionally, salinity can influence microbial processes such as nitrification and denitrification through direct inhibition (Rysgaard et al. 1999). Alternately, with increases in salinity, SO_4^{2-} concentrations increase, and sulfide produced from SO_4^{2-} reduction can inhibit nitrification (Joye & Hollibaugh 1995). We noted a slight but significant decrease of NO_x pools with increasing $(SO_4^{2-})_{Dep}$ inventories (Table 4.3), suggesting that net nitrification was lower when SO_4^{2-} reduction rates were high. However, coupled nitrification-denitrification occurs at the oxic-anoxic boundary in sediments (Seitzinger 1988), and in the estuarine sediments of this study oxygen is depleted within a few mm (Joye & Lee unpublished data). Porewater equilibration samplers may not have the depth resolution (1.5 cm intervals) to adequately capture the steep gradients at the depths where nitrification occurs. Nutrient dynamics are discussed further in the "*Inorganic N:P Ratios*" section.

Increased SO_4^{2-} availability associated with higher salinities also influences the balance between SO_4^{2-} reduction and methanogenesis, as methanogens are usually out-competed by SO_4^{2-} reducers for certain substrates when SO_4^{2-} is not limiting (Capone & Kiene 1988). There was, not surprisingly, a strong correlation between Cl^- and SO_4^{2-} inventories (data not shown), such that the less saline sites (STL1, OKT1 and OKT2) had significantly lower SO_4^{2-} than the more saline sites (SAP1, SAP2, OKT3 and SAP2). SO_4^{2-} concentrations declined with depth in porewaters at the less saline sites, and at the STL2 site, to concentrations of SO_4^{2-} (<1 mM) that likely were limiting to SO_4^{2-} reducers (Roychoudhury et al. 1998). At the other saline sites

(excluding STL2), SO_4^{2-} concentrations did not limit SO_4^{2-} reducers. Methanogenesis at depth in the fresher (STL1, OKT1 and OKT2) and STL2 sites, due to substrate limitation of SO_4^{2-} reducers, resulted in a trend of higher CH_4 inventories. While this pattern was not evident seasonally at any single site, the effect of salinity on CH_4 inventories was apparent across sites independent of time (Table 4.3). The differences in CH_4 inventories between the fresh (and STL2) and saline sites were not significant due to high variability, but the fresher sites did have higher CH_4 pools (Fig. 4.4). This suggests a larger fraction of organic carbon was oxidized via methanogenesis at the STL1, STL2, OKT1 and OKT2 sites where SO_4^{2-} availability limited the extent of SO_4^{2-} reduction.

Influence of Development in the Upland

The higher porewater inventories of $(SO_4^{2-})_{Dep}$, NH_4^+, PO_4^{3-}, DIC and DON at the STL2 site (Fig. 4.4) clearly set this site apart from the other sites we studied. The STL2 site is adjacent to a residential community that utilizes septic systems to process household waste. Septic-derived materials may influence porewater concentrations and rates of microbial transformations at this site. Septic systems do not appear to efficiently process human waste, and septic-derived nutrient inputs can lead to the eutrophication of surface waters (Moore et al. 2003). Septic-derived waste also has high concentrations of inorganic nutrients and dissolved organic matter (Ptacek 1998).

The relationships between $(SO_4^{2-})_{Dep}$ and DIC inventories were similar at all sites and at site STL2 alone (Fig. 4.6). However, NH_4^+ and PO_4^{3-} increased considerably more with increasing $(SO_4^{2-})_{Dep}$ inventories at the STL2 site compared to other sites (Fig. 4.6). The $(SO_4^{2-})_{Dep}$ to NH_4^+ and PO_4^{3-} ratios, derived from the slopes of these lines, were about 50% lower at the

STL2 site [except for the $(SO_4^{2-})_{Dep}$ to PO_4^{3-} ratio in surface sediments; Table 4.5]. This pattern may be due in part to the advection of nutrient-rich septic water from the upland, but the close coupling with $(SO_4^{2-})_{Dep}$ (Fig. 6) suggests microbial processing *in situ*. The high $(SO_4^{2-})_{Dep}$ inventories (Fig. 4.4) and measured SO_4^{2-} reduction rates (Table 4.4) provide further evidence that these patterns result from something more than simply increased nutrient inputs. It is impossible to estimate the stoichiometric composition of mineralized organic matter from measured porewater inventories unless differential adsorption and diffusion corrections are made (Berner 1977). It does, however, appear that there is large difference between the SO_4^{2-}:C:N:P ratios at STL2 compared to all other sites in this study.

Septic waste contains high concentrations of DOC (Ptacek 1998), and although DOC inventories were not significantly higher at the STL2 site than other sites due to variability between sites and dates, DOC inventories were slightly elevated at this site (Fig. 4.4). Furthermore, DON pools were elevated significantly at the STL2 site (Fig. 4.4). We hypothesize that N- and P-rich labile septic-derived DOM from the upland stimulated the coupled fermentative and SO_4^{2-} reducing community at this site. The stimulation of microbial sulfate reduction and mineralization of this N- and P-rich DOM resulted in increased porewater inventories of NH_4^+, PO_4^{3-} and $(SO_4^{2-})_{Dep}$. Stimulation of benthic and water-column primary production in the estuary by nutrient inputs from the upland may have also provided additional organic matter for metabolism in these sediments. Advection of nutrient-rich septic-influenced water from the upland also likely contributed to the higher NH_4^+ and PO_4^{3-} inventories. On-going work is addressing this hypothesis directly.

Inorganic N:P Ratios

The increasing NH_4^+:PO_4^{3-} ratios of porewater pools with higher $(SO_4^{2-})_{Dep}$ inventories (Fig. 4.8) suggests either that the N:P ratio of the organic matter undergoing mineralization changed with the rate of metabolism (i.e., seasonally), or that nitrification-denitrification preferentially removed nitrogen from the sediments relative to phosphorus, particularly when SO_4^{2-} reduction rates were low. The second mechanism is tempting to consider as (discussed above) NO_x inventories were higher when $(SO_4^{2-})_{Dep}$ inventories were lower (Table 4.3). NH_4^+:PO_4^{3-} inventory ratios were quite low when $(SO_4^{2-})_{Dep}$ was low, often below the Redfield (1958) ratio of 6.6 (Fig. 4.8), again indicating that NH_4^+ may have been removed via coupled nitrification-denitrification. The inhibitory effects of H_2S produced from SO_4^{2-} reduction on nitrification (Joye & Hollibaugh 1995) when SO_4^{2-} reduction rates were high [i.e. high $(SO_4^{2-})_{Dep}$] may account for this trend in NH_4^+:PO_4^{3-} ratios.

System-Scale Patterns of Porewater Creek-bank DOM

DOC and DON concentrations were higher than most previous studies have reported for coastal sediments. DOC and DON in excess of 10 mM and 500 μM, respectively, were often measured at depth in the sediment porewater (Fig. 4.2). We examined intertidal sediment DOM in relatively small tidal creeks, and are unaware of any published DOM data from similar systems. Coastal subtidal marine sediment DOC concentrations of generally <3 mM (Burdige 2001) and DON <200 μM (Burdige & Zheng 1998) have been observed in Chesapeake Bay. Cape Lookout Bight porewater DOC reached concentrations of 10 mM in the summer, although concentrations were generally <5 mM (Alperin et al. 1994). Continental margin sediment DOC concentrations are typically lower, with <3 mM DOC off North Carolina (Alperin et al. 1999)

and <1 mM in California margin sediments (Burdige et al. 1999). A study of sandy sediments in an estuarine lagoon found DON concentrations in excess of 100 μM (Yamamuro & Koike 1998), and DON in sediments of the Northern Adriatic approached 400 μM (Cermelj et al. 1997), which were similar to the DON concentrations presented here.

Burdige and Zheng (1998) observed a positive correlation between mineralization rates and DOC and DON concentrations, such that concentrations of the dissolved organics were highest in the summer. Similarly, DOC production during summer was observed in Cape Lookout Bight sediments (Alperin et al. 1994). However, in the present study DOC and DON concentrations were not correlated with temperature (Table 4.3), and did not appear to vary seasonally. Profiles were obtained over a range of seasons (Table 4.2), and the data do not show seasonal accumulation of dissolved organics in these sediments.

The relationships observed between $(SO_4^{2-})_{Dep}$, DIC, NH_4^+ and PO_4^{3-} inventories in the estuarine porewaters (Fig. 4.6, Table 4.3) suggests a close coupling between SO_4^{2-} reduction and the terminal metabolic end-products of organic matter mineralization (DIC, NH_4^+, PO_4^{3-}). However, there is a much less obvious coupling of $(SO_4^{2-})_{Dep}$ and DOC, presumably the substrate for SO_4^{2-} reduction in these sediments. $(SO_4^{2-})_{Dep}$ and DOC were not correlated at any of the sites except for surface 10 cm at SAP1 and deeper porewater at STL2 (Table 4.3), and there is no overall relationship when data from all sites is pooled (Fig.4.7). Similar regressions between DIC and DOC inventories yielded no significant results, with again the exception of the STL2 site ($p > 0.05$, data not shown).

DOC concentrations measured in these porewaters are the net result of both DOC production through hydrolytic breakdown of POM and transport of DOM into and out of the sediments, and the fermentative and terminal metabolic oxidation of DOM (Fenchel & Findlay

1995). In saltmarshes, plant root exudates can fuel SO_4^{2-} reduction independently of hydrolytic DOM production (Hines et al. 1999) and may contribute to the strong seasonal cycle of SO_4^{2-} reduction in saltmarshes coincident with the growing season (King 1988, Kostka et al. 2002*b*). Unvegetated intertidal creek-bank sediments are somewhat removed from this DOM exudate, and may rely more on the hydrolytic production of DOM from sediment POM.

The initial hydrolysis of POM can exceed the subsequent rates of fermentation and terminal metabolism, resulting in the accumulation of DOC in porewaters (Arnosti & Repeta 1994, Brüchert & Arnosti 2003). However, it appears that production and mineralization of DOC may be more tightly coupled in the intertidal creek-bank sediments in this study, resulting in little change in the bulk DOC inventory. We speculate that the DOC we measured represents a refractory pool of organic carbon that is largely unavailable for further microbial degradation. In this scenario, the labile DOC utilized by SO_4^{2-} reducers and by other terminal metabolizers is a small but rapidly cycled pool of DOC that is not detectable over or within the bulk pool. Measurements of specific organic compounds, such as acetate (Kostka 2002*b*) or ethanol (Hines et al. 1999), would potentially provide insight on the coupling of metabolic pathways in these sediments and such studies are planned for the future.

There was a significant positive relationship between DON and $(SO_4^{2-})_{Dep}$ inventories for data pooled from all the sites excluding STL2 (Table 3, Fig.4.7). The overall porewater inventories of DON are relatively low (around 5 μmol cm^{-2}) compared with inventories of other metabolites (Fig. 4.4). The higher pools of DON associated with higher rates of SO_4^{2-} reduction may be due to the coupling of DON production and terminal metabolism. In Chesapeake Bay sediments, Burdige and Zheng (1998) observed that, as rates of DOM utilization increased, consumption became non-selective and the C:N ratio of the DOM decreased, leading to a

negative correlation between both the DOC and DON versus the DOC:DON ratio. It appears that there may be selective utilization of DON in sediments with lower SO_4^{2-} reduction rates (i.e. lower overall rates of metabolism) in this study as well. The DOC:DON inventory ratio decreased significantly with increasing $(SO_4^{2-})_{Dep}$, suggesting non-selective utilization of DOM at higher SO_4^{2-} reduction rates (Fig. 4.9).

The hypothesis of selective utilization of DON at lower metabolic rates would require that the DIC:DIN ratio, as products of the mineralization of DOC and DON, mirror the DOC:DON ratio, i.e. the DIC:DIN would be low when metabolic rates are low due to the preferential mineralization of DON and production of DIN relative to mineralization of DOC and production of DIC. This is not the trend we observed. In contrast, the DIC:DIN ratio followed a pattern very similar to the DOC:DON ratio (Fig. 4.9). Denitrification and the preferential removal of inorganic nitrogen relative to DIC alone would not account for this pattern. The decrease in DIC:DIN and DOC:DON ratios with increasing terminal metabolism must be driven, therefore, by fermentation and hydrolysis of particulate organic matter. During the summer, either preferential degradation of PON to DON compared with POC degradation, or a change in the organic matter source to more N-rich POM appears to be the mechanism driving the changes in DOC:DON and DIC:DIN ratios (Fig. 4.9).

The POC and PON data (Table 4.4) from the STL2 and OKT4 sites, where a seasonal record was obtained, indicate that sediment POC:PON increased in the summer. The POC:PON ratio of inventories to 40 cm increased during the summer at both sites in a very similar manner (Fig. 4.10). Although this may be due in part to changes in particulate organic matter inputs, the pattern suggests that preferential degradation of PON to DON by the hydrolytic bacterial community in the summer, rather than variable inputs of POM or preferential utilization of DON

by terminal metabolizers, exerted overall control on the DOC:DON and DIC:DIN ratios in these sediments (Fig. 4.9).

The apparent hydrolytic control of the C:N ratio, along with the lack of seasonal accumulation of porewater DOC and the weak seasonal trend in SO_4^{2-} reduction rates (Table 4.4) and terminal metabolite porewater inventories (Table 4.3) suggests that the overall mineralization of organic matter is limited by the initial hydrolysis of POM in these sediments. Controls on the hydrolytic/fermentative/terminal metabolic organic matter-oxidizing consortium in sediments remain unclear, and an important avenue for future research.

SUMMARY

The large dataset obtained through the use of porewater equilibration samplers at eight intertidal estuarine sites allowed us to evaluate system-scale seasonal and spatial patterns of sediment metabolism, with an emphasis on the role of DOC and DON. We have come to the following conclusions:

1) Seasonality was observed, suggesting temperature does in part control rates of organic matter oxidation in unvegetated intertidal creekbank sediments. However, temperature alone cannot adequately describe the patterns of sulfate depletion, terminal metabolic products (DIC, NH_4^+, PO_4^{3-}), dissolved organic carbon and nitrogen, and sulfate reduction observed in this study.
2) There were significant system-scale correlations between the inorganic products of terminal metabolism (DIC, NH_4^+ and PO_4^{3-}) and sulfate depletion, and sulfate reduction appeared to be the dominant terminal carbon oxidation pathway in these sediments.

3) The data suggest that septic-derived waste from a residential community in the developed upland provided N- and P-rich labile DOM that stimulated rates of metabolism at the STL2 site, as well as contributing to inorganic nutrient and DIC inventories via the advection of septic water.

4) Hydrolytic production and fermentative and terminal metabolic consumption of labile DOC is closely coupled in these sediments. Bulk measurements of DOC did not aid in elucidating controls or pathways of carbon oxidation, and bulk DOC in these sediments is likely a recalcitrant pool. Terminal organic matter mineralization in these sediments appeared to be limited by hydrolytic/fermentative breakdown of POM and DOM when overall rates of metabolism were high. Hydrolysis also appears to control the C:N ratio of the POM and DOM. Controls on the breakdown of organic matter and the coupling between the hydrolytic/fermentative and terminal metabolic bacterial communities is an important topic for future research.

ACKNOWLEDGMENTS

We thank R. Lee, S. Carini, L. Velasquez, T. Roberts, and P. Olecki for help in the field and laboratory; W. Sheldon for providing Matlab mapping tools; and, C. Meile and three anonymous reviewers for providing comments that substantially improved this paper. This research was supported by the National Science Foundation's Georgia Coastal Ecosystems Long Term Ecological Research Program (OCE 99-82133) and National Oceanic and Atmospheric Administration Sea Grant Programs in Georgia (award numbers NA06RG0029-R/WQ11 and R/WQ12A) and South Carolina (award number: NA960PO113).

LITERATURE CITED

Aller RC & Aller JY (1998) The effect of biogenic irrigation intensity and solute exchange on diagenetic reaction rates in marine sediments. J. Mar. Res. 56: 905-936

Alperin MJ, Albert STL2 & Martens CS (1994) Seasonal variations in production and consumption rates of dissolved organic carbon in an organic-rich coastal sediment Geochim. Cosmochim. Acta 58: 4909-4930

Alperin MJ, Martens CS, Albert STL2, Suayah IB, Benninger LK, Blair NE, & Jahnke RA (1999) Benthic fluxes and porewater concentration profiles of dissolved organic carbon in sediments from the North Carolina continental slope. Geochim. Cosmochim. Acta 63: 427-448

Álvarez-Salgado XA & Miller AEJ (1998) Simultaneous determination of dissolved organic carbon and total dissolved nitrogen in seawater by high temperature catalytic oxidation: conditions for precise shipboard measurements. Mar. Chem. 62: 325-333

Amon RMW & Benner R (1996) Bacterial utilization of different size classes of dissolved organic matter. Limnol. Oceanogr. 41: 41-51

Arnosti C & Repeta DJ (1994) Oligosaccharide degradation by anaerobic marine bacteria: characterization of an experimental system to polymer degradation in sediments. Limnol. Oceanogr. 39: 1865-1877

Berner RA (1977) Stoichiometric models for nutrient regeneration in anoxic sediments. Limnol. Oceanogr. 22: 781-786

Boynton WR & Kemp WM (1985) Nutrient regeneration and oxygen consumption by sediments along an estuarine salinity gradient. Mar. Ecol. Prog. Ser. 23: 45-55

Brüchert V & Arnosti C (2003) Anaerobic carbon transformation: experimental studies with flow-through cells. Mar. Chem. 80: 171-183

Burdige DJ & Martens CS (1988) Biogeochemical cycling in an organic-rich coastal marine basin: 10. The role of amino acids in sedimentary carbon and nitrogen cycling. Geochim. Cosmochim. Acta 52: 1571-1584

Burdige DJ & Gardner KG (1998) Molecular weight distribution of dissolved organic carbon in marine sediment pore waters. Mar. Chem. 62: 45-64

Burdige DJ & Zheng S (1998) The biogeochemical cycling of dissolved organic nitrogen in estuarine sediments. Limnol. Oceanogr. 43: 1796-1813

Burdige DJ, Berleson WM, Coale KH, McManus J & Johnson KS (1999) Fluxes of dissolved organic carbon from California continental margin sediments. Geochim. Cosmochim. Acta 63: 1507-1515

Burdige DJ (2001) Dissolved organic matter in Chesapeake Bay sediment pore waters. Org Geochem 32: 487-505

Canfield DE, Raiswell R, Westrich JT, Reaves CM & Berner RA (1986) The use of chromium reduction in the analysis of reduced inorganic sulfur in sediments and shales. Chem Geol 54: 149-155

Capone DG & Kiene RP (1988) Comparison of microbial dynamics in marine and fresh-water sediments - contrasts in anaerobic carbon catabolism. Limnol. Oceanogr. 33: 725-749

Cermelj B, Bertuzzi A & Faganeli J (1997) Modeling of pore water nutrient distribution and benthic fluxes in shallow coastal waters (Gulf of Trieste, Northern Adriatic). Water Air Soil Pollut. 99: 435-444

Enoksson V (1993) Nutrient recycling by coastal sediments: effects of added algal material. Mar. Ecol. Prog. Ser. 92: 245-254

Fenchel TM & Findlay BJ (1995) Ecology and evolution of anoxic worlds. Oxford University Press, Oxford

Froelich PN, Klinkhammer GP, Bender ML, Luedtke NA, Heath GR, Cullen D, Dauphin P, Hammond D, Hartman B & Maynard V (1979) Early oxidation of organic-matter in pelagic sediments of the eastern equatorial Atlantic - suboxic diagenesis. Geochim. Cosmochim. Acta 43: 1075-1090

Hesslein RH (1976) An in situ sampler for close interval pore water studies. Limnol. Oceanogr. 21: 912-914

Hines ME, Evans RS, Genthner BRS, Willis SG, Friedman S, Rooney-Varga JN & Devereux R (1999) Molecular phylogenetic and biogeochemical studies of sulfate-reducing bacteria in the rhizosphere of *Spartina alterniflora*. Appl Environ Microbiol 65: 2209-2216

Hopkinson CS (1987) Nutrient regeneration in shallow-water sediments of the estuarine plume region of the nearshore Georgia Bight, USA. Mar Biol 94: 127-142

Hopkinson CS, Giblin AE, Tucker J & Garritt RH (1999) Benthic metabolism and nutrient cycling along an estuarine salinity gradient. Estuaries 22: 825-843

Howarth RW (1988) Nutrient limitation of net primary production in marine ecosystems. Ann Rev Ecol 19: 89-110

Howarth RW (1993) Microbial processes in salt-marsh sediments. In: Ford TE (ed) Aquatic microbiology: an ecological approach. Blackwell, Cambridge, p 239-259

Iversen N & Jørgensen BB (1985) Anaerobic methane oxidation rates at the sulfate-methane transition in marine sediments from Kattegat and Skagerrak (Denmark). Limnol. Oceanogr. 30: 944-955

Jørgensen BB (1977) Sulfur cycle of a coastal marine sediment (Limfjorden, Denmark). Limnol. Oceanogr. 22: 814-832

Jørgensen BB (1978) A comparison of methods for the quantification of bacterial sulfate reduction in coastal marine sediments. 1. Measurements with radiotracer techniques. Geomicrobiol J 1: 11-27

Jørgensen BB (1982) Mineralization of organic-matter in the sea bed - the role of sulfate reduction. Nature 296: 643-645

Jørgensen BB & Sørensen J (1985) Seasonal cycles of O_2, NO_3^- and SO_4^{2-} reduction in estuarine sediments: the significance of an NO_3^- reduction maximum in spring. Mar. Ecol. Prog. Ser. 24: 65-74

Jørgensen BB (2000) Bacteria and marine biogeochemistry. In: Schulz HD & Zabel M (Eds) Marine geochemistry (pp 173-207). Springer, New York

Joye SB & Hollibaugh JT (1995) Influence of sulfide inhibition of nitrification on nitrogen regeneration in sediments. Science 270: 623-624

King GM (1988) Patterns of sulfate reduction and the sulfur cycle in a South Carolina salt marsh. Limnol. Oceanogr. 33: 376-390

Kostka JE, Gribsholt B, Petrie E, Dalton D, Skelton H & Kristensen E (2002*a*) The rates and pathways of carbon oxidation in bioturbated saltmarsh sediments. Limnol. Oceanogr. 47: 230-240

Kostka JE Roychoudhury A & Van Cappellen P (2002*b*) Rates and controls of anaerobic microbial respiration across spatial and temporal gradients in saltmarsh sediments. Biogeochemistry 60: 49-76

Lomstein BA, Blackburn TH & Henriksen K (1989) Aspects of nitrogen and carbon cycling in the northern Bering Shelf sediment I. The significance of urea turnover in the mineralization of NH_4^+. Mar. Ecol. Prog. Ser. 57: 237-247

Lowe KL, DiChristina TJ, Roychoudhury AN, & Van Cappellen P (2000) Microbiological and geochemical characterization of microbial Fe(III) reduction in salt marsh sediments. J. Geomicrobiol. 17: 163-178

Marvin-DiPasquale MC, Boynton WR & Capone DG (2003) Benthic sulfate reduction along the Chesapeake Bay central channel. II. Temporal controls. Mar. Ecol. Prog. Ser. 260: 55-70

Meile C, Koretsky CM & Van Cappellen P (2001) Quantifying bioirrigation in aquatic sediments: an inverse modeling approach. Limnol. Oceanogr. 46: 164-177

Middelburg JJ, Soetart K & Herman PMJ (1997) Empirical relationships for use in global diagenetic models. Deep-Sea Res. 44: 327-344

Moore JW, Schindler DE, Scheuerell MD, Smith D & Frodge J (2003) Lake eutrophication at the urban fringe, Seattle region, USA. Ambio 32: 13-18

Murphy J & Riley JP (1962) A modified single solution method for the determination of phosphate in natural systems. Anal. Chim. Acta 27: 31-36

Nielsen OI, Kristensen E & Macintosh DJ (2003) Impact of fiddler crabs (*Uca* spp) on rates and pathways of benthic mineralization in deposited mangrove shrimp pond waste. J. Exp. Mar. Biol. Ecol 289: 59-81

Pilson MEQ (1998) An introduction to the chemistry of the sea. Prentice Hall, New Jersey

Ptacek CJ (1998) Geochemistry of a septic-system plum in a coastal barrier bar, Point Pelee, Ontario, Canada. J. Cont. Hydrol. 33: 293-312

Redfield AC (1958) The biological control of chemical factors in the environment. Am. Sci. 46: 205-222

Roden EE & Wetzel RG (1996) Organic carbon oxidation and suppression of methane production by microbial Fe(III) oxide reduction in vegetated and unvegetated freshwater wetland sediments. Limnol. Oceanogr. 41: 1733-1748

Rosenfeld JK (1979) Ammonium adsorption in anoxic nearshore sediments. Limnol. Oceanogr. 24: 356-364

Rowe GT, Clifford CH & Smith KL (1976) Benthic nutrient regeneration and its coupling to primary productivity in coastal waters. Nature 255: 215-217

Roychoudhury AN, Viollier E & Van Cappellen P (1998) A plug flow-through reactor for studying biogeochemical reactions in undisturbed aquatic sediments. Appl. Geochem. 13: 269-280

Rysgaard S, Thastum P, Dalsgaard T, Christensen OKT2 & Sloth NP (1999) Effects of salinity on NH_4^+ adsorption capacity, nitrification, and denitrification in Danish estuarine sediments. Estuaries 22: 21-30

Sansone FJ & Martens CS (1978) Methane oxidation in Cape Lookout Bight, North Carolina. Limnol. Oceanogr. 23: 349-355

Sarazin G, Michard G & Prevot F (1999) A rapid and accurate spectroscopic method for alkalinity measurements in sea water samples. Water Res. 33: 290-294

Seitzinger SP (1988) Denitrification in freshwater and coastal marine ecosystems: ecological and geochemical significance. Limnol. Oceanogr. 33: 702-724

Solorzano L (1969) Determination of ammonia in natural waters by the phenolhypochlorite method. Limnol. Oceanogr. 14: 799-801

Stookey LL (1970) Ferrozine - a new spectrophotometric reagent for iron. Anal. Chem. 42: 779-781

Stumm W & Morgan JJ (1996) Aquatic chemistry, third edition. Wiley, New York

Sundareshwar PV & Morris JT (1999) Phosphorus sorption characteristics of intertidal marsh sediments along an estuarine salinity gradient. Limnol. Oceanogr. 44: 1693-1701

Teal JM (1958) Distribution of fiddler crabs in Georgia salt marshes. Ecology 39: 185-193

Westrich JT & Berner RA (1988) The effect of temperature on rates of sulfate reduction in marine sediments. Geomicrobiol. J. 6: 99-117

Yamamuro M & Koike I (1998) Concentrations of nitrogen in sandy sediments of a eutrophic estuarine lagoon. Hydrobiologia 386: 37-4

Table 4.1. Schedule of porewater equilibration meter sampling, sediment solid phase POC and PON measurement and sulfate reduction (SR) rate determination at the Georgia and South Carolina field sites. Abbreviations correspond to sites in Figure 1.

	Date	Georgia	South Carolina
Porewater Equilibration Samplers	September 2000	STL2, SAP1, SAP2	
	January 2001	STL2, SAP1, SAP2	
	April 2001	STL2, SAP1, SAP2	OKT1
	August 2001[1]	STL2, SAP1, SAP2	OKT4, OKT3
	January 2002	STL2, SAP1, SAP2	OKT1, OKT3, OKT4, OKT2
	August 2002	STL2, SAP1, SAP2, STL1	OKT1, OKT3, OKT4, OKT2
	January 2003	STL2, STL1	OKT1, OKT3, OKT4, OKT2, Survey[2]
POC, PON, and SR	April 2002	STL2, SAP1, SAP2	OKT4, (OKT1, OKT3)[3]
	June 2002	STL2	OKT4
	August 2002	STL2, SAP2	OKT4
	January 2003	STL2	OKT4

[1]Single porewater equilibration meter at each site during August 2001, [2]Single meter at five survey sites between the OKT3 and OKT4 sites (Fig. 1), [3]Sediment solid phase measurements only.

Table 4.2. Porewater equilibration chamber subsampling.

Analysis	Sample	Volume (ml)	Vial	Preservation
CH_4, DIC[a]	Unfiltered	1	6 ml headspace vial with rubber septa and aluminum crimp seal	0.1 ml concentrated phosphoric acid
Alkalinity[b]	Unfiltered	0.1	7 ml glass vial	3 ml bromophenol blue reagent[‡], analyzed within 2 hr
H_2S	Unfiltered	0.1-0.5	7 ml glass vial	0.5 ml 20% zinc acetate
NH_4^+	0.2 µm filtered	0.1 - 0.5	7 ml glass vial	0.2 ml phenol reagent[‡], analyzed within 2 d
NOx, DON[c]	0.2 µm filtered	balance of sample	7 ml glass vial	Refrigerated
DOC[c], PO_4^{3-}, Cl^-, SO_4^{2-}, Fe^{2+}	0.2 µm filtered	4	7 ml glass vial	0.1 ml concentrated nitric acid, refrigerated

[a]Measured April 2001 and all subsequent samplings; [b] September 2000 and January 2001 samples; [c] not measured on September 2000 samples; [‡] reagent added to sample vial prior to sampling

Table 4.3. Slopes of significant ($p<0.05$) regressions of the measured porewater inventories from 0 to 10 cm and from 10 to 40 cm at each site (except for STL1) against temperature [μmol cm^{-2} (degree C)$^{-1}$], Cl^- inventories [μmol (mmol Cl^-)$^{-1}$] and $(SO_4^{2-})_{Dep}$ inventories [μmol (μmol [$(SO_4^{2-})_{Dep}$]$^{-1}$]. 'All sites' is data pooled from all sites with the exception of the STL2 site.

(following page)

=		Site	NH_4^+	NO_x	PO_4^{3-}	DIC	$(SO_4^{2-})_{Dep}$	CH_4	Fe^{2+}	H_2S	DON	DOC
Temperature	10 - 40 cm	STL2										
		SAP1	0.158		0.024		2.931		-0.059	0.401		
		SAP2									-0.294	
		OKT1										
		OKT2					8.11					
		OKT3					12.36			15.71		
		OKT4								12.50		
		All Sites	**0.33**				**3.25**			**5.12**		
	10 cm	STL2					3.228			3.432		
		SAP1			0.010		0.788					-2.145
		SAP2										
		OKT1										
		OKT2										
		OKT3	0.347							3.164		
		OKT4										
		All Sites	**0.072**				**0.703**			**0.492**		
Chloride	10 - 40 cm	STL2										
		SAP1										
		SAP2		-0.056			34.68					
		OKT1							-1.846			12.87
		OKT2			-0.451							
		OKT3										16.15
		OKT4										
		All Sites						**-0.967**	**0.310**			
	10 cm	STL2										
		SAP1				-36.82	15.547				-0.784	
		SAP2								-1.339		
		OKT1										
		OKT2										
		OKT3										8.483
		OKT4										20.707
		All Sites						**-0.184**				
SO_4^{2-} Depletion Inventories	10 - 40 cm	STL2	0.242		0.026	2.309	NA	0.030				-1.445
		SAP1			0.007		NA					
		SAP2					NA					
		OKT1	0.049			2.503	NA			1.992		
		OKT2				1.972	NA					
		OKT3	0.081			1.525	NA			0.937		
		OKT4	0.094				NA					
		All Sites	**0.078**	**>-0.001**	**0.010**	**1.842**	**NA**			**1.061**	**0.012**	
	10 cm	STL2	0.143		0.019	4.803	NA		-0.017		0.027	
		SAP1					NA					-2.831
		SAP2					NA					
		OKT1					NA					
		OKT2	0.103			1.842	NA					
		OKT3	0.085		0.020	1.557	NA			0.763	0.009	
		OKT4	0.122		0.036		NA			0.431		
		All Sites	**0.074**	**>-0.001**	**0.019**	**1.334**	**NA**			**0.431**	**0.012**	

Table 4.4. Sediment particulate organic carbon (POC) and nitrogen (PON) and sulfate reduction (SR) rates integrated to 40 cm depth.

	Site	POC mmol cm^{-2}	PON mmol cm^{-2}	SR µmol cm-2 d^{-1}
April 2002				
	STL2	51.9	5.0	5.2
	SAP1	59.1	7.5	
	SAP2	25.7	4.7	1.4
	OKT1	39.3	6.1	
	OKT3	30.8	5.5	
	OKT4	43.6	4.4	0.9
June 2002				
	STL2	56.3	4.1	2.1
	OKT4	44.8	3.2	2.0
August 2002				
	STL2	58.6	3.8	5.2
	SAP2	22.5	2.7	2.0
	OKT4	54.0	2.9	0.3
January 2003				
	STL2	55.6	4.3	1.1
	OKT4	46.8	3.9	0.4

Table 4.5. Ratios of porewater inventories from 0 to 10 and 10 to 40 cm for data from all sites except STL2 and site STL2 alone, derived from the slopes of regressions (Table 2).

	0-10 cm Inventories		10-40 cm inventories	
Ratio	All sites	STL2	All sites	STL2
$DIC:(SO_4^{2-})_{Dep}$	1.3	4.8	1.8	2.3
$(SO_4^{2-})_{Dep}:NH_4^+$	13.4	7.0	12.8	4.1
$(SO_4^{2-})_{Dep}:PO_4^{3-}$	54.1	53.8	104	38.5

FIGURE LEGENDS

Figure 4.1. Map of the sampling sites in the Okatee River Estuary (South Carolina), Sapelo Island and Satilla River Estuary (Georgia).

Figure 4.2. Example of porewater equilibration profiles of NH_4^+, NO_x, PO_4^{3-}, DIC, DOC, DON, H_2S, Fe^{2+}, SO_4^{2-}, pH, Cl^- and CH_4 (from the STL2 and SAP1 sites in August 2002).

Figure 4.3. Example of duplicate porewater equilibration profiles of Cl^-, DIC, $(SO_4^{2-})_{Dep}$, and NH_4^+ from sites STL2 (January 2003), OKT3 and (August 2002). The porewater inventory to 40 cm for each profile is indicated.

Figure 4.4. Average porewater inventories of Cl^-, $(SO_4^{2-})_{Dep}$, NH_4^+, PO_4^{3-}, DIC, H_2S, Fe^{2+}, CH_4, DOC and DON to a depth of 40 cm at eight sites in Georgia and South Carolina (± standard deviation). Sites that do not share the same letter are significantly different ($p < 0.05$, Tukey pairwise comparison).

Figure 4.5. Altamaha River discharge (data from the United States Geological Survey) and porewater Cl^- inventories at the SAP1 site (± standard deviation except for August 2001).

Figure 4.6. Sediment porewater inventories to 40 cm depth of NH_4^+, PO_4^{3-} and DIC against $(SO_4^{2-})_{Dep}$ inventories. Regressions are calculated for the STL2 site data separately from data from all of the other sites. Equations are given for significant relationships.

Figure 4.7. $(SO_4^{2-})_{Dep}$ inventories plotted against DON and DOC pools to 40 cm depth. Regressions are calculated for the STL2 site data separately from data from the other sites. Equations are given for significant relationships.

Figure 4.8. Molar ratios of DIN:DIP (top), DIC:DIN and DOC:DON (bottom) inventories versus sulfate depletion inventories to 40 cm. Regressions against log-transformed sulfate depletion inventories were made for the DIC:DIN and DOC:DON data (data pooled from all sites).

Figure 4.9. Particulate organic carbon (POC) to nitrogen (PON) molar ratios of sediment inventories to 40 cm at the STL2 and OKT4 sites on four dates.

Figure 4.10. Average sulfate depletion inventories and depth-integrated sulfate reduction rates at the STL2, SAP2 and OKT4 sites (± standard deviation).

Figure 4.1

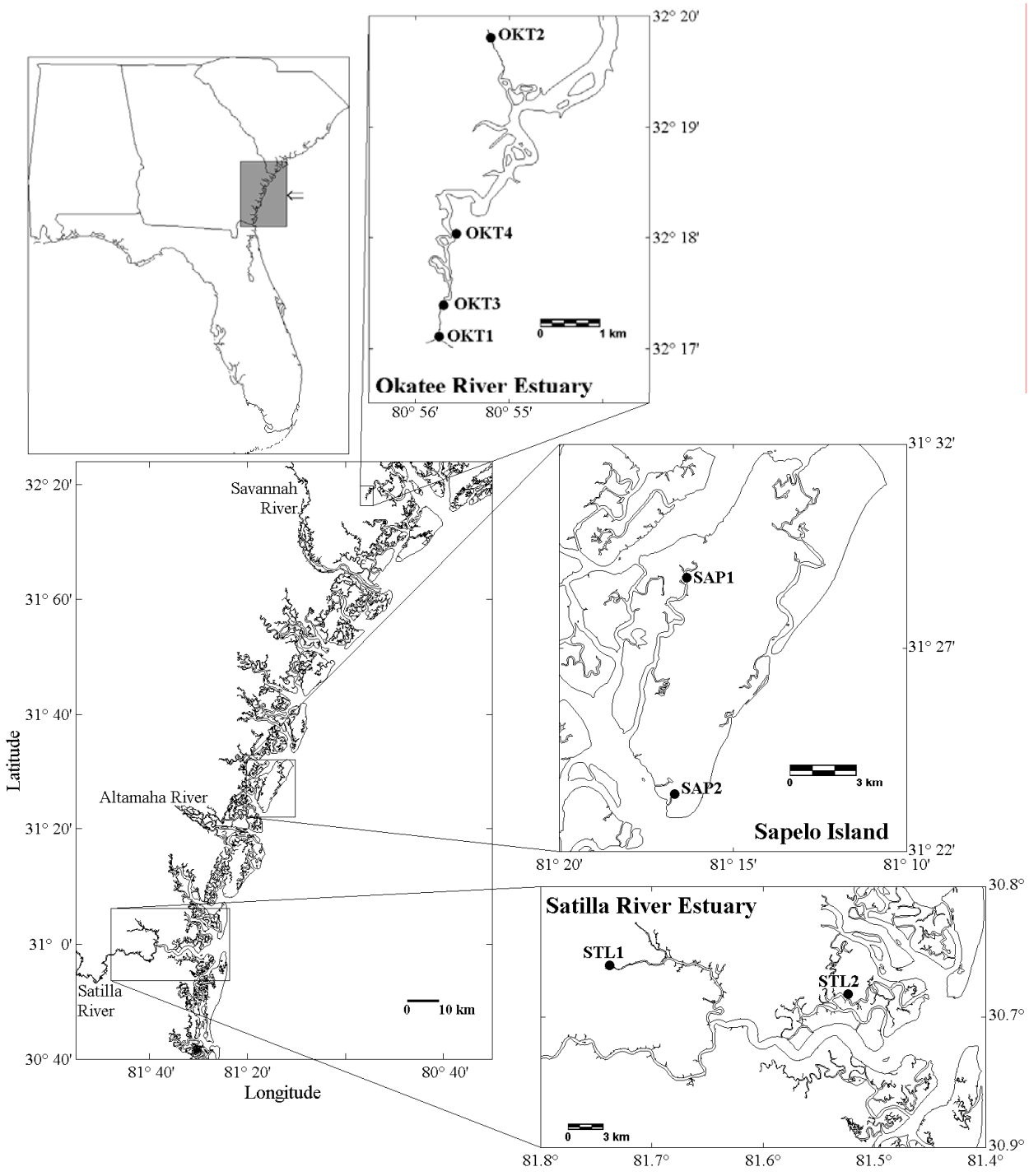
OKT2
OKT4
OKT3
OKT1
0 1 km
Okatee River Estuary
32° 20'
32° 19'
32° 18'
32° 17'
80° 56'
80° 55'
Savannah River
Altamaha River
Satilla River
0 10 km
32° 20'
31° 60'
31° 40'
31° 20'
31° 0'
30° 40'
81° 40'
81° 20'
80° 40'
Latitude
Longitude
SAP1
SAP2
0 3 km
Sapelo Island
31° 32'
31° 27'
31° 22'
81° 20'
81° 15'
81° 10'
Satilla River Estuary
STL1
STL2
0 3 km
30.8°
30.7°
30.9°
81.8°
81.7°
81.6°
81.5°
81.4°

Figure 4.2

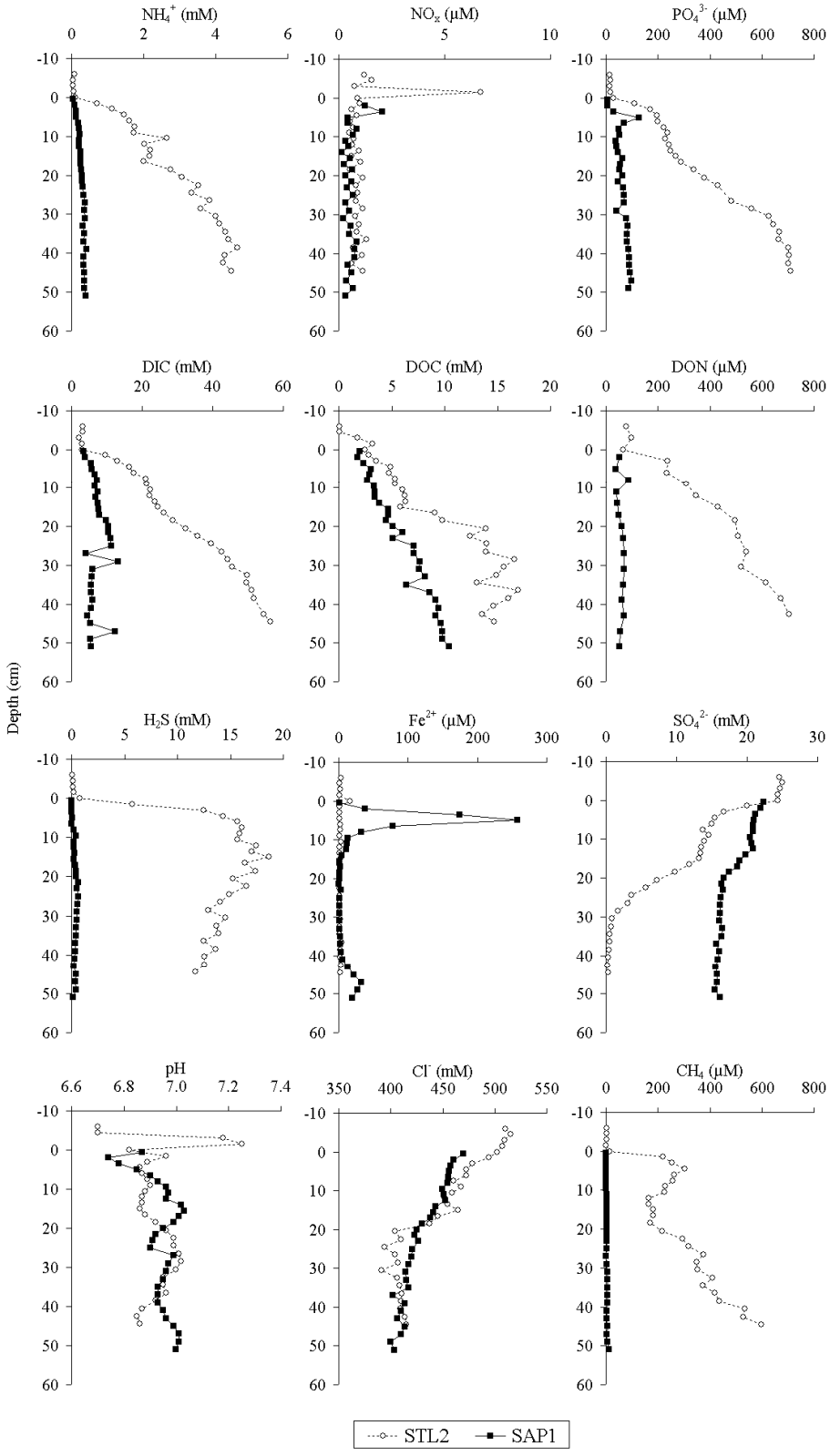
NH4+ (mM)
NOx (µM)
PO43- (µM)
DIC (mM)
DOC (mM)
DON (µM)
H2S (mM)
Fe2+ (µM)
SO42- (mM)
pH
Cl- (mM)
CH4 (µM)
Depth (cm)
STL2
SAP1

Figure 4.3

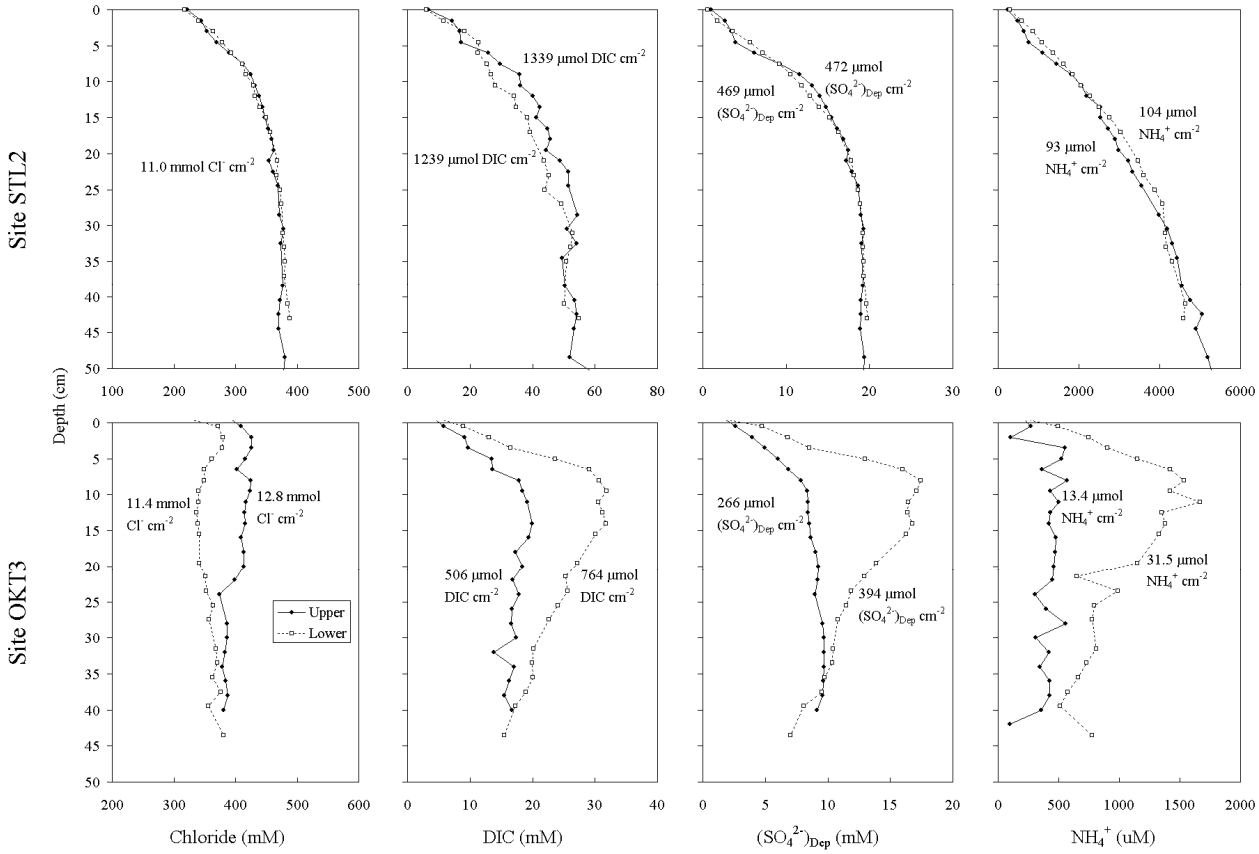
Site STL2
Site OKT3
Depth (cm)
11.0 mmol Cl⁻ cm⁻²
1339 µmol DIC cm⁻²
1239 µmol DIC cm⁻²
472 µmol (SO4 2-)Dep cm⁻²
469 µmol (SO4 2-)Dep cm⁻²
104 µmol NH4+ cm⁻²
93 µmol NH4+ cm⁻²
11.4 mmol Cl⁻ cm⁻²
12.8 mmol Cl⁻ cm⁻²
Upper
Lower
506 µmol DIC cm⁻²
764 µmol DIC cm⁻²
266 µmol (SO4 2-)Dep cm⁻²
394 µmol (SO4 2-)Dep cm⁻²
13.4 µmol NH4+ cm⁻²
31.5 µmol NH4+ cm⁻²
Chloride (mM)
DIC (mM)
(SO4 2-)Dep (mM)
NH4+ (uM)

Figure 4.4

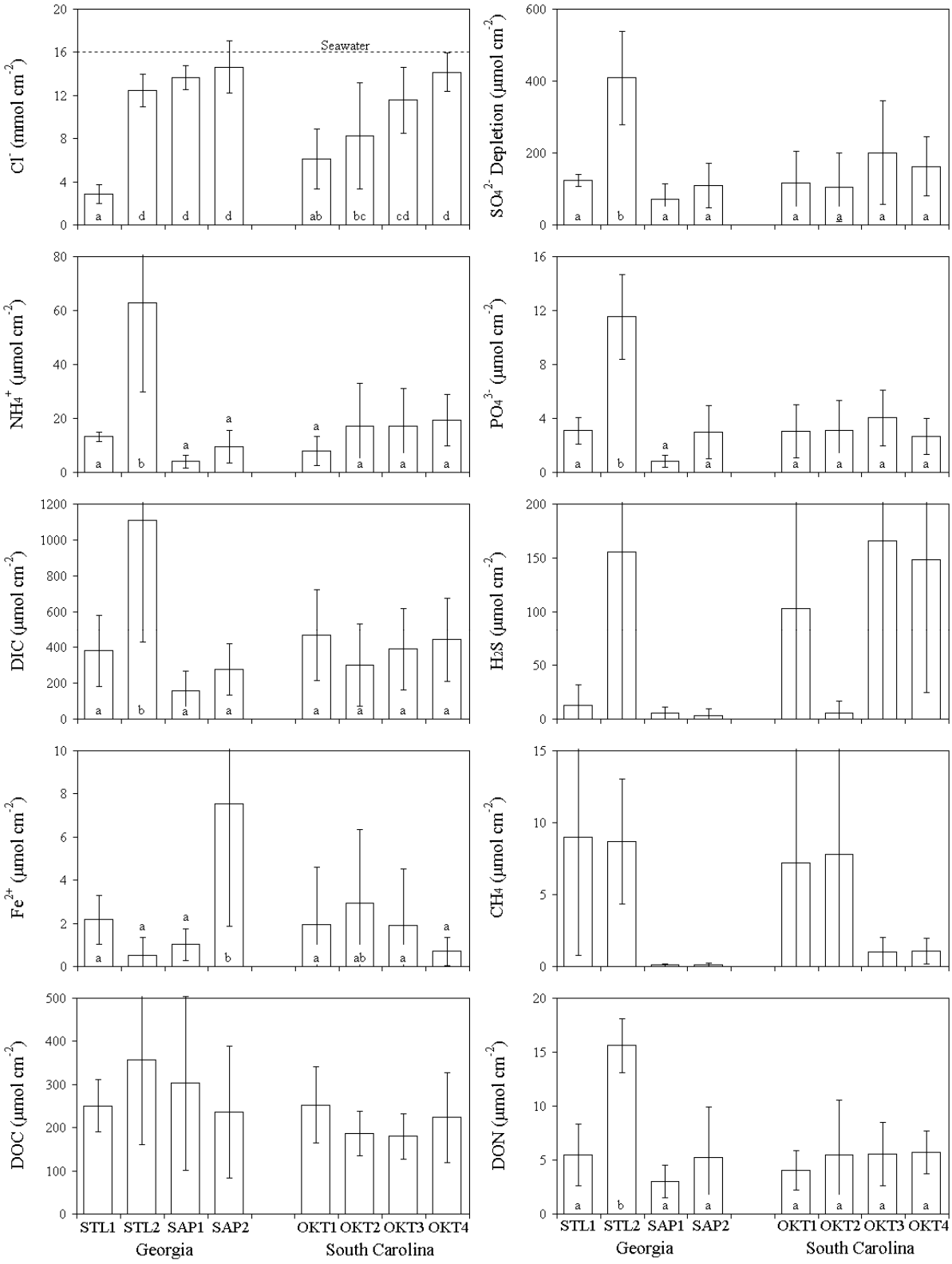
Cl- (mmol cm-2)
Seawater
SO4 2- Depletion (µmol cm-2)
NH4+ (µmol cm-2)
PO4 3- (µmol cm-2)
DIC (µmol cm-2)
H2S (µmol cm-2)
Fe2+ (µmol cm-2)
CH4 (µmol cm-2)
DOC (µmol cm-2)
DON (µmol cm-2)
STL1 STL2 SAP1 SAP2
OKT1 OKT2 OKT3 OKT4
Georgia
South Carolina

Figure 4.5

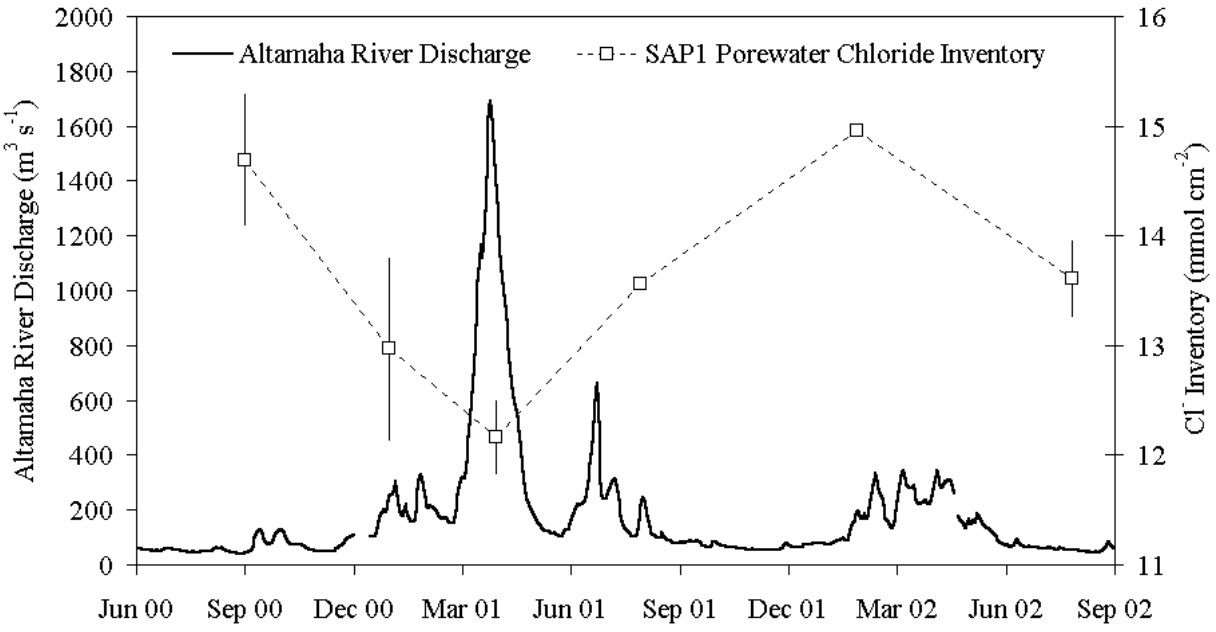
Altamaha River Discharge
SAP1 Porewater Chloride Inventory
Altamaha River Discharge (m3 s-1)
Cl- Inventory (mmol cm-2)
2000
1800
1600
1400
1200
1000
800
600
400
200
0
16
15
14
13
12
11
Jun 00
Sep 00
Dec 00
Mar 01
Jun 01
Sep 01
Dec 01
Mar 02
Jun 02
Sep 02

Figure 4.6

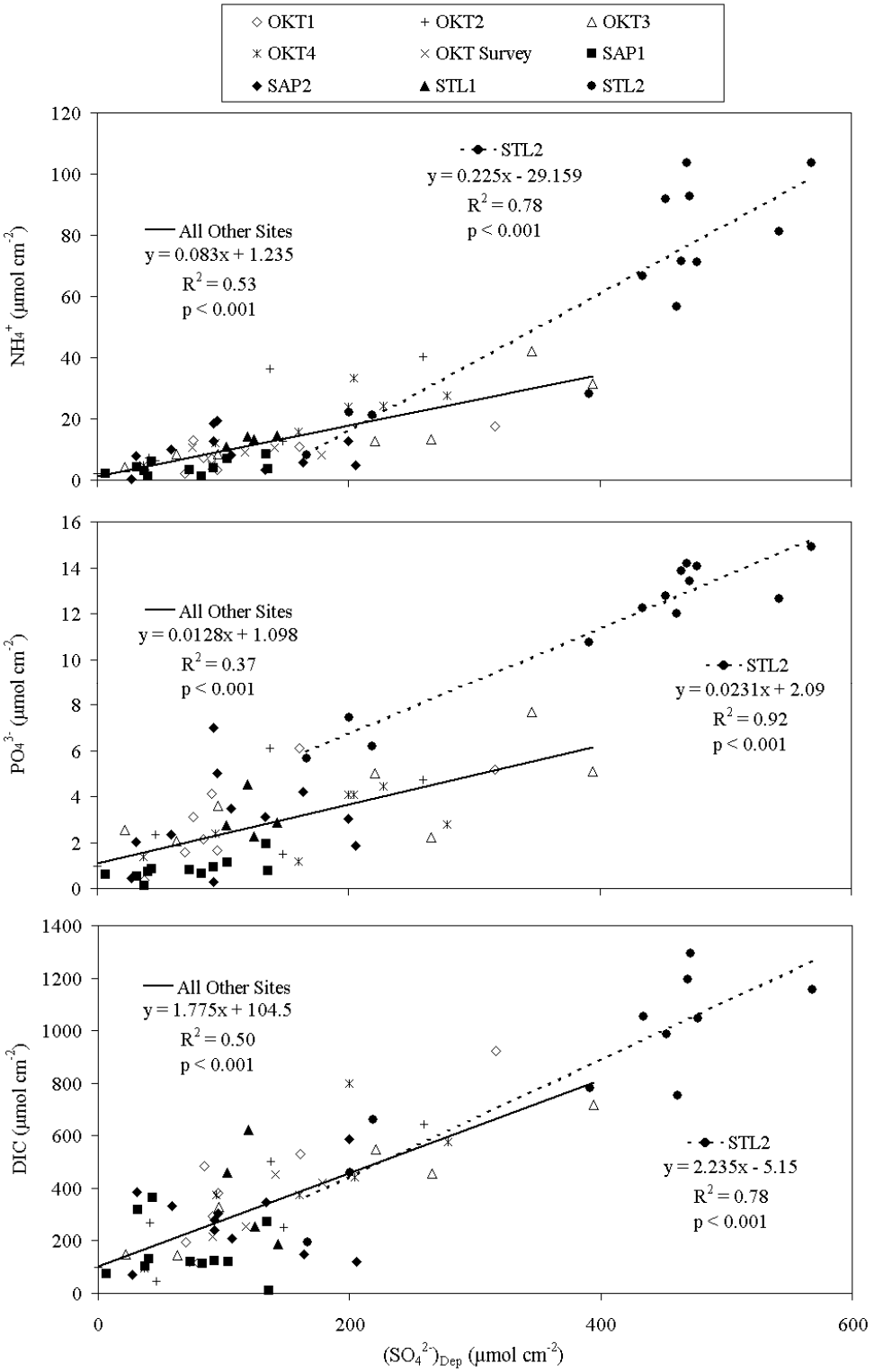
OKT1
OKT2
OKT3
OKT4
OKT Survey
SAP1
SAP2
STL1
STL2
NH4+ (µmol cm-2)
STL2
y = 0.225x - 29.159
R2 = 0.78
p < 0.001
All Other Sites
y = 0.083x + 1.235
R2 = 0.53
p < 0.001
PO43- (µmol cm-2)
All Other Sites
y = 0.0128x + 1.098
R2 = 0.37
p < 0.001
STL2
y = 0.0231x + 2.09
R2 = 0.92
p < 0.001
DIC (µmol cm-2)
All Other Sites
y = 1.775x + 104.5
R2 = 0.50
p < 0.001
STL2
y = 2.235x - 5.15
R2 = 0.78
p < 0.001
(SO42-)Dep (µmol cm-2)

Figure 4.7

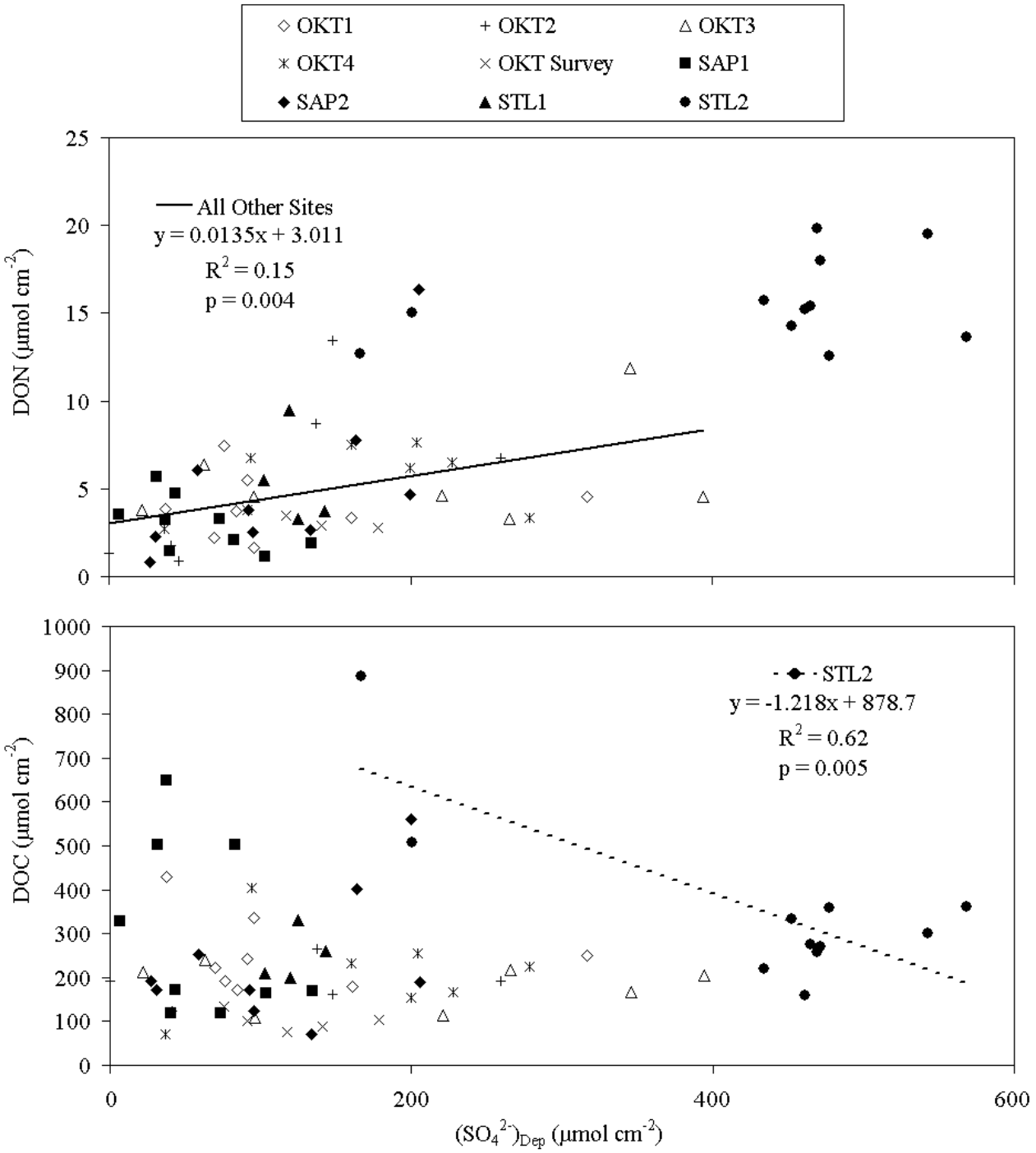
◇ OKT1
+ OKT2
△ OKT3
✳ OKT4
× OKT Survey
■ SAP1
◆ SAP2
▲ STL1
● STL2
All Other Sites
y = 0.0135x + 3.011
R2 = 0.15
p = 0.004
DON (µmol cm-2)
STL2
y = -1.218x + 878.7
R2 = 0.62
p = 0.005
DOC (µmol cm-2)
(SO4 2-)Dep (µmol cm-2)

Figure 4.8

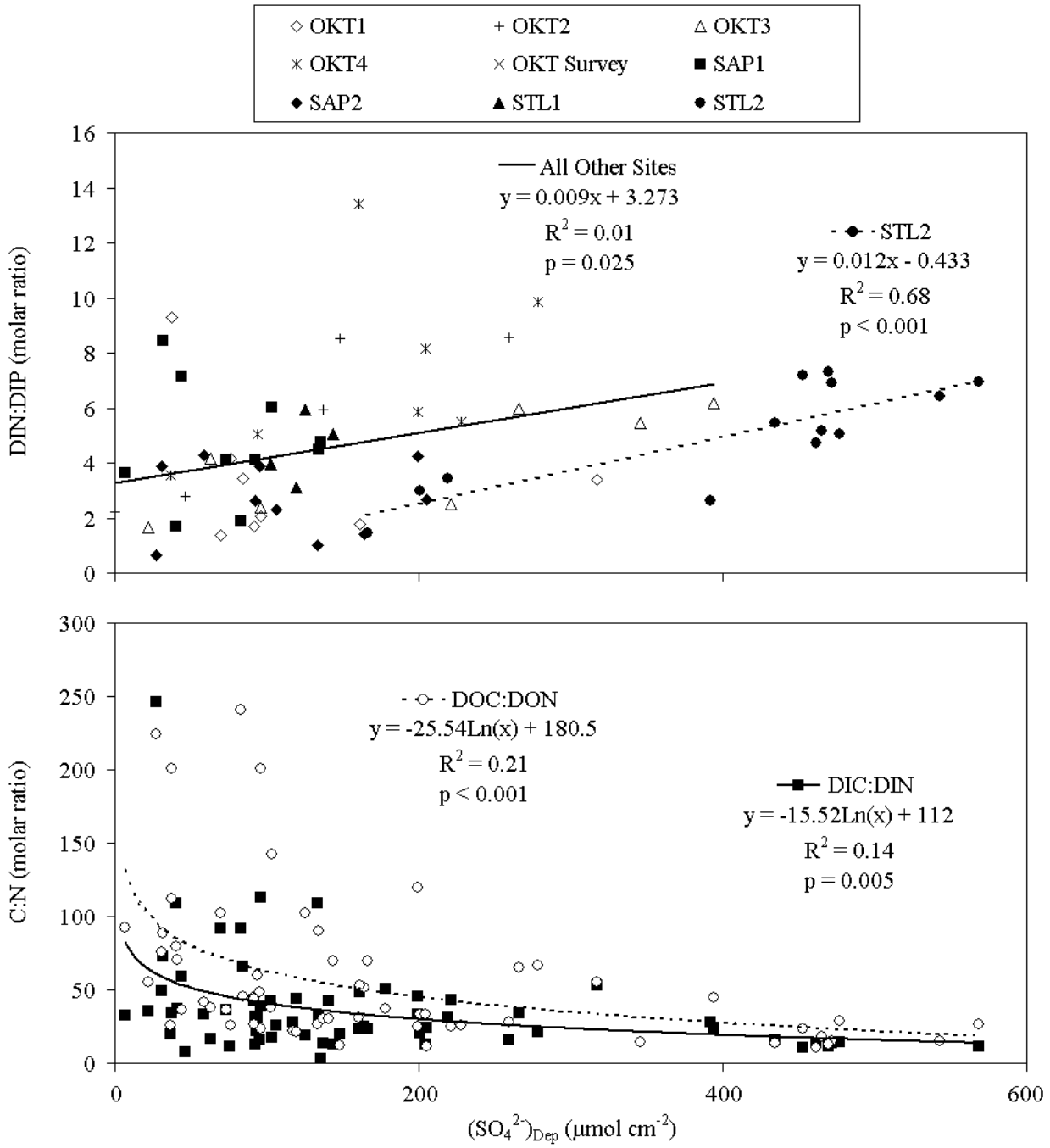
OKT1
OKT2
OKT3
OKT4
OKT Survey
SAP1
SAP2
STL1
STL2
All Other Sites
y = 0.009x + 3.273
R2 = 0.01
p = 0.025
STL2
y = 0.012x - 0.433
R2 = 0.68
p < 0.001
DIN:DIP (molar ratio)
DOC:DON
y = -25.54Ln(x) + 180.5
R2 = 0.21
p < 0.001
DIC:DIN
y = -15.52Ln(x) + 112
R2 = 0.14
p = 0.005
C:N (molar ratio)
(SO4 2-)Dep (µmol cm-2)

Figure 4.9

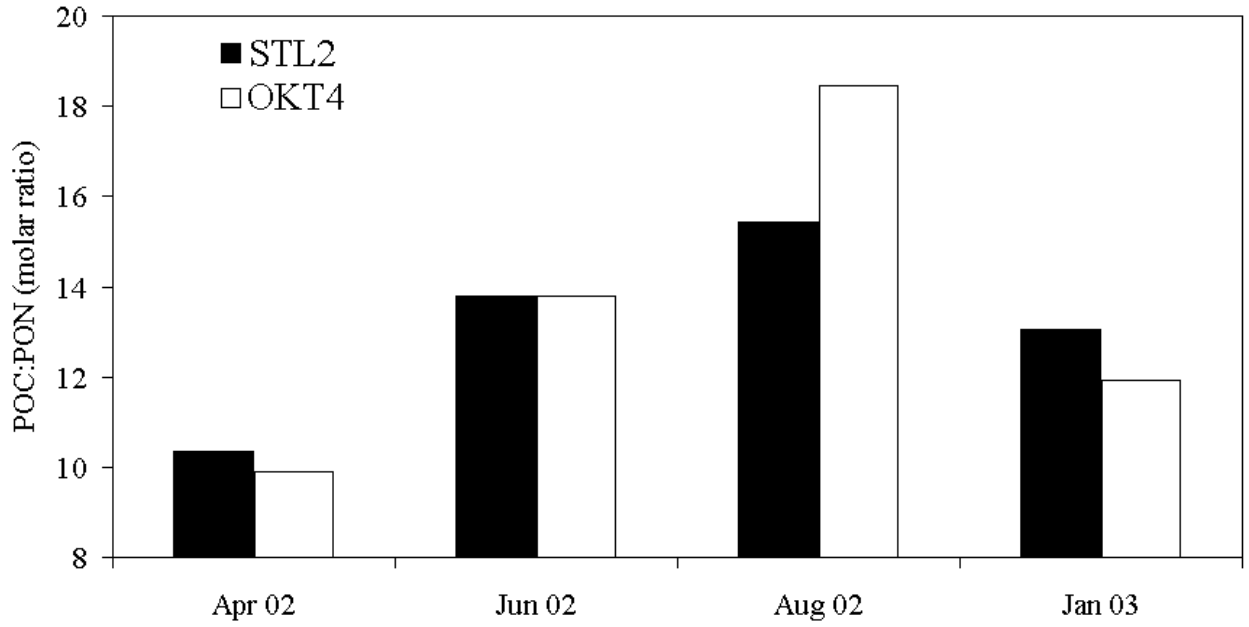
20
18
16
14
12
10
8
POC:PON (molar ratio)
STL2
OKT4
Apr 02
Jun 02
Aug 02
Jan 03

Figure 4.10

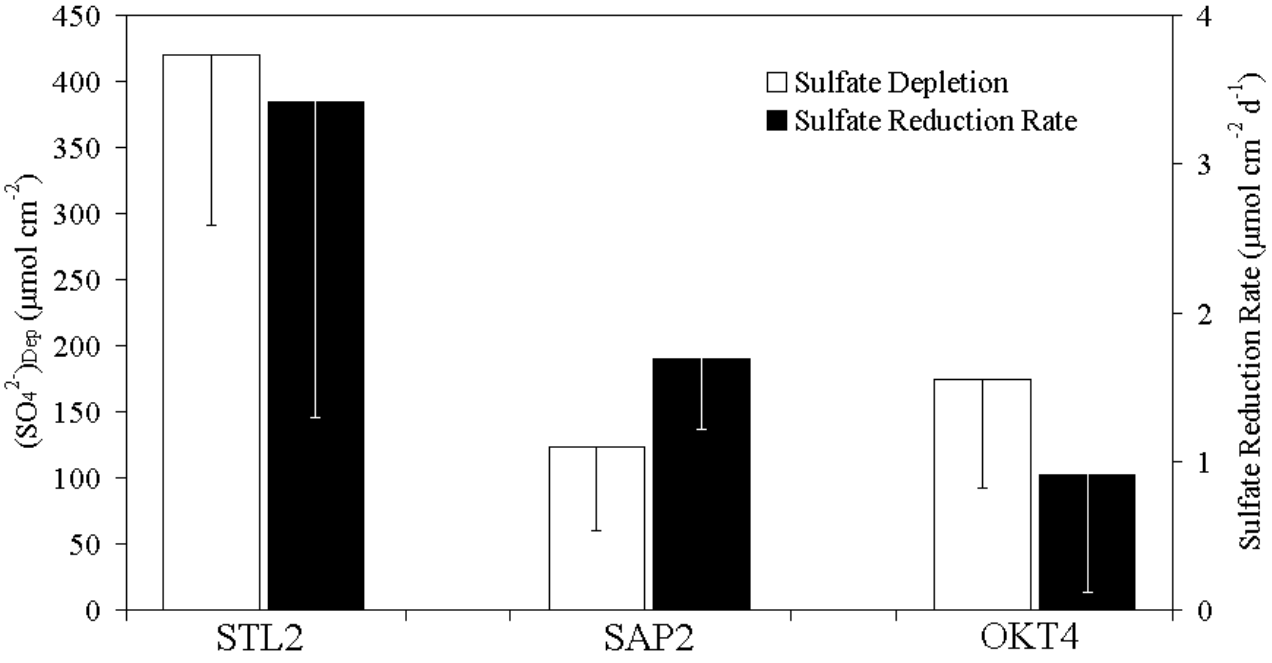
Sulfate Depletion
Sulfate Reduction Rate
$(SO_4^{2-})_{Dep}$ (µmol cm^{-2})
Sulfate Reduction Rate (µmol cm^{-2} d^{-1})
0
50
100
150
200
250
300
350
400
450
0
1
2
3
4
STL2
SAP2
OKT4

CHAPTER 5

TEMPERATURE DRIVEN ACCUMULATION OF LABILE DISSOLVED ORGANIC CARBON IN MARINE SEDIMENTS[1]

[1] Weston, N.B., S.B. Joye. Prepared for submission to *Proceedings of the National Academy of Sciences*

ABSTRACT

The mineralization of complex organic matter in sediments is mediated by a diverse consortium of microbes that hydrolyze, ferment, and terminally oxidize organic compounds. Here we document the temperature-driven decoupling of the production and consumption of key organic intermediates due to variable temperature responses of these functional microbial groups. Rates of labile dissolved organic carbon production exceeded those of terminal oxidation at temperatures less than 25°C, resulting in net production and accumulation of labile dissolved organic carbon. Above 25°C, potential terminal oxidation rates exceeded those of labile organic carbon production and labile organic carbon availability limited rates of terminal oxidation.

Understanding the controls on organic matter mineralization has long been a focus of terrestrial and aquatic biogeochemical studies because the long-term burial of organic carbon corresponds to the net accumulation of oxygen in the atmosphere, thus mediating the redox state of the Earth's biosphere and atmosphere (*1*). Though organic matter inputs to aquatic systems derive from allochthonous and autochthonous sources, organic matter mineralization is mediated by a similar series of microbial-processes across systems (Fig. 5.1). Organic matter mineralization supplies inorganic nutrients to fuel primary and secondary production and also influences the long-term burial of organic carbon and other materials in sediments (*1*, *2*, Fig. 5.1).

The microbes performing the terminal mineralization of organic matter to metabolic end products (Fig. 5.1) are limited largely to low molecular weight, labile dissolved organic carbon that can be transported across cellular membranes (< 600 Da, *3*). Terminal metabolism thus

requires the production of labile dissolved organic matter (*4*). Extracellular enzymatic hydrolysis initially converts particulate organic matter to high molecular weight dissolved organic matter, which is further hydrolyzed and fermented to labile and refractory low molecular weight dissolved organic matter and fermentation end products (*4-6*). Labile dissolved organic matter, which includes compounds such as volatile fatty acids (VFAs) and amino acids, is available for terminal metabolism (Fig. 5.1; *4, 7, 8*).

Despite the importance of hydrolysis/fermentation in organic matter mineralization, relatively little is known about environmental controls on this process. Here we show that the variable temperature responses of the microbial functional groups mediating the mineralization of complex organic matter in anaerobic marine sediments results in the temperature-driven decoupling of production and consumption of organic intermediates and the accumulation of labile dissolved organic matter at low temperatures. Temperature-driven changes in rates of organic carbon processing result in significant changes in coupling between VFA production and consumption, leading to either VFA accumulation or VFA limitation of terminal metabolism.

Coastal sediments account for only a small fraction (~7%) of the total area of marine sediments but receive and mineralize a disproportionately high fraction of organic matter (~55%; *9, 10*). High metabolic rates in coastal sediments deplete available oxygen, and the majority of organic matter mineralization proceeds via anaerobic metabolic pathways (*11*), mainly sulfate reduction (*11-14*). A majority of carbon mineralized by sulfate reduction flows through labile VFA intermediates such as acetate and propionate (*7, 8*). Temperature and substrate availability are primary drivers of microbial activity (*15*) and may regulate rates of organic matter mineralization (*16*). Rates of sulfate reduction in coastal sediments, for instance, generally follow a seasonal pattern similar to that of temperature (*12, 17*). Although sulfate reduction and

other anaerobic terminal metabolic processes depend on the labile organic carbon substrates produced by fermentation, the temperature dependence of organic carbon production via hydrolysis and fermentation and consumption via terminal metabolism may be quite different. A variable temperature dependence of the hydrolytic/fermentative and the terminal metabolic microbial communities could decouple these phases of organic matter mineralization.

We examined the role of temperature on the hydrolytic/fermentative production and terminal metabolic consumption of labile VFAs in anaerobic sediments from a temperate coastal estuary using two independent approaches. Anaerobic sediment slurry incubations were conducted between 5 and 32°C (*18*). Potential rates of hydrolysis/fermentation were determined in sulfate-free slurries with 2 mM 500,000 Da dextran, a dextrose polysaccharide. Rates of potential terminal metabolism were determined by amending slurries with acetate in the presence of sulfate (*18*). Rates of hydrolysis/fermentation and terminal metabolism, mainly (97%) sulfate reduction, were determined by measuring changes in substrates (sulfate, dissolved organic carbon) and products (carbon dioxide and VFAs) over time. Rates of hydrolysis/fermentation and terminal metabolism increased with increasing temperature while net VFA production decreased with increasing temperature (Fig. 5.2A). Production of acetate and propionate accounted for over 80% of VFA produced from dextran. From 10% (at 5°C) to > 90% (at 32°C) of the added dextran-carbon was fermented to VFAs during the course of the experiment. The rates of hydrolysis/fermentation and potential terminal metabolism exhibited significantly different temperature responses. Rates of hydrolysis/fermentation exceeded rates of terminal metabolism at temperatures less than 25°C ($p < 0.05$, Fig. 5.2A). At about 25°C, the two processes were equal, and at temperatures exceeding 25°C, rates of terminal metabolism exceeded rates of hydrolysis/fermentation ($p < 0.05$, Fig. 5.2A). This variable temperature

control resulted in net VFA production at temperatures less than 25°C, and net VFA consumption at temperatures greater than 25°C (Fig. 5.2A).

The slurry experiments, reflecting the response of a sediment microbial community sampled at one temperature to a range of temperatures, showed a temperature-driven decoupling of VFA production via hydrolysis/fermentation and consumption via terminal metabolism. To investigate whether this decoupling occurred in microbial communities adapted to *in situ* temperatures, flow-through bioreactor experiments were conducted using sediments collected four times over the course of a year. Bioreactor experiments have the advantage of retaining the natural sediment matrix, evaluating the response of the microbial community at *in situ* temperatures (12°C January, 20°C April, 27°C May and 29°C August), and measuring directly the coupling of hydrolysis/fermentation and terminal metabolism in a given sediment microbial population (*18*). Rates of hydrolysis/fermentation and terminal metabolism were determined in carbon-amended bioreactors (2 mM as 500,000 Da dextran) and in control bioreactors (no carbon addition) (*18*). Rates from dextran-amended reactors are reported as net rates and reflect the subtraction of rates in control bioreactors, thus differentiating between hydrolysis/fermentation of added dextran and that of natural sediment organic matter.

The bioreactor data validated the results from the slurry experiments (Fig. 5.2B, 5.2C). Rates of hydrolysis/fermentation were significantly greater than rates of terminal metabolism at 12 and 20°C ($p < 0.05$), resulting in net VFA production from dextran at these temperatures. Over 80% of the VFAs produced in the dextran-amended flow-through reactors were in the form of acetate and propionate. Rates of terminal metabolism and hydrolysis/fermentation coupled to autochthonous sediment organic matter in the control bioreactors increased over the temperature range of 12 to 27°C (January to May), as did net hydrolytic/fermentative DOC production from

particulate organic matter (Fig. 5.2C). Rates of terminal metabolism, hydrolysis/fermentation, and net DOC production declined sharply from 27 to 29°C (May to August) in the control reactors, potentially as a consequence of carbon limitation of the microbial community in the late summer.

Concentrations of bacterial phospholipid fatty acids (PLFA) measured upon termination of the flow-through experiments were used to evaluate changes in microbial abundance (Fig. 5.2D, *18*). The PLFA content in control bioreactors increased through the spring and early summer, indicating an increase in the microbial population. However, a marked drop in microbial biomass in late summer (Fig. 5.2D, August, 29°C) coincided with decreased rates of terminal metabolism, hydrolysis/fermentation and net DOC production (Fig. 5.2C). Carbon limitation of terminal metabolizing microbes at temperatures greater than 25ºC was confirmed by the significant increase ($p < 0.05$) in microbial PLFAs observed following dextran addition in May (30% increase) and August (>50% increase) (Fig. 5.2D).

A metabolic coupling index was determined for slurry and bioreactor experiments using the ratio of terminal metabolism to hydrolysis/fermentation (Fig 5.2E). When hydrolytic/fermentative production and terminal metabolic consumption of intermediates are tightly coupled, there is little or no net VFA accumulation and the index approaches 1. As the index approaches zero, production outpaces consumption and there is net VFA (in dextran-amended reactors) or DOC (in control reactors) accumulation due to temperature limitation of terminal metabolic activity.

The metabolic coupling index increased with temperature in the slurry and bioreactor experiments (Fig. 5.2E). The metabolic coupling index fell below 0.5 at temperatures below 14°C in both the slurry and dextran-amended flow-through bioreactor experiments, indicating

that rates of dextran hydrolysis/fermentation were more than double those of terminal metabolism. At temperatures above 25°C, the coupling index either approached (flow-through) or exceeded (slurry) 1 (Fig. 5.2E). In the bioreactor experiments, hydrolysis/fermentation of added dextran was the dominant source of labile dissolved organic matter available for terminal metabolism (rates in dextran-amended bioreactors were control-bioreactor-corrected, *18*), and therefore the metabolic coupling index could not exceed 1. This is not the case in the slurry experiments, where acetate was added to measure potential terminal metabolism and the coupling index could exceed 1, indicating that potential rates of terminal metabolism exceeded rates of hydrolysis/fermentation.

The metabolic coupling index increased from January to May (12 to 27°C) in the control reactors but remained below 0.5 in all experiments (Fig. 5.2E), meaning that < 50% of the DOC generated by particulate organic matter hydrolysis was consumed by terminal metabolizers. The close coupling of hydrolysis/fermentation and terminal metabolism observed in dextran-amended bioreactors at temperatures above 25ºC suggests that the DOC produced in control bioreactors was largely refractory and unavailable to terminal metabolizers. The significant ($p < 0.05$) increase of microbial biomass in response to carbon addition, evidenced by the increase in sediment PLFA content (Fig. 5.2D), corresponded to times (May, 27°C and August, 29°C) when the hydrolytic/fermentative-terminal metabolic coupling index in dextran-amended bioreactors was ~1, indicating complete consumption of fermentation products by terminal metabolizers (Fig. 5.2E).

The apparent activation energy (E_a, a measure of the temperature response of a microbial pathway, *17*) of hydrolysis/fermentation and terminal metabolism was calculated for slurry and flow-through experiments (*18*). The E_a values for terminal metabolism were similar between the

slurry experiment and the control and carbon amended bioreactor experiments (89.2, 82.7 and 85.5 kJ mol^{-1}, respectively), as were E_a values for hydrolysis/fermentation (47.8, 45.6 and 53.4 kJ mol^{-1}, respectively). The average E_a for terminal metabolism (85.8 kJ mol^{-1}) was significantly higher ($p < 0.05$) than the E_a for hydrolysis/fermentation (48.9 kJ mol^{-1}), underscoring the higher temperature sensitivity of terminal metabolism, in this case sulfate reduction. These E_a values are similar to those reported for sulfate reduction (83 kJ mol^{-1}, *14*; 36-132 kJ mol^{-1}, *17*) and overall organic matter degradation (54-125 kJ mol^{-1}, *19*) in marine sediments but are the first to differentiate the E_a for *in situ* terminal metabolic and hydrolytic/fermentative microbial communities. A general assumption in geochemical models is that the rates and E_a of anaerobic terminal metabolism reflects the response of the sediment microbial community as a whole to temperature and organic matter reactivity (*17*). Our results indicate that this is not necessarily the case, and that the functional groups mediating distinct phases of organic matter mineralization exhibit different temperature responses. A fundamental difference between the temperature response of terminal metabolism and hydrolysis/fermentation would be predicted based on the relationship between the thermodynamic energy yield of either process and temperature (*18*).

We constructed a simple model of anaerobic organic carbon processing over a seasonal temperature curve using a constant input of high molecular weight dissolved organic matter (0.5 μM d^{-1}) and first-order reaction rate constants (k) for terminal metabolism and hydrolysis/fermentation derived from the slurry experiment (Fig. 5.3A, *18*). The model results illustrate accumulation of labile VFAs in during colder periods due to the differential temperature response of terminal metabolic and hydrolysis/fermentative microbial communities (Fig. 5.3B). This seasonal accumulation of acetate and other labile dissolved organic carbon

substrates is largely attenuated if the temperature response of terminal metabolism is equal to that of hydrolysis/fermentation (Fig. 5.3B), underscoring the significance of temperature in regulating the fate of organic matter cycling in the environment. In natural systems, organic matter inputs are seasonally and spatially variable, thus, the timing of organic matter inputs will influence the potential for VFA accumulation in sediments. For instance, VFA accumulation would be expected during a spring phytoplankton bloom when temperatures remain low but phytoplankton-derived carbon inputs are high. The observed accumulation of acetate in Long Island Sound surficial sediments (*20*) following spring phytoplankton-derived inputs of organic matter is a potential example of this phenomenon in a natural environment.

The concentrations of dissolved organic substrates, like VFAs, in anaerobic sediments may exceed those anticipated for labile compounds (*20, 21*) and the mechanisms responsible for such accumulations have not been identified (*22*). Shifts in the microbial community composition could contribute to patterns of substrate abundance (*23*); however, accumulation of labile VFAs can occur in the apparent absence of microbial population transitions or substrate limitation, and such accumulations have been observed at lower temperatures (*8, 20, 21, 22, 24, 25*). The differential temperature control of the hydrolytic/fermentative and terminal metabolic microbial communities that we document here provides a clear mechanism for decoupling the production and consumption of labile organic intermediates and a robust explanation for the accumulation of labile dissolved organic carbon in anaerobic sediments. The temperature-limited capacity of the hydrolytic/fermentative production of labile dissolved organic carbon during warm summer months may generate a 'bottleneck' in organic matter mineralization that results in carbon limitation of the terminal metabolic microbial community.

Anaerobic habitats occur throughout the aquatic and terrestrial biospheres, and organic matter processing in these zones contributes substantially to the global cycling of carbon, nutrients, and other elements (*1*, *4, 9, 11*). Variable temperature responses of key functional components may be a fundamental feature of the anaerobic microbial community involved in organic matter mineralization and has significant implications for organic matter turnover within and across ecosystems and geographic zones, and with respect to global climate change. Given the lower thermodynamic energy yield of methanogenesis compared to sulfate reduction, temperature-driven decoupling of hydrolysis/fermentation and terminal metabolism may be more pronounced in freshwater habitats where methanogenesis accounts for the majority of terminal metabolism (*18*). Acetate accumulation has been documented in freshwater methanogenic environments at lower temperatures (*22*), and temperature driven decoupling of hydrolysis/fermentation and terminal metabolism may drive this pattern. Increased global temperatures could reduce temperature-driven decoupling in methanogenic systems, leading to increased fluxes of methane, a potent radiative trace gas, from these environments. If the temperature-limited capacity of the hydrolytic/fermentative production of labile dissolved organic carbon at temperatures exceeding 25 ºC occurs generally, then terminal metabolizers in tropical anaerobic habitats may be limited by labile organic carbon availability during much of the year. Similarly, in polar environments, the activity of terminal metabolizers may be restricted by low temperatures consistently, resulting in the accumulation of labile dissolved organic matter in sediment porewaters and loose coupling between hydrolysis/fermentation and terminal metabolism. The data presented here show clearly that small changes in temperature impact the efficiency of organic matter turnover in anaerobic marine sediments by influencing coupling between different components of the anaerobic microbial community. Differential

temperature-regulation of key phases of organic matter mineralization may also influence coupling between processes, e.g., primary production, that depend on regenerated metabolites, e.g., inorganic nutrients (Fig. 5.1), and the microbes involved in organic matter mineralization.

LITERATURE CITED

1. Berner, R.A. *Nature* **426**, 323 (2003).
2. G.T. Rowe, C.H. Clifford, K.L. Smith, *Nature* **255**, 215 (1976).
3. M. S. Weiss et al., *Science* **254**, 1627 (1991).
4. T. M. Fenchel, B. J. Findlay, *Ecology and Evolution of Anoxic Worlds* (Oxford University Press, Oxford, 1995).
5. C. Arnosti, D. J. Repeta, N. V. Blough, *Geochim. Cosmochim. Acta* **58**, 2639 (1994).
6. D. J. Burdige, A. Skoog, K. Gardner, *Geochim. Cosmochim. Acta* **64**, 1029 (2000).
7. J. Sørensen, D. Christensen, B. B. Jørgensen, *Appl. Environ. Microbiol.* **42**, 5 (1981).
8. P. Wellsbury, R. J. Parkes, *FEMS Micobiol. Ecol.* **17**, 85 (1995).
9. J. J. Middelburg, K. Soetart, P. M. J. Herman, *Deep-Sea Res.* **44**, 327 (1997).
10. R. Wollast, in *Ocean Margin Processes in Global Change*, R. F. C. Mantoura, J. M. Martin, R. Wollast, Eds. (Wiley, Chichester, 1991), pp. 365-381.
11. D. E. Canfield, in *Interactions of C, N, P and S Biogeochemical Cycles*, R. Wollast, L. Chou, F. Mackenzie, Eds. (Springer, Berlin, 1993), pp. 333-363.
12. G. M. King, *Limnol. Oceanogr.* **33**, 376 (1988).
13. E. E. Roden, J. H. Tuttle, *Mar. Ecol. Prog. Ser.* **93**, 101 (1993).
14. E. E. Roden, J. H. Tuttle, W. R. Boynton, W. M Kemp, *J. Mar. Res.* **53**, 799 (1995).
15. L. R. Pomeroy, W. J. Wiebe, *Aquat. Microb. Ecol.* **23**, 187 (2001).

16. P. Westermann, *World J. Microbiol. Biotech.***12**, 497 (1996).

17. J. T. Westrich, R. A. Berner, *Geomicrobiol. J.* **6**, 99 (1988).

18. Materials and methods are available as supporting material.

19. J. J. Middelburg *et al., Mar. Ecol. Prog. Ser.* **132**, 157 (1996).

20. H. Wu, M. Green, M. I. Scranton, *Limnol. Oceanogr.* **42**, 705 (1997).

21. D. B. Albert, C. Taylor, C. S. Martens, *Deep-Sea Res.* **42**, 1239 (1995).

22. A. Fey, R. Conrad, *Appl. Environ. Microbiol.* **66**, 4790 (2000).

23. T. M. Hoehler, D. B. Albert, M. J. Alperin, C. S. Martens, *Limnol. Oceanogr.* **44**, 662 (1999).

24. C. Arnosti, B. B. Jørgensen, *Mar. Ecol. Prog. Ser.* **249**, 15 (2003).

25. N. Finke, Ph.D. Dissertation, University of Bremen (2003).

26. This work was supported by the National Oceanic and Atmospheric Administration's Georgia Sea Grant Program (NA06RG0029-R/WQ11 and R/WQ12A). We thank D. Albert, J. Dai, H. Ding, M. Erickson, J. Menken, W. Porubsky, T. Roberts, V. Samarkin, and M. Sun for analytical assistance and J. Edmonds, T. Hollibaugh, P. Megonigal, C. Meile, M. Moran, B. Orcutt, and H. Schulz for providing comments that substantially improved this paper.

FIGURE LEGENDS

Figure 5.1: A simplified diagram showing organic matter dynamics in aquatic ecosystems. Inputs of organic matter derive from allochthonous and autochthonous sources. The dashed-line indicates the suite of microbial processes that mineralize organic matter. Particulate organic matter is hydrolyzed to high molecular weight dissolved organic matter, which is then further hydrolyzed and fermented to labile, low molecular weight dissolved organic matter. Terminal metabolizers then mineralize labile dissolved organic matter to terminal end products. Organic matter recycling provides inorganic nutrient sources to support production in aquatic ecosystems and influences the amount of organic carbon subject to long-term burial.

Figure 5.2: Net rates (± standard deviation) of hydrolysis/fermentation (HF –□–), terminal metabolism (TM –●–) and volatile fatty acid production (R_{VFA} ··▲··) or net dissolved organic carbon production (R_{DOC} ··△··) in **(panel A)** anaerobic sediment slurries incubated at different temperatures and **(panel B)** in dextran-amended and **(panel C)** control flow-through reactor experiments incubated at *in situ* temperatures (12°C, January 2005; 20°C, April 2004; 27°C, May 2004; 29°C, August 2004). Note that rates in dextran-amended reactors are corrected for rates in control reactors, and are estimates of rates of processing of added dextran only, and rates in control reactors are estimates of sediment POM processing. **(Panel D)** Sediment phospholipid fatty acid content (± standard deviation) in control ($PLFA_{Con}$ ···+···) and dextran-addition ($PLFA_{Dex}$ –×–) flow-through reactors at the termination of the 10 day experiments. **(Panel E)** Hydrolytic/fermentative and terminal metabolic coupling index calculated from the ratio of terminal metabolism to hydrolysis/fermentation in the slurry (–○–) and dextran-amended (–◆–) and control (–◇–) flow-through reactor experiments.

Figure 5.3: Seasonal model of coupled hydrolytic/fermentative production and terminal metabolic consumption of volatile fatty acids (VFA) in a closed sediment system with constant inputs of high-molecular weight organic matter (0.5 μM d-1). **(Panel A)** Temperature (T ▬) and first-order rate constants for hydrolysis/fermentation (kHF – –) and terminal metabolism (kTM ▬) derived from the slurry experiment and **(panel B)** resulting sediment VFA concentrations using these measured rate constants (·····) and when kTM is set equal to kHF (▬).

Figure 5.1.

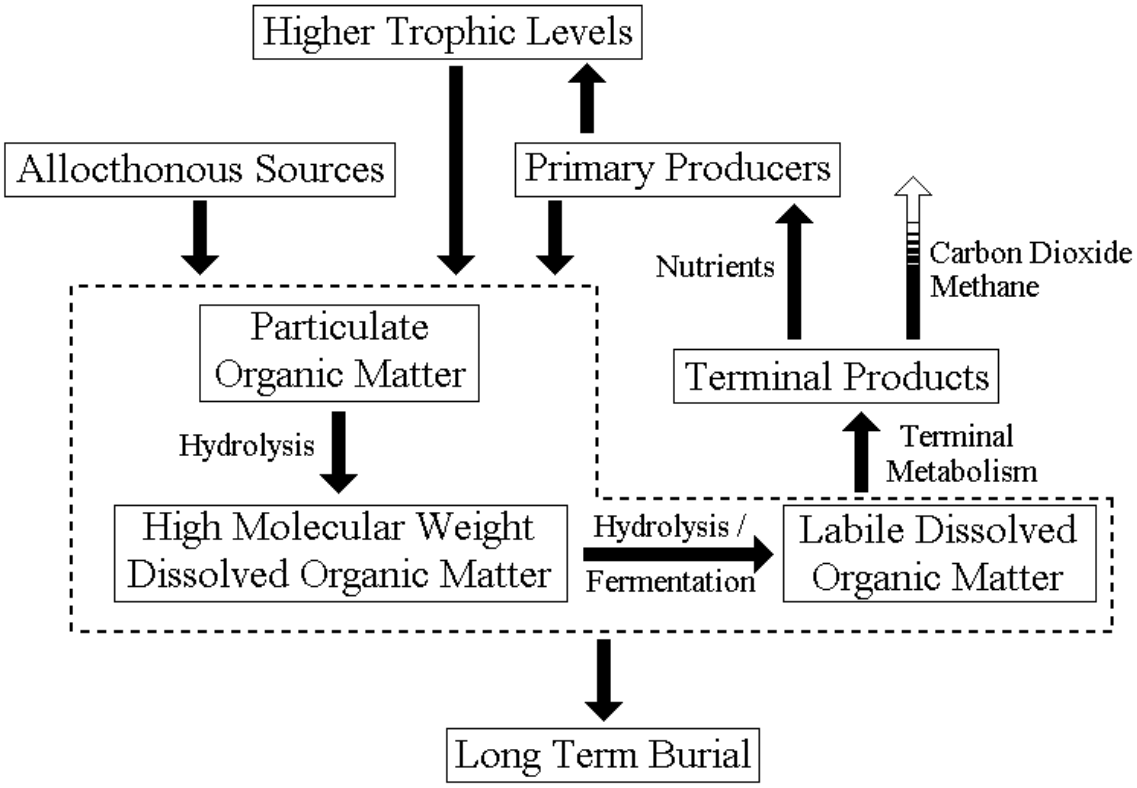
Higher Trophic Levels
Allocthonous Sources
Primary Producers
Nutrients
Carbon Dioxide
Methane
Particulate
Organic Matter
Terminal Products
Hydrolysis
Terminal
Metabolism
High Molecular Weight
Dissolved Organic Matter
Hydrolysis /
Fermentation
Labile Dissolved
Organic Matter
Long Term Burial

Figure 5.2.

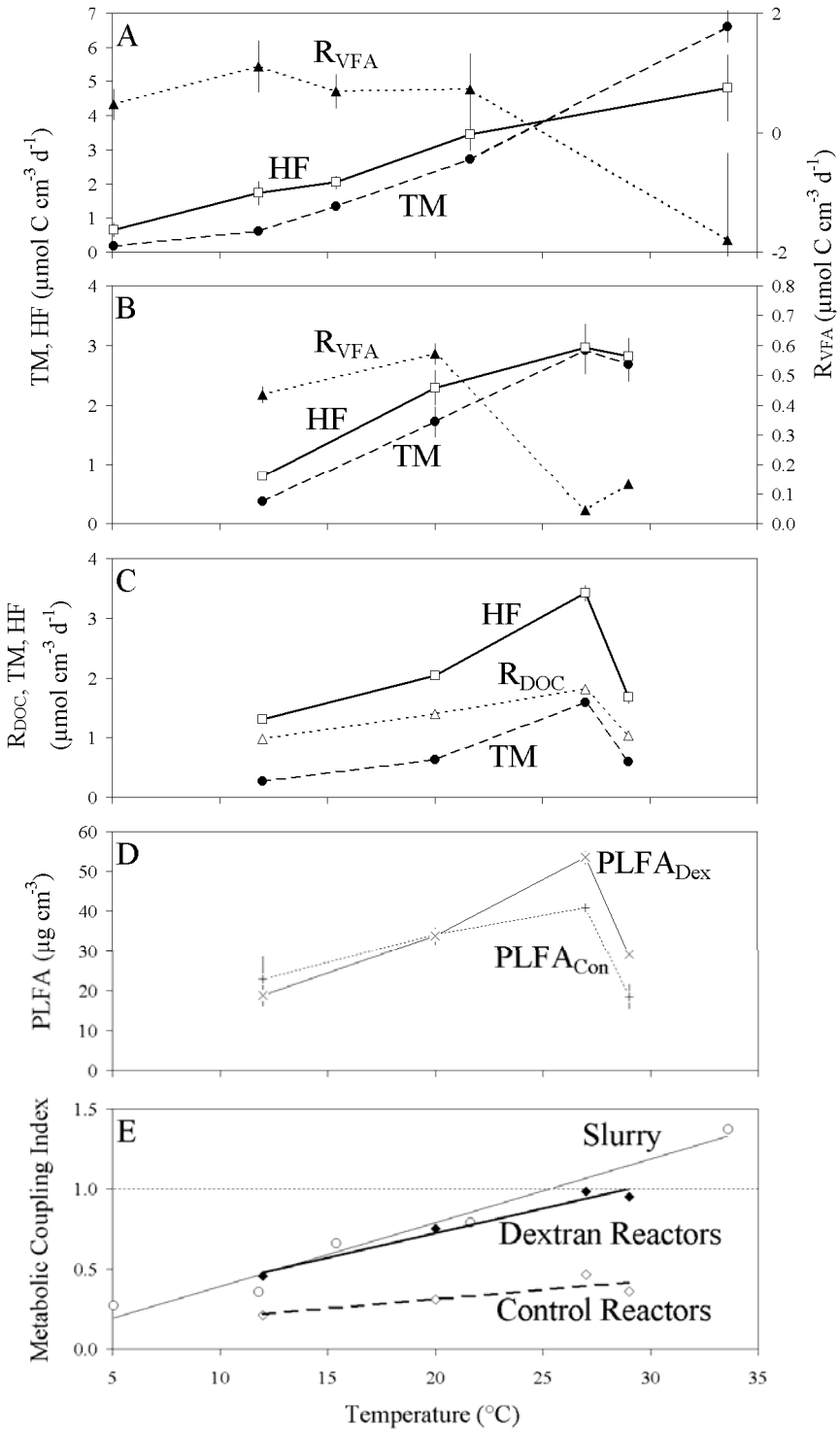
A
R_{VFA}
HF
TM
TM, HF (µmol C cm^{-3} d^{-1})
R_{VFA} (µmol C cm^{-3} d^{-1})
B
R_{VFA}
HF
TM
C
HF
R_{DOC}
TM
R_{DOC}, TM, HF (µmol cm^{-3} d^{-1})
D
$PLFA_{Dex}$
$PLFA_{Con}$
PLFA (µg cm^{-3})
E
Slurry
Dextran Reactors
Control Reactors
Metabolic Coupling Index
Temperature (°C)

Figure 5.3.

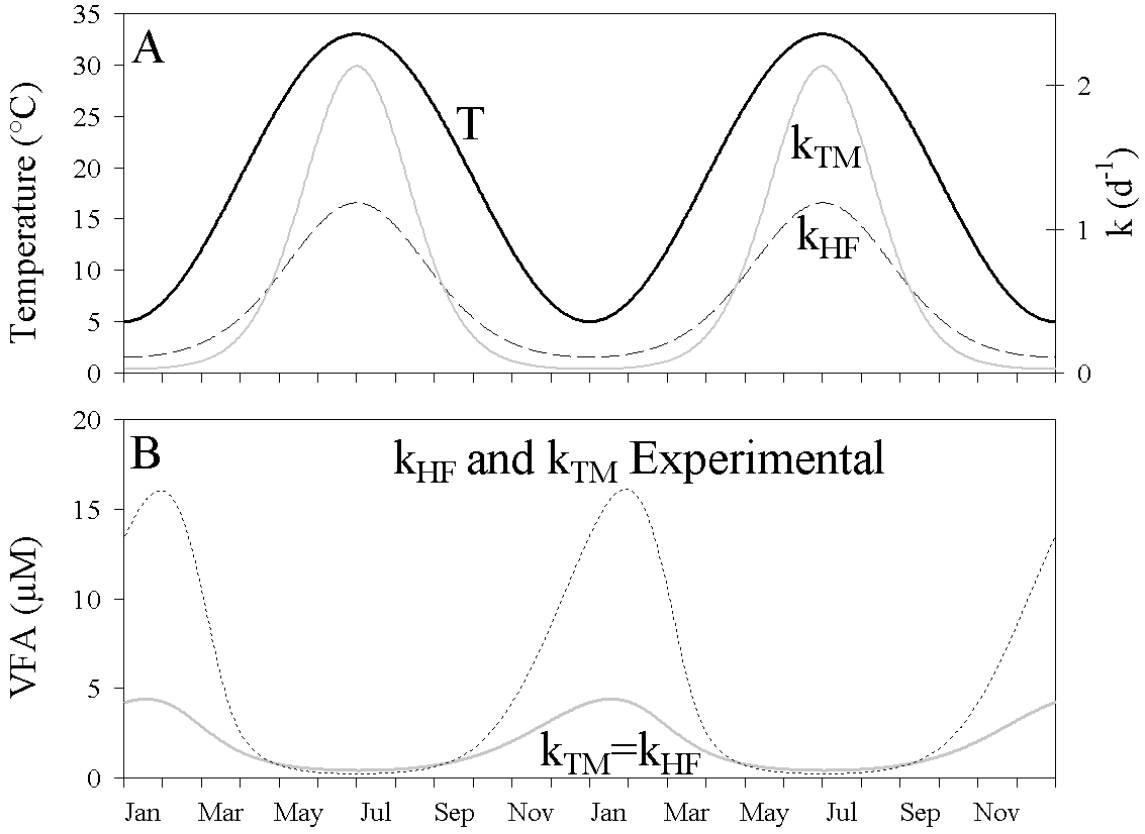
A
T
k_{TM}
k_{HF}
Temperature (°C)
k (d^{-1})
35
30
25
20
15
10
5
0
2
1
0
B
k_{HF} and k_{TM} Experimental
VFA (μM)
20
15
10
5
0
k_{TM}=k_{HF}
Jan
Mar
May
Jul
Sep
Nov
Jan
Mar
May
Jul
Sep
Nov

SUPPORTING MATERIALS

Slurry Experiment

Sediment cores were obtained from the bank Umbrella Creek, a tidal creek off the Satilla River in Georgia, USA for a slurry experiment in December 2004. Cores were transported to the laboratory and the 2-4 cm depth of several cores was homogenized anaerobically (in a Coy chamber). Homogenized sediment was separated into two equal portions. Each portion was then mixed with anaerobic artificial porewater (292 mM NaCl, 12.6 mM $MgCl_2$, 0.9 mM $CaCl_2$, 4 mM NH_4Cl, 1.2 mM KH_2PO_4, 5.7 mM KCl and 9.5 mM $NaHCO_3$), one of with sulfate (5 mM Na_2SO_4) and one without, in an approximately 2:1 water to sediment ratio. The slurry was shaken for 10 minutes, gently centrifuged, and the supernatant removed and discarded. This rinsing procedure was repeated four times. After the final rinse, sediment was slurried in a 2:1 artificial porewater to sediment ratio and distributed into headspace-free 6 ml vials. Vials were sealed, placed in a secondary gas-tight container in an atmosphere of N_2, removed from the Coy anaerobic chamber and placed at various temperatures (5, 12, 15, 22 and 34°C) for a three day equilibration period.

Acetate (2 mM as sodium acetate) was then added to the vials containing sulfate, and high molecular weight organic carbon (2 mM carbon as 500,000 nominal molecular weight dextran, Sigma®) was added to the sulfate-free vials (15 vials from each temperature and treatment). Vials were then sampled immediately and over a time course for the next several days (22 and 34°C) to weeks (5, 12, and 15°C). At each sampling, vials were centrifuged and the supernatant sampled for dissolved inorganic carbon (DIC), sulfate (SO_4^{2-}), volatile fatty acids (VFAs) and methane (CH_4; Table 5.S1). Rates of processes were determined from slopes of

concentration versus time during period of linear change for each treatment (see *Rates and Reaction Pathways* section).

Seasonal Flow-through Bioreactor Experiments

Intact sediment cores (8.8 cm i.d.) and sediment temperature profiles were obtained from the unvegetated creek-bank in Umbrella Creek in April, May and August 2004 and January 2005. Cores were transported to the laboratory, stored at *in situ* temperatures overnight, and sectioned the following day for porewater analysis and preparation for the sediment flow-through reactor experiments (Roychoudhury 1997, 2003; Brüchert and Arnosti 2003). Duplicate sediment cores were sectioned anaerobically (in a Coy chamber) at 1 cm intervals to 4 cm. Porewater was analyzed for sulfate (SO_4^{2-}; Table 5.S1) to ensure that SO_4^{2-} was not limiting to sulfate reducers at the time of sampling. Porewater SO_4^{2-} was > 5 mM on all dates, above limiting concentrations (Roychoudhury et al. 1997, 2003).

Sediment flow-through reactor experiments were initiated on the day following sampling. Sediment from the 2-4 cm depth of four intact sediment cores was extruded into separate (2 x 8.8 cm height x i.d.) sections and placed in flow-through reactor housings. Sediment flow-through reactors were constructed of polycarbonate plastic and consisted of a 2 cm section of sediment, capped on either end with 0.6 cm of 15 μm frit and held in place with an upper and lower housing. The polycarbonate housings had an inlet/outlet in the center, and spiral grooves on the inner surface to promote diffuse flow across the surface of the frit. The assembly was bolted lightly together and sealed with viton o-rings between the core, frit and housing. A peristaltic pump was used to pump anaerobic artificial porewater (292 mM NaCl, 12.6 mM $MgCl_2$, 0.9 mM $CaCl_2$, 5 mM Na_2SO_4, 4 mM NH_4Cl, 1.2 mM KH_2PO_4, 5.7 mM KCl and 9.5 mM $NaHCO_3$) from

a reservoir through the reactors at a slow flow rate (~10 ml hr^{-1}). The entire assembly (reservoir, pump and reactors) was placed in a nitrogen-flushed glove bag in an incubator. A mixture of 2.5% CO_2 in N_2 (to maintain constant DIC concentration in reservoir) was used to purge the reservoirs for 4 hours initially, and then 0.5 hour per day for the duration of the experiment to maintain anaerobic conditions. Oxygen content of the reservoirs was checked periodically by microelectrode (Unisense®) and was always below detection (~1 μM) following the initial purge.

Reactor experiments were conducted at 12°C (January), 20°C (April), 27°C (May) and 29°C (August). Duplicate reactors were used for two treatments; a control and a high molecular weight carbon addition. Anaerobic artificial porewater was pumped through all reactors for an initial 4 day period to establish flow and flush sediment porewater. Inflow water for both treatments was then spiked with 1 mM KBr, and the reservoir for the carbon treatment was also spiked with 2 mM carbon as dextran (Sigma®, nominal molecular weight 500,000).

Water exiting the flow-through reactors was sampled at least once daily (more often during initial breakthrough) for 10 days following carbon addition. Sample was obtained from the outflow of the sediment reactors by placing the outflow tubing in a glass vial for 2 hours (allowing the vial to overflow for at least one volume). This sample was then split into various vials for analysis of DIC, SO_4^{2-}, CH_4, VFA, and dissolved organic carbon (DOC), reduced iron (Fe^{2+}), hydrogen sulfide (H_2S) and bromide (Br^-) (Table 5.S1). Flow rate and pH of the flow-through reactors was also monitored throughout the experiment. The breakthrough of Br^- was used to calculate a dispersion coefficient (Yu et al. 1999) and validate diffuse flow through the reactors, and concentrations and flow rates were used to calculate rates of reactions (see *Rates and Reaction Pathways*). Upon termination of the flow-through reactor experiments, the reactors

were disassembled and sediment was immediately frozen (-80° C) for bacterial phospholipid fatty-acid (PLFA) analysis.

Analytical Methods

Analytical methods are summarized in Table 5.S1. Methods requiring further description (PLFA and VFA) are described below.

PLFAs were measured following the protocol of Boschker et al. (1999). Briefly, lipids were extracted using the method of Bligh and Dyer (1959) followed by sequential extraction of lipid classes on silica columns with solvents of increasing polarity. The final methanol (PLFA) fraction was collected, subjected to a mild alkaline methanolysis, and analyzed by gas chromatography (Hewlett-Packard 6890 GC system with a 30 m HP-5 column, 20°C/min from 50-170 C and 4°C/min to 310°C). Identification of PLFAs by retention time was compared with standards of known composition. The extraction scheme was validated using an L-alpha-phosphatidylcholine-beta-oleoyl-gamma-myristoyl phospholipid standard, and an internal standard (nonadecanoic acid methyl ester) was used to quantify PLFAs in samples.

VFAs were analyzed by a modified Albert and Martens (1997) 2-nitrophenylhydrazide derivitization. Following derivitization samples were concentrated and rinsed on an Alltech Instruments PRP-1 cartridge, and then eluted (with Solvent B from Albert and Martens 1997) into a separate vial. This derivitized and pre-eluted sample was then directly injected onto a Browlnee Spheri-5 RP-8 column for high performance liquid chromatographic detection at 400 nm. VFAs quantified include glycolate, lactate, acetate, formate, propionate, iso-butyrate, butyrate, succinate, iso-valerate and valerate.

Rates and Reaction Pathways

Rates of metabolic processes (μmol cm^{-3} d^{-1}) in the slurry experiment were calculated from changes in concentration of DIC, SO_4^{2-}, DOC, and VFAs during periods of linear increase or decrease with time, based on the original volume (cm^3) of sediment. Rates in the flow-through reactors (μmol cm^{-3} d^{-1}) were estimated by the difference in concentration of DIC, SO_4^{2-}, VFA, and DOC between the reactor outflow (C_{out}) and reservoir inflow water (C_{in}), correcting for flow rate (Q) through the reactors (equation 5.1). The effects of added HMW-carbon on rates (R_D) were determined by correcting the rates in the carbon addition reactors (R_A) for rates measured in control reactors (R_C, equation 5,2).

(5.1) $$R = Q(C_{out} - C_{in})$$

(5.2) $$R_D = R_A - R_C$$

All rates for in the dextran-addition reactors are expressed as R_D (corrected for rates in the control reactors) to differentiate effects of carbon addition.

Rates of terminal metabolism in the flow-through reactor and slurry experiments were calculated from changes in metabolic substrates (SO_4^{2-}) and products (DIC and CH_4) in two ways:

(5.3) $$TM_{DIC} = R_{DIC} + R_{CH4}$$

(5.4) $$TM_{SO4} = 2(R_{SO4}) + 2(R_{CH4})$$

where terminal metabolism (TM) on a per carbon basis is calculated from either DIC production (TM_{DIC}; equation 5.3), which is the sum of DIC and CH_4 production (R_{DIC} and R_{CH4}, respectively), or from sulfate uptake (TM_{SO4}; equation 5.4), which is double the rates of sulfate uptake (R_{SO4}) and R_{CH4}. In all experiments, R_{CH4} was negligible (< 1%) and Fe^{2+} concentrations in the slurries and in flow-through reactor samples were measurable but low, and may have been due to iron mineral dissolution rather than microbial iron oxide reduction. TM_{DIC} agreed well with TM_{SO4} in all cases (within 5%), indicating that sulfate reduction was the dominant pathway of terminal metabolism and other pathways (methanogenesis, aerobic respiration, metal-oxide reduction, denitrification) were negligible. TM_{DIC} values were used in all further calculations, graphs, and discussion.

Rates of hydrolysis/fermentation (HF_D; equation 5.5) in the slurry and dextran-addition flow-through experiments were then calculated from the rate of terminal metabolism and the rate of volatile fatty acid production (R_{VFA}) on a per carbon basis:

$$HF_D = TM + R_{VFA} \quad (5.5)$$

Note that these are minimum estimates of hydrolysis/fermentation, as intermediates produced by fermentation and available to terminal metabolizers other than those measured by the VFA analysis (such as other low molecular weight dissolved organic carbon compound or molecular hydrogen) were not quantified. Rates of hydrolysis/fermentation in control flow-through reactors (HF_C) were also determined from rates of terminal metabolism and R_{DOC} (DOC production rate) in the control reactors:

(5.6) $HF_C = TM_C + R_{DOC}$

With no carbon addition to the control reactors, DOC is produced from particulate organic matter, and must therefore be a product of hydrolysis/fermentation.

Apparent Activation Energies

The apparent activation energies (E_a) of terminal metabolism and hydrolysis/fermentation were calculated using Arrhenius equation (Westrich and Berner 1988):

(5.7) $TM \text{ or } HF = Ae^{(-Ea/RT)}$

where A is a constant, R is the gas constant and T is temperature (in K). The slope of the linear best-fit of the natural log of the rate against T^{-1} is equal to $-E_a/R$. E_a was determined separately for terminal metabolism and hydrolysis/fermentation for the slurry experiment and the dextran-addition and control flow-through reactor experiments. Data from August (29°C) was not included in the control E_a calculation due to the sharp decline in rates on this date. E_a as it is calculated here is influenced by the interactions of temperature and population size and composition. When rates of TM and HF in the control reactors were calculated on a per μg PLFA basis, plots of ln(TM) and ln(HF) versus T^{-1} including August were linear ($r^2 \sim 0.9$) and the estimated E_a of TM remained about 50% that of HF.

Thermodynamic Considerations

The thermodynamics of glucose fermentation to acetate and terminal metabolism of acetate (sulfate reduction and methanogenesis) were calculated at standard state (1 M or 10^5 Pa and 25°C; Table 5.S2). The Gibbs free energy (ΔG) for glucose fermentation is only slightly effected by changes in temperature (4.7 J mol C^{-1} K^{-1}; *9*) while the ΔG of acetoclastic methanogenesis is more effected by changes in temperature (156.7 J mol C^{-1} K^{-1}) as calculated from the state equation

$$\Delta G = \Delta H - T\Delta S \quad (5.8)$$

where ΔH and ΔS are the enthalpies and entropies of reaction, respectively (Table 5.S2), and T is temperature (in Kelvin). The ΔG for sulfate reduction of acetate has an intermediate sensitivity to temperature (98.8 mol C^{-1} K^{-1}; Table 5.S2).

The sensitivity of ΔG for sulfate reduction and methanogenesis to changes in temperature as compared to ΔG for fermentation, suggests that thermodynamics may in part control the temperature-driven decoupling between hydrolysis/fermentation and terminal metabolism at lower temperatures. Furthermore, the temperature-driven decoupling observed in this study (Fig. 5.3) may be amplified in systems dominated by methanogenesis due to the larger temperature sensitivity of this metabolic pathway (Table 5.S2).

Sediment Metabolism Model

A simple seasonal model of terminal metabolic consumption of VFAs coupled to hydrolyic/fermentative production of VFAs from high molecular weight dissolved organic matter

was constructed, using first-order rate constants derived from the slurry incubation experiment. Rate constants were determined using plots of the natural log of substrate (dextran for hydrolysis/fermentation and acetate for terminal metabolism) disappearance with time. Dextran concentrations were calculated from a known starting concentration and the accumulation of fermentative and terminal metabolic end-products (equation 5.5), and acetate disappearance was measured directly. The temperature dependence of the first-order rate constants was determined using Arrhenius-type plots of as above (equation 5.7) to derive the E_a of each metabolic pathway. The E_a for first-order rate constants were 59.9 kJ mol^{-1} for hydrolysis/fermentation and 112.4 kJ mol^{-1} for terminal metabolism. These relationships were then used to determine the first-order rate constants during a seasonal temperature cycle (Fig. 5.3A).

A constant high molecular weight dissolved organic matter input of 0.5 μM d^{-1} into a closed sediment system with seasonally oscillating temperature (from 5 to 33°C) was modeled. The rate of hydrolysis/fermentation and VFA production was a product of the first-order rate constant and the high molecular weight dissolved organic matter concentration, and the rate of terminal metabolism was a product of its first-order rate constant and the concentration of VFAs. A second model scenario was run, in which the first-order rate constant for terminal metabolism was set equal to that of hydrolysis/fermentation to clarify the role of temperature sensitivity on the seasonal accumulation of VFAs in the sediment. The model results shown (Fig. 5.3B) are after several years to ensure appropriate beginning-of-year starting conditions.

SUPPORTING MATERIAL LITERATURE CITED

1. D. B. Albert, C. S. Martens. *Mar. Chem.* **56**, 27 (1997).
2. E. G. Bligh, W. J. Dyer, Can. J. *Biochem. Physiol.* **37**, 911 (1959).

3. H. T. S. Boschker, J. F. C. de Brouwer, T. E. Cappenburg, *Limnol. Oceanogr.* **44**, 309 (1999).
4. A. N. Roychoudhury, P. Van Cappellen, J. E. Kostka, E. Viollier, *Est. Coast. Shelf Sci.* **56**, 1001 (2003).
5. A. N. Roychoudhury, E. Viollier, P. Van Cappellen, *Appl. Geochem.* **13**, 269 (1998).
6. V. Brüchert, C. Arnosti. *Mar. Chem.* **80**, 171 (2003).
7. C. Yu, A. W. Warrick, M. H. Conklin, *Water Res. Res.* **35**, 3567 (1999).
8. J. T. Westrich, R. A. Berner, *Geomicrobiol. J.* **6**, 99 (1988).
9. A. Fey, R. Conrad, *Appl. Environ. Microbiol.* **66**, 4790 (2000).

Table 5.S1. Sampling, preservation and analytical methods for methane (CH_4), dissolved inorganic carbon (DIC), dissolved organic carbon (DOC), sulfate (SO_4^{2-}), volatile fatty acids (VFAs) and bromide (Br^-).

Analyte	Sample	Preservation	Analytical Method
Aqueous Measurements			
CH_4	Unfiltered in He purged headspace vial	4.4 N phosphoric acid	Shimadzu® GC 14A flame ionization detector gas chromatograph
DIC	Unfiltered	Run immediately	Shimadzu® TOC 5000 infra-red gas analyzer
DOC	0.2 µm filtered	0.2 N nitric acid, refrigerated	Shimadzu® TOC 5000 high-temperature combustion infra-red gas analyzer after sparging with CO_2-free air
SO_4^{2-}	0.2 µm filtered	0.2 N nitric acid, refrigerated	Dionex® ion chromatograph
VFA	0.2 µm filtered	Frozen	Modified 2-nitrophenylhydrazide derivatization and high performance liquid chromatography (Albert & Martens 1997) S*ee text for further description*
Br^-	0.2 µm filtered	0.1 M zinc acetate	Colorimetric (Lachat® Quikchem 8000 autoanalyzer method 30-135-21-1B)
Sediment Solid-Phase Measurements			
PLFA	Sediment	Frozen (-80 °C)	Phospholipid extraction followed by gas chromatographic analysis (Boschker et al. 1999) S*ee text for further description*

Table 5.S2. Gibbs free energies (ΔG^0), enthalpies (ΔH^0) and entropies (ΔS^0), per mol of carbon, for fermentation, sulfate reduction and methanogenesis under standard (1 M or 1 atm, 25°C).

Pathway	Reaction	ΔG^0 kJ mol^{-1} C	ΔH^0 kJ mol^{-1} C	ΔS^0 J (K mol C)$^{-1}$
Fermentation	$C_6H_{12}O_6 \rightarrow 3CH_3COO^-$	-33.1	-31.7	4.7
Sulfate Reduction	$CH_3COO^- + SO_4^{2-} + H^+ \rightarrow H_2S + 2HCO_3^-$	-43.7	-14.3	98.8
Methanogenesis	$CH_3COO^- + H^+ \rightarrow CH_4 + CO_2$	-37.9	8.9	156.7

CHAPTER 6

CONCLUSIONS

Two main themes have been addressed here; the influence of human activities in the watersheds of coastal systems (**Chapters 2, 3 & 4**), and the controls on organic matter processing in estuarine sediments (**Chapter 3, 4 & 5**). Excess nutrient loading and the eutrophication of coastal waters continues to be a major concern globally. The salt marshes and estuaries of Georgia are perhaps the least developed coastal areas in the contiguous United States. Nevertheless, this work demonstrates that changes over the past three decades have altered nutrient delivery from the Altamaha River watershed (**Chapter 2**), and delivery of nutrients and organic matter can effect processes in estuarine sediments (**Chapter 4**). Upriver salinity intrusion due to water withdrawals, climate change and natural seasonal variation in precipitation within the watershed may further exacerbate nutrient loading to coastal waters (**Chapter 3**). Future population growth and development within this watershed, if not managed wisely, will adversely effect coastal waters in Georgia.

The research presented here expands our knowledge of the anaerobic mineralization of organic matter in sediments. Upriver salinity intrusion results in a rapid shift from methanogenesis to sulfate reduction as the dominant pathway of terminal organic matter mineralization (**Chapter 3**). There has been abundant work on the terminal oxidative step of organic matter mineralization, but we know surprisingly little about the hydrolytic and fermentative steps, which are required for the breakdown of complex organic matter in anaerobic systems. This work demonstrates that, while sulfate depletion and the terminal products of sulfate reduction are strongly correlated in estuarine porewater on a system-wide scale, bulk

dissolved organic carbon (DOC) does not clearly reflect metabolic processes. The hydrolytic/fermentative production and terminal metabolic consumption of labile DOC intermediates is relatively tightly coupled, such that bulk porewater DOC is largely unavailable to the microbial community (**Chapter 4**). However, process studies show that the temperature-driven decoupling of labile DOC production and consumption can result in accumulation of DOC at lower temperatures, and that fermentative/hydrolytic production of labile intermediates limits terminal metabolism at warmer temperatures (**Chapter 5**). We suspect this is a fundamental process that reflects to some degree the thermodynamics of these metabolic processes. Further work is needed to determine if this temperature-driven decoupling occurs in freshwater methanogenic sediments, as we believe it does to an even greater degree. This may be a previously unrecognized important aspect of global carbon cycling.